CNIC-01075
CNDC-0018
INDC(CPR)-040/L

中国核科技报告

CHINA NUCLEAR SCIENCE AND TECHNOLOGY REPORT

COMMUNICATION OF NUCLEAR DATA PROGRESS

No. 15(1996)

China Nuclear Data Center

中国核情报中心
原子能出版社

China Nuclear Information Centre
Atomic Energy Press

CNIC-01075
CNDC-0018
INDC(CPR)-040 / L

COMMUNICATION OF NUCLEAR DATA PROGRESS

No. 15 (1996)

China Nuclear Data Center

China Nuclear Information Centre

Atomic Energy Press

Beijing, June, 1996

EDITORIAL NOTE

This is the 15th issue of *Communication of Nuclear Data Progress* (CNDP), in which the nuclear data achievements and progress in China during the last year are presented, including measurements of the energy spectrum and angular distributions of protons from stainless steel bombarded by 14.6 MeV neutrons, and of $^{Nat}Ni(n,x\alpha)$ reaction cross sections; calculating methods in program CCRMN, theoretical calculations of ^{59}Co and ^{90}Zr neutron reaction data, progress in calculation of direct inelastic scattering cross section of neutron, consistent dynamical and statistical description, a set of optical potential parameters of natural zinc; the method and program CABEI for adjusting consistency between natural and its isotope data, production cross sections of ^{18}F, ^{77}Br and ^{186}Re medical radioisotopes, evaluations of H total cross section from 20 MeV to 2 GeV, $^{58, 60, 61, 62, 64, Nat}Ni(n,p)$, ^{59}Co, $^{90}Zr(n,x)$ and ^{84}Rb decay data, the comparison of gamma-ray spectrum calculation with semi-empirical method and some model codes, nuclear data sheets update for $A = 197$ and nuclear high-spin data for $A = 174$, 176 and 178; thermal reactor benchmark testing of CENDL-2 and ENDF/B-6, the status of CENDL-2.1 and progress on Chinese Evaluated Nuclear Parameter Library, activities and cooperations on nuclear data in China in 1995.

We hope that our readers and colleagues will not spare their comments, in order to improve the publication

Please write to Drs. Liu Tingjin and Zhuang Youxiang
Mailing Address: China Nuclear Data Center
China Institute of Atomic Energy
P. O. Box 275 (41), Beijing 102413
People's Republic of China
Telephone 86-10-69357729 or 69357830
Telex: 222373 IAE CN
Facsimile 86-10-6935 7008
E-mail: CIAEDNP@BEPC2.IHEP.AC.CN

EDITORIAL BOARD

CONTENTS

I EXPERIMENTAL MEASUREMENT

Progress on Measurement of (n,x) Cross Sections at HST in 1995

Ye Bangjiao Wang Zhongmin Fan Yangmei
Han Rongdian Yu Xiaoqi Du Huaijiang

(Department of Modern Physics, Univ.
of Sci. and Tech. of China)

1 The Measurement of Energy Spectrum and Angular Distributions of Protons Emission from Reaction induced by 14.6 MeV Neutron Bombarding Stainless Steel

This experiment has been performed at Univ. of Sci and Tech of China, Hefei (HST) by using multitelescope system[1]. 14.6 MeV neutrons were produced by 150 keV Cockcroft–Walton accelerator. The 1Cr 18Ni 9Ti (type 321) stainless steel target with 0.8 mm thick and 40 mm height was used. The elemental composition of type 321 stainless steel is given in Table 1.

Table 1 Elemental composition of type 321 stainless steel target

Element	Fe	Cr	Ni	Mo	Mn	Si	Co	Ti	C	S	W	P
Wt %	70.298	18.4	9.2	0.033	1.38	0.48	0.032	0.012	0.1	0.004	0.030	0.031

The target (in multitelescope system) was irradiated about 40 h with a neutron source strength $\sim 1.5 \times 10^9$ n / s. During the entire experiment, the background telescope was equipped with a weak ^{241}Am α–source. This telescope was used to monitor the energy calibration of the CsI(Tl) crystal. The stability of the entire measuring system was checked continually by monitoring all the important single counter rates. The target foil was rotated 180 deg. at the

midpoint of the experiment to reduce the asymmetry effects of the two different halves of the reaction chamber. The total number of true events turned out to be ~84000.

Data analysis processes are similar to that of Ref. [2]. The double differential proton emission cross sections for type 321 stainless steel (n,xp) reaction have been obtained in 16 angles from 24 to 165 deg. The errors consist of statistical error and all identified systematic errors. The statistical error corresponds to 1 σ and the total systematic error is 6.2%. The angle-integrated proton emission cross sections were derived from least-squares fitting the double differential data with Legendre polynomials. This is shown in Fig. 1. Because stainless steels are complex, the theoretical calculations are very difficult. So present result has not been compared with calculation. The total proton emission cross section for proton energy >2 MeV is 229 ± 16 mb

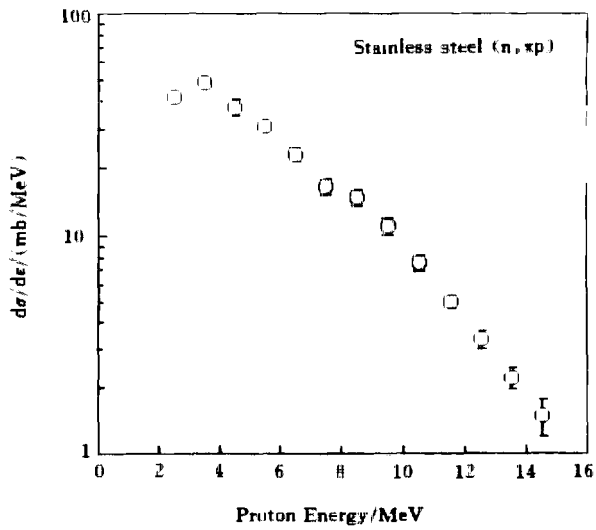

Fig. 1 Proton spectra from the type 321 stainless steel (n,xp) reaction

2 The Energy Calibration of the CsI(Tl) Crystal for α-Particles

In order to measure cross sections of (n,xα) reaction, the HST multitelescope system must be calibrated for alpha particles. This was done once several years ago[3], but now the work voltage of CsI(Tl) crystal and electronics system have been changed much. Due to nonlinearity of the energy respond to α-particles, CsI(Tl) crystal must be carefully calibrated. Based on this

aim, 32 weak ^{241}Am α–sources have been used in this system. Each chamber is equipped with an α–source. Different thickness of Al foils are used to change the energy of α–particles. Besides, the energy data used for the calibration in Ref. [3] are also adopted after normalizing these data to ^{241}Am α–sources. All data used for the calibration is listed in Table 2. When pass through 97 mm length of 5% CO_2+95% Ar_2 gas mixture at pressure of 100 mPa, α–particle energy loss is 0.834 MeV. So in this table, the energy of ^{241}Am α–particles is 4.652 MeV instead of 5.486 MeV.

Table 2 The energy of α–particle used for the calibration

	^{239}Pu α–source		^{241}Am α–source			$^{3}T(d,n)^{4}He$		$^{6}Li(d,\alpha)^{4}He$		
Al foil thick / μm	11	1	6.2	7.7	—	1	31	21	11	1
Energy / MeV	3.07	4.97	3.269	3.473	4.652	3.30	7.87	9.05	10.1	11.1
Channels	15.6	31.2	16.3	18.0	28.7	17.8	61.0	71.4	84.5	93.8

Because the energy respondence of CsI(Tl) crystal for α–particles is non–linear at $E_\alpha < 8$ MeV and linear at $E_\alpha > 8$ MeV, the calibration curve consists of two parts : in $E_\alpha < 8$ MeV region, all data are fitted with 4 order polynomial and in $E_\alpha > 8$ MeV region only 4 higher energy data are used to fit with linear function. Fig. 2 shows the result, which has been used in measurement of $^{Nat}Ni(n,x\alpha)$ reaction cross sections.

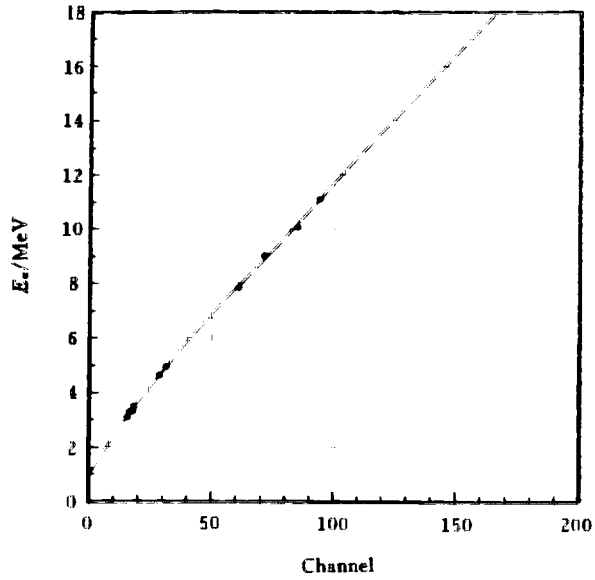

Fig. 2 The energy calibration curve of α–particle for HST multitelescope system

3 Progress on Measurement of $^{Nat}Ni(n,x\alpha)$ Reaction Cross Sections

In 1995 the data acquirement has been performed for the measurement of double differential α–particles emission cross sections of $^{Nat}Ni(n,x\alpha)$ reaction. The natural nickel target with 0.5 mm thick and 40 mm height was used. 16 telescopes were used for Ni targets, which were fixed in the ringlike Pb holder, and the other 16 telescopes were used for simultaneous measurement of the background. Pb was used for the target holder and background–measuring material because it has very small cross sections of (n,α) reaction. The proportional counters were operated with a gas mixture of 5% CO_2+95% Ar_2 at pressure of 100 mPa and voltage of −740 V.

20 cm Fe was used to shield CsI(Tl) from neutrons. The distance between neutron source (T–Ti target) and CsI(Tl) is 400 mm. The whole system was irradiated for about 160 h with a neutron source strength $\sim 2 \times 10^9$ n / s

The data analysis will be finished in the near future.

References

[1] Ye Bangjiao et al., CNDP, 10, 19(1993)

[2] Ye Bangjiao et al., Nucl. Sci. Eng., 117, 67(1994)

[3] Ye Bangjiao, Ph. D thesis, HST, 42(1992)

II THEORETICAL CALCULATION

Progress on Study of Nuclear Data Theory and Related Fields at the Theory Group of CNDC

Ge Zhigang

(China Nuclear Data Center, CIAE)

The theory group of CNDC has made a lot of progress in nuclear reaction theory and its application as well as many other related fields in 1995. The recent progress in those fields are presented as the following.

1 Nuclear Reaction Theory Study and Its Applications

1.1 Consistent Dynamic and Statistical Description of Fission and Comparison

(See paper 2.4 of this issue)

1.2 Transition Between the P and Q Chains in FKK Theory

Recently a major development in FKK is considered as the flux reduced by the direct inelastic reaction, and transition from scattering states (P chains) to bound states (Q chains) beyond the initial states.

The original FKK theory considered the P and Q chains remain distinct after the initial interaction, the transition between the P and Q chains are small and average out, but many subsequent analyses show that MSC cross sections are too large compared with experimental data.

The fluctuating component of the transition matrix element T_{fi} is given by

$$T_{fi}^{MSC} = \langle \psi_f^{(-)} \mid V_{PQ} \frac{1}{1_E - h_{PP}} V_{QP} \mid \psi_i^{(+)} \rangle$$

where the wave function can be expressed by Lippman–Schwinger equation :

$$| \psi_{i,f}^{(\pm)} > = | \varphi_{i,f}^{(\pm)} > + \frac{1}{E^{(\pm)} - H_{\mathrm{OPT}}} v \, | \varphi_{i,f}^{(\pm)} >$$

where v is off–diagonal component of H_{OPT}, and satisfies $(E^{(\pm)} - H_{\mathrm{OPT}}^{(\mathrm{D})}) \, | \varphi_{i,f}^{(\pm)} \geqslant 0$. Where $H_{\mathrm{OPT}}^{(\mathrm{D})}$ is diagonal component of H_{OPT} In the original paper, the wave function is approximated by its first term. If complete expression is considered, additional three terms are obtained, the three terms describe transition between P and Q chains beyond initial interaction, in other words, at each stages of the P chain P to Q transition takes place This is called gradual absorption model

The optical model reaction cross sections are accounted for all flux removed from the elastic channel However the removed flux feeds not only the bound, compound states of the MSC reaction chain but also the direct inelastic reaction Therefore to calculate the MSC and the CN cross sections the optical model absorption has to be reduced by the amount of the direct inelastic reactions So that the fraction feeding of the MSC reaction chain is R ($R<1$), the fraction reduced by direct inelastic reaction is ($1-R$) Gradual absorption splits R into the partial Rm's that describe feeding of separate reaction stages m.

By using the scheme mentioned above, the computer program has been made and the calculated results were compared with experimental data. The results show that after considering transition from P to Q chains MSC cross sections are lower and CN cross sections are greater than the former analyses and better agreement was obtained

1.3 Systematics of Nucleon–Nucleon Total, Elastic and Inelastic Scattering Cross Sections and Elastic Scattering Angular Distributions up to 10 GeV

Based on a large amount of the experimental data, the systematics of n–p or p–n, n–n or p–p total, elastic and inelastic scattering cross sections and elastic scattering angular distributions up to 10 GeV have been obtained For n–p or p–n interaction, the cross section systematics formula are as follows

$$\sigma_{\mathrm{el}} = 9.9958 - 0.0020726 U_0^{-1.5} + 2.7903 U_0^{-1} + 0.29492 U_0^{-0.5}$$

$$-0.13088U_0^{0.5}+0.021252U_0+633.36\ \exp\left[-109.89U_0^{0.9439}\right]$$
$$+3.0101\ \exp\left[-0.57247\ (U_0-0.2127)^2\right]$$
$$-1548.4\ \exp\left[-0.79448\times10^7\ (U_0-0.0005)^2\right],$$
$$\text{For } 0.001\ \text{GeV}\leqslant E_n\leqslant 10\ \text{GeV} \tag{1}$$

$$\sigma_{in}=\frac{29.444U_1^{2.0628}}{0.041667+U_1^{2.0727}}\Theta(U_1)\quad \text{For } E_n\leqslant 10\ \text{GeV} \tag{2}$$

$$U_0=\sqrt{s}-(m_1+m_2)$$

$$U_1=\sqrt{s}-(m_1+m_2+m_\pi)$$

$$\sqrt{s}=\left[m_1^2+m_2^2+2m_2(m_1+E_L)\right]^{1/2}$$

Here, $\sqrt{s}$ represents the energy of the two nucleons system. $\Theta(U_1)$ is step function.

The comparisons between the calculated results and the experimental data show that our systematics can reproduce the experimental data pretty well.

1.4 Properties of Hot Nuclear and Neutron Matter in a Relativistic Hartree–Fock Theory

It is very interesting to investigate hadronic matter at various temperatures and densities. To study the equation of state for hot hadronic matter is an important subject in the context of heavy–ion reactions. Walecka's model is quite useful for studying various nuclear and neutron properties at different temperatures and densities based on relativistic quantum field theory and field dynamics. In this work the temperature–dependent relativistic Hartree–Fock equations for an infinite system of mesons and baryons have been obtained on the basis of the thermofield dynamics and Walecka's model. The equations have been applied to nuclear and neutron matter. The Hartree–Fock binding energy, the self–consistent nucleon spectrum, the effective mass and Schrodinger equivalent optical potential have been studied.

1.5 Effective Nucleon–Nucleon Cross Sections Based on Skyrme Interactions

A major goal in the study of intermediate–energy heavy–ion collisions is to measure the time evolution process of nuclear matter under violet collisions as well as nuclear properties under extreme conditions of high density and temperature. However, the interesting information on these problems can only be obtained indirectly through certain theoretical model. Thus one has to choose a good theoretical tool, which should be as general and basic as possible on the one hand and as practicable as possible on the other hand. At present, there exist various approaches to this subject; the most ambitious one is to obtain the transport equation starting from the time–dependent G–matrix theory. In this approach the time evolution of the heavy–ion collision process is described by a kinetic equation, the G matrix serves as a dynamical input of two–body interaction. It would be more practical to take the effective interaction rather than the G matrix as the transport model for heavy–ion collision. In this work we obtain a self–consistent Boltzmann–Uehling–Uhlenbeck approach which is used to study heavy–ion collisions based on the effective Skyrme interactions, and reproduced empirical optical potentials. The temperature and density dependence of the effective elastic cross section in nuclear matter have been studied. Because of the fundamental assumption of the temperature independence of the effective Skyrme interaction and the limitation due to the zero–range force used, our results might be considered to be reasonable for $T \lesssim 10$ MeV and for kinetic energies $E_p \lesssim 120$ MeV.

2 Chinese Evaluated Nuclear Parameter Library (CENPL)

(See paper 5.3 of this issue)

3 The Nuclear Data Calculation and Related Code Development

3.1 Calculation of Various Cross Section for n+^{169}Tm Reaction in Energy Range up to 100 MeV

The activation products ^{168}Tm (half life is 93.1 d), ^{167}Tm (half life is 9.25 d), ^{166}Tm (half life is 7.7 h), and ^{165}Tm (half life is 30.06 h) can be produced from n+^{169}Tm reaction through (n,2n), (n,3n), (n,4n) and (n,5n) reactions, respectively. In order to determine the neutron optical potential parameters for n+^{169}Tm reaction in the energy region up to 100 MeV, more neutron experimental data of ^{169}Tm, some inelastic scattering cross sections of W and Pb, and some total cross sections of neighboring nucleus ^{165}Ho above 20 MeV were

used. Then various cross sections of n+^{169}Tm reaction were calculated. The calculated results show that the activation products $^{168, 167, 166, 165}$Tm are important neutron monitor reaction products for n+^{169}Tm reaction in energy range up to 100 MeV.

3.2 Theoretical Calculation of n+^{59}Co Reaction in Energy Region up to 100 MeV

(See paper 2.3 of this issue)

3.3 Calculation of Neutron Monitor Reaction Cross Sections of ^{90}Zr in Energy Region Up to 100 MeV

(See paper 2.8 of this issue)

3.4 Calculations of the Production Rate of Radioactive Nuclear Beam Induced by 70 MeV Protons on ^{72}Ge Target

The intensive beam proton cyclotron is adopted in Beijing Radioactive Nuclear Beam Facility designed by China Institute of Atomic Energy. This facility is designed with a maximum proton energy of 70 MeV and a intensity of 200 μA. The production rate [atoms / (s μA)] of radioactive nuclear beam induced by 70 MeV protons on ^{72}Ge target were calculated. Since the calculated (p,n), (p,2n), (p,3n), and (p,nα) cross sections of ^{72}Ge are in good agreement with the experimental data, the calculated production rate of radioactive nuclear beam is reliable. The calculated results are as follows :

Reaction	$T_{1/2}$	Zr_5Ge_3	^{72}Ge
^{72}Ge(p,n)^{72}As	1.1 d	0.100×10^{11}	0.298×10^{11}
^{72}Ge(p,2n)^{71}As	2.7 d	0.150×10^{11}	0.449×10^{11}
^{72}Ge(p,3n)^{70}As	52 m	0.590×10^{10}	0.177×10^{11}
^{72}Ge(p,4n)^{69}As	15.2 m	0.934×10^{9}	0.280×10^{10}
^{72}Ge(p,2p3n)^{68}Ga	67.3 m	0.429×10^{10}	0.129×10^{11}

3.5 Improvement of UNF Code Series

A version of UNF code, used for the light nuclei, has been developed, and related works on the improvement of UNF code series were made in 1995.

Progress on Nuclear Data Work at Nankai University in 1995

Cai Chonghai Yu Ziqiang Zuo Yixin

(Nankai University, Tianjin)

In 1995, we finished two nuclear model calculation programs CCRMN and OMHF, further improved the optical model parameters library, and made very significant progress in the theoretical research on quantum molecular dynamics (QMD).

1 Research and Making of Nuclear Model Programs

1.1 Code CCRMN

(See paper 2.5 of this issue)

1.2 Code OMHF

An optical model program with Hauser–Feshbach statistical theory, in addition to the total, absorptive, shape elastic cross section and its angular distribution, it can also calculate the compound–nucleus elastic scattering cross section and its angular distribution. The projectile can be n, p, t, ^{3}He, d and α.

2 Improvement of Optical Model Parameters Library

(See paper 5.3 of this issue)

3 The Research Work on QMD Theory

1 The nuclear equation of state was derived. The nuclear force parameters for normal nuclear matter property was established.

2 The collision cross sections of two particle (N–N or N–Δ) in the collision term were given by BUU (Boltzman–Uehling–Uhlenbeck) theory.

3. The mechanizm of the formation of nuclear fragments was investigated and their probabilities were calculated. Also the excited energy of the residual-fragment through evaporating some light particles in de-excitation was calculated.

Theoretical Calculation of n+^{59}Co Reaction in Energy Region up to 100 MeV

Shen Qingbiao Yu Baosheng Cai Dunjiu

(China Nuclear Data Center, CIAE)

Abstract

A set of neutron optical potential parameters for ^{59}Co in energy region of 2 ~ 100 MeV was obtained based on concerned experimental data. Various cross sections of n+^{59}Co reactions were calculated and predicted. The calculated results show that the activation products $^{58,\ 57}$Co, ^{59}Fe, and ^{56}Mn are main neutron monitor reaction products for n+^{59}Co reaction in energy range up to 100 MeV. ^{54}Mn production reaction can be a promising neutron monitor reaction in the energy region from 30 to 100 MeV.

Introduction

The activation products ^{58}Co (half life is 70.82 d), ^{57}Co (half life is 271.80 d), ^{56}Co (half life is 77.2 d), ^{59}Fe (half life is 44.496 d), ^{56}Mn (half life is 2.5785 h), ^{54}Mn (half life is 312.12 d), and ^{52}Mn (half life is 5.591 d) can be produced from n+^{59}Co reaction. $^{58,\ 57,\ 56}$Co can be produced through (n,2n), (n,3n), (n,4n) reactions, respectively. ^{59}Fe can be obtained through (n,p) reaction. ^{56}Mn can be produced through (n,α), (n,2n2p), (n,npd), (n,2d), (n,n^{3}He), and (n,pt) reactions, ^{54}Mn can be produced through (n,2nα), (n,4n2p), (n,3npd), (n,2n2d), (n,3n^{3}He), (n,2npt), (n,ndt), and (n,2t) reactions; ^{52}Mn can be produced through (n,4nα), (n,6n2p), (n,5npd), (n,4n2d), (n,5n^{3}He), (n,4npt),

(n,3ndt), and (n,2n2t) reactions.

In order to determine the neutron optical potential parameters for n+^{59}Co reaction in the energy region up to 100 MeV, more neutron experimental data of ^{59}Co and some total and nonelastic scattering cross sections of neighboring nucleus Cu above 20 MeV were used. Then various cross sections of n+^{59}Co reaction were calculated. If the calculated results were in pretty agreement with the existed experimental data, the production cross sections of the activation products mentioned above can be predicted.

In Sec. 1, the theories and parameters used in our calculations are described. The calculated results and analyses are given in Sec. 2. Finally, a summary is given in Sec. 3.

1 Theories and Parameters

The calculation was made with the program SPEC[1] including the first to the sixth particle emission processes. In this program, the optical model, evaporation model, and exciton model are included. The preequilibrium and direct reaction mechanisms of γ emission[2] are also included in program SPEC. The direct inelastic scattering cross sections were obtained by the collective excitation distorted-wave Born approximation[3]. The compound-nucleus elastic scattering contributions were calculated by Hauser-Feshbach model. The calculations of the production cross sections of ^{54,52}Mn were made by program CCRMN[4] including the first to the tenth particle emission processes, the others were made by program SPEC. Thus all reaction channels mentioned above were included in our calculations.

For composite particle emissions, the pick-up mechanism of cluster formation[5~7] was included in the first and second particle emission processes.

Firstly, based on various neutron experimental data of ^{59}Co and neighboring nucleus Cu from EXFOR library and recent information a set of optimum neutron optical potential parameters in energy region 2~ 100 MeV was obtained as follows:

$$V = 53.3398 - 0.26759E + 0.00008938E^2 - 24.0(N-Z)/A \quad (1)$$

$$W_S = \max\{0,\ 10.6945 - 0.08068E - 12.0\,(N-Z)/A\} \quad (2)$$

$$W_V = \max\{0,\ -2.45323 + 0.18447E - 0.0008014E^2\} \quad (3)$$

$$U_{SO} = 6.2 \quad (4)$$

$$r_r = 1.18156,\ r_S = 1.21528,\ r_V = 1.22334,\ r_{SO} = 1.18156 \quad (5)$$

$$a_r = 0.76703,\ a_s = 0.51985,\ a_v = 0.68083,\ a_{so} = 0.76703 \qquad (6)$$

The Gilbert–Cameron level density formula[8] is applied in our calculations, and the exciton model constant K is taken as 700 MeV^3.

2 Calculated Results and Analyses

Fig 1 shows the comparison of neutron total cross sections between the calculated values and the experimental data in the energy region 2~100 MeV for n+^{59}Co reaction. The theoretical values are in good agreement with the experimental data. Figs. 2 and 3 show that the calculated neutron elastic and nonelastic cross sections are in good agreement with the experimental data for n+^{59}Co reaction. The calculated neutron inelastic scattering cross sections of ^{59}Co are shown in Fig. 4. Fig. 5 gives the comparison of calculated and experimental (n,2n) cross sections of ^{59}Co. They are basically agreement with the experimental data.

The experimental data and calculated results show that the larger values of (n,2n) cross sections producing ^{58}Co are lying in 13~30 MeV energy region; for (n,3n) reaction producing ^{57}Co in 23~40 MeV energy region; for (n,p) reaction producing ^{59}Fe in 6~25 MeV energy region. The larger values of (n,4n) cross sections producing ^{56}Co are lying in 40~60 MeV energy region, but their values are much smaller than others mentioned above.

Fig. 6 shows the calculated $^{56,\ 54,\ 52}$Mn production cross sections for n+^{59}Co reaction in energy range up to 100 MeV. The $^{56,\ 54}$Mn production cross sections for n+^{59}Co reaction in energy range up to 50 MeV were calculated by using program GNASH in Ref. [9] The ^{56}Mn production cross sections below 35 MeV are mainly obtained from (n,α) reaction and our calculated results basically agree with the experimental data. For higher energy region, they come from many reaction channels. The second peak of the ^{56}Mn production cross sections in energy region 45~70 MeV was obtained by our calculation, but it does not appear in Ref. [9] since only (n,α) and (n,2n2p) channels were included in their calculation The first and second peaks of the ^{54}Mn production cross sections appear in 30~50 and 70~100 MeV energy regions, respectively. The first peak of the ^{54}Mn production cross sections also appears in 30~50 MeV energy region in Ref. [9]. This reaction can be used as a neutron monitor reaction for the long term irradiation purpose in the energy range between 30 and 100 MeV, because the decay data of ^{54}Mn are very well established, and the estimated cross section is large enough From Fig. 6 one can see that the esti-

mated ^{52}Mn production cross sections are much smaller than $^{56,\ 54}$Mn below 100 MeV.

3 Summary

Based on the available experimental data, a set of neutron optical potential parameters for ^{59}Co in energies of 2 ~ 100 MeV was obtained. Then many cross sections for n+^{59}Co reaction were calculated based on optical model, evaporation model, and exciton model. Because the calculated results for many channels are in pretty agreement with the existed experimental data, the predicted production cross sections of the activation products are reasonable.

The calculated results show that the activation products $^{58,\ 57}$Co, ^{59}Fe, and ^{56}Mn are main neutron monitor reaction products for n+^{59}Co reaction in energy range up to 100 MeV. ^{54}Mn production reaction can be a promising neutron monitor reaction in the energy region from 30 to 100 MeV.

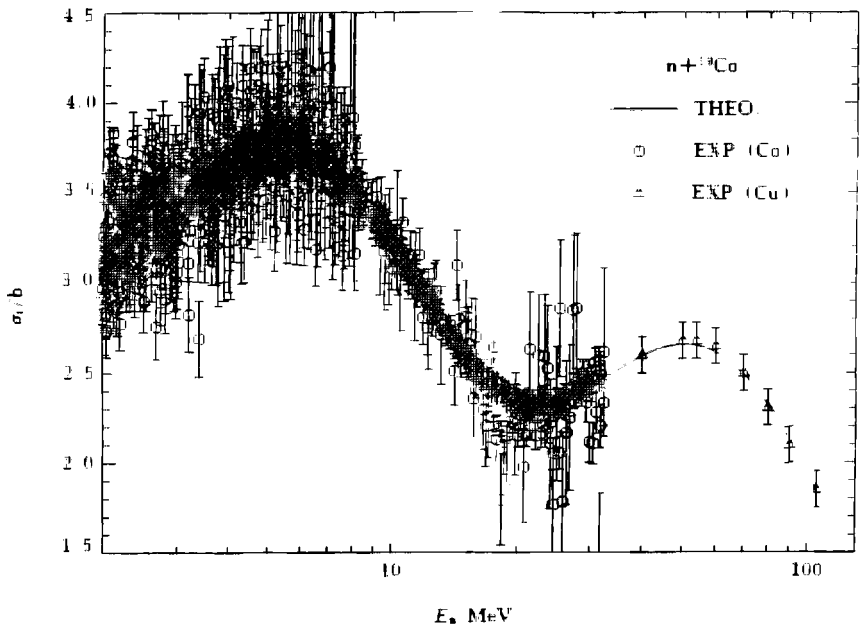

Fig. 1 Neutron total cross sections of ^{59}Co

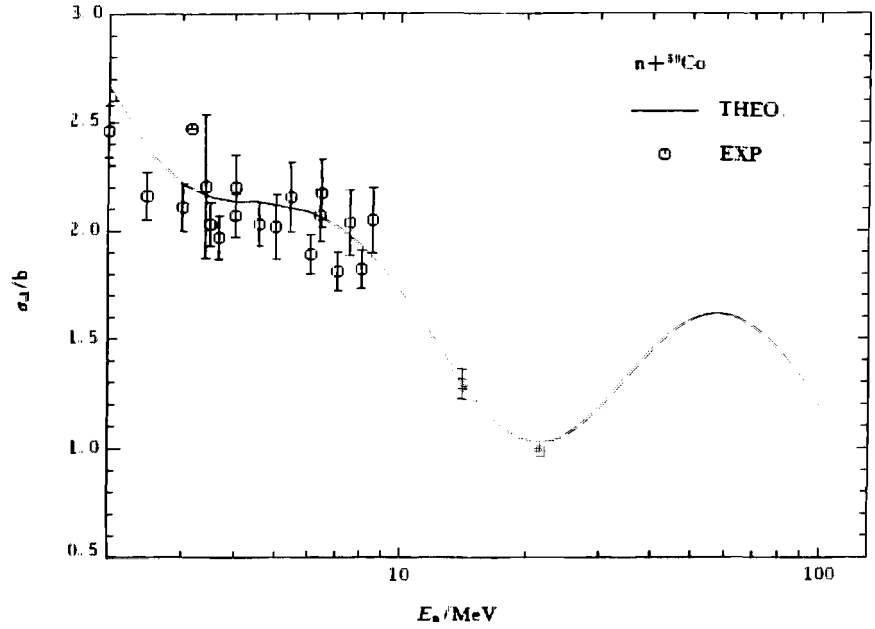

Fig. 2 Neutron elastic scattering cross section of ^{59}Co

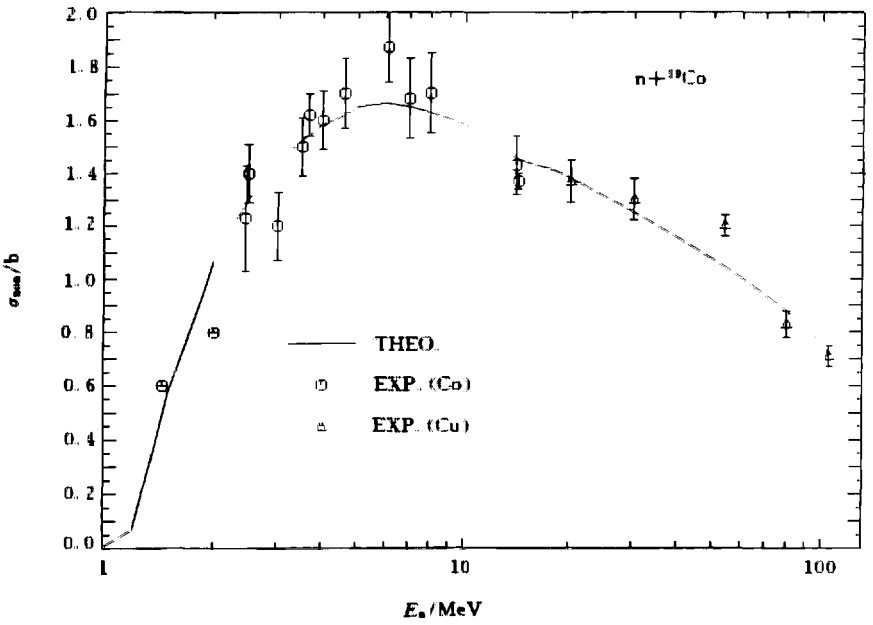

Fig 3 Neutron nonelastic scattering cross section of ^{59}Co

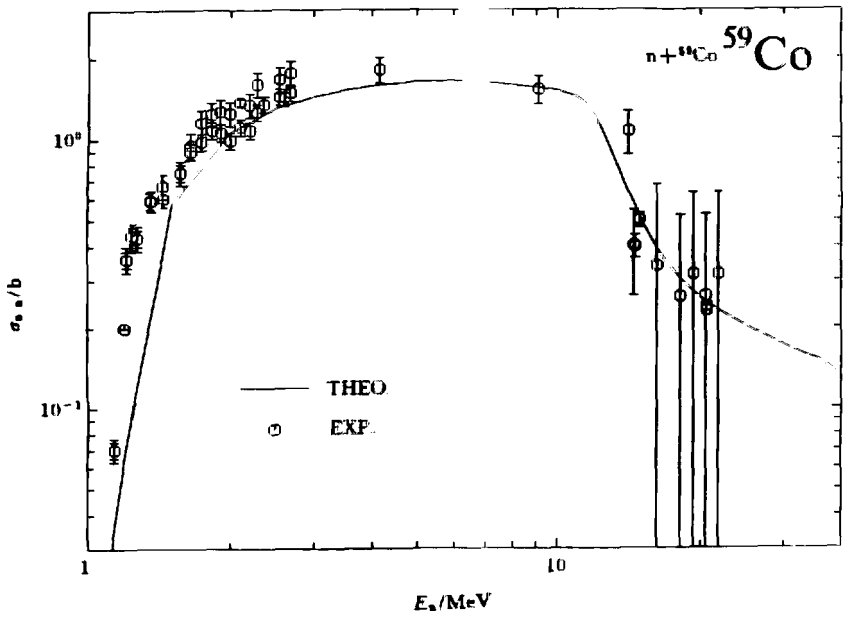

Fig. 4 Neutron inelastic scattering cross section of ^{59}Co

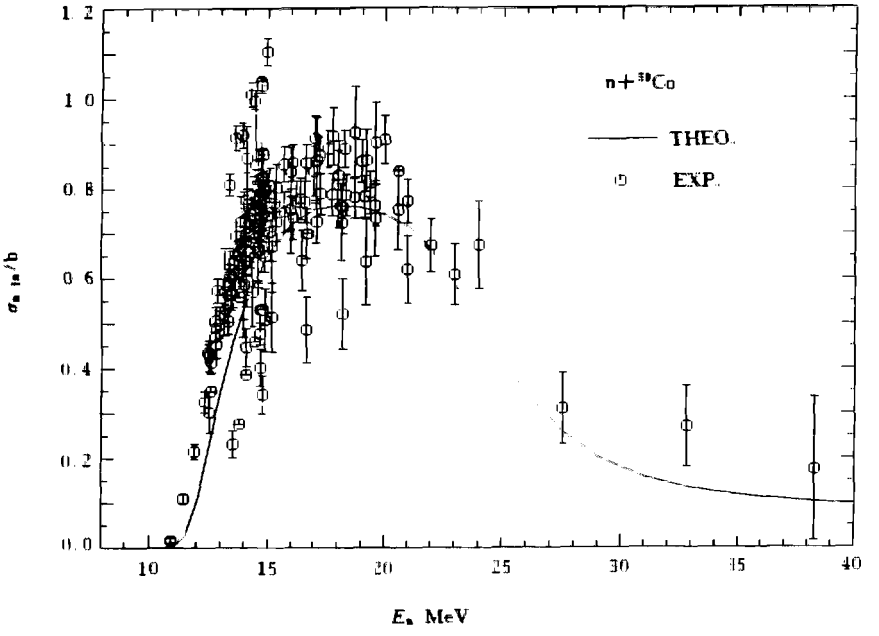

Fig. 5 (n,2n) cross section of ^{59}Co

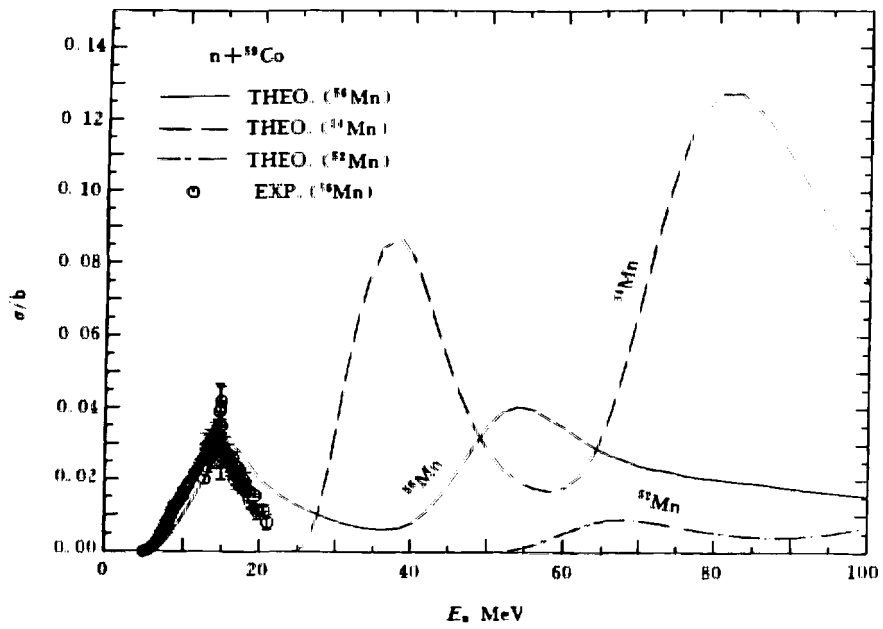

Fig. 6 The calculated $^{56, 54, 52}$Mn production cross sections for n+^{59}Co reaction

References

[1] Shen Qingbiao et al , CNDP, 11, 28(1994)

[2] J. M. Akkermans et al , Phys. Let , 157B, 95(1985)

[3] P. D. Kunz, "Distorted Wave Code DWUCK4", University of Colorado, unpublished

[4] Cai Chonghai et al., CNDP, 15(1996)

[5] A Iwamoto et al , Phys Rev., C26, 1821(1982)

[6] K. Sato et al., Phys. Rev., C28, 1527(1983)

[7] Zhang Jingshang et al , Commun. in Theor. Phys (Beijing, China), 10, 33(1988)

[8] A Gilbert et al., Can J. Phys., 43, 1446(1965)

[9] S. Iwasaki et al., Nuclear Data for Sci. & Tech, Proc Inter Conf., Gatlinburg, Tennessee, May 9~13, p 627, 1994

Consistent Dynamical and Statistical Description of Fission and Comparison

Wang Shunuan

(China Nuclear Data Center, CIAE)

Abstract

The research survey of consistent dynamical and statistical description of fission is briefly introduced. The channel theory of fission with diffusive dynamics based on Bohr channel theory of fission and Fokker–Planck equation and Kramers–modified Bohr–Wheeler expression according to Strutinsky method given by P. Frobrich et al. are compared and analyzed

Within the framework of the Bohr channel theory, and the assumption of that the fission barrier is single–humped as predicted by liquid drop model calculations and that the shape of fission barrier is well approximated by a parabola, the Bohr–Wheeler[1] fission width formula Γ_f^{BW} and Hill–Wheeler[2] fission width formula with quantum penetration of fission barrier Γ_f^{HW} are presented.

As far as it goes that nearly all of the theoretical and experimental research for neutron induced fission are based on information obtained at relatively low incident energies, and the number of neutron induced fission cross section measurements in the energy region above 20 MeV is very small Thus, the statistical model of nuclear fission originally developed by Bohr and Wheeler was for a long time sufficient to describe the observed effects. This model assumes that the thermal equilibrium is kept in all relevant degrees of freedom of the nucleus and that the fission decay rate depends on a particular transition state on saddle point. This theory has been applied to calculate fission cross section and other fission–related quantities for many years up to now.

Recently, using the 800 MeV pulsed proton beam from LAMPF to produce neutron by spallation, the WNR target–4 facility provides a source extending from 100 keV to nearly 800MeV making it possible to perform fission cross section measurements for multiple samples in a single experiment over a broad energy range[3~5]. The neutron data obtained[4] show that the results of

fission cross section calculated by traditional channel theory of fission, i. e., the Bohr–Wheeler or Hill–Wheeler formulas are significantly above the experimental data, and provide completely new information about the fission process and a challenge for theorists to develop a model that can describe the behaviors of the fission cross sections at the energy above 20 MeV to nearly 800 MeV. Actually, for neutron induced reactions on U, Pu elements, some discrepancy between theoretical calculation (higher than the experimental data) given by traditional channel theory of fission with enhancement effects of level density on saddle point and experimental data above 15 MeV has been obviously seen[6]. The theoretical one is somehow higher than the experimental data. It turned out however in the recent years that not only in describing the rise of precision neutron multiplicity with increasing bombarding energy observed in heavy-ion induced fission reaction[7], but also in describing behaviors of fission cross section induced by neutron on actinide nuclides at energy above 20 MeV to 1000 MeV [3~5], the standard or traditional statistical Bohr–Wheeler or Hill–Wheeler formula fails. It was realized that one has to include dynamical effects in the description of fission for higher energy excited nuclei, in particular one has to introduce the concept of nuclear friction as considered in Refs. [8, 9].

In order to understand the fission cross section behaviors at the energy range above 20 MeV by neutron induced reactions on actinides, the channel theory of fission with diffusive dynamics is proposed based on Bohr channel theory of fission and Fokker–Planck equation in the way of dynamical and statistical consistent description of fission for excited nuclei[10]. The influence of the details of fission process for nucleus deforming from its ground state to saddle point is properly taking into account in fission width calculation.

The fission width formula Γ_f^{WSN} based on channel theory of fission with diffusive dynamics is described and analyzed in detail in Ref. [10].

There are some other fission width calculations in consistent dynamical and statistical descriptions. In order to make an analysis and a comparison among them, other two fission width expressions are introduced in the present paper. The other two are so called Kramers–modified Bohr–Wheeler expressions according to Strutinsky method[11] given in Refs. [12~14]. Read as the following respectively:

$$\Gamma_f^{KMBW}(E)=\frac{\hbar\omega_{gs}}{kT}\ \Gamma_f^{BW}(E)\ \left[\ \left(\ 1+\frac{\beta^2}{4\omega^2}\ \right)^{\frac{1}{2}}-\frac{\beta}{2\omega}\ \right]$$

for over damped case, i. e., for large friction coefficient β case, the expression

shown above can be reduced as :

$$\Gamma_f^{KMBWR}(E)=\frac{\omega h\omega_{gs}}{\beta kT}\Gamma_f^{BW}(E)$$

Here, the quantities ω and ω_{gs} are the frequencies at the saddle point and at the ground state, respectively.

In the interests of making a comparison among fission width calculation expressions

$$\Gamma_f^{WSN},\ \Gamma_f^{BW},\ \Gamma_f^{KMBW},\ \Gamma_f^{KMBWR}$$

introduced above respectively in the present paper, the n+^{238}U reaction has been taken as an example, in the range of excitation energy below 80 MeV. In the calculation, level densities ρ_c and ρ_f take the form of Gilbert–Cameron, but for ρ_f the level density parameter a_f decreasing as excitation energy increasing is considered, $V_f=6.22$ MeV, $h\omega=0.5$ MeV, $h\omega_{gs}=1$ MeV are adopted. The friction coefficient varies from 0 to 300×10^{20} s^{-1} and kT varies from 0.5 to 3 MeV to see how their sensitivities are, although the varying ranges are not so reasonable. For example, as we known that kT should be taken as a function of excitation energy of the system according to the Fermi gas model[15]. As regards to taking the value of friction coefficient,there are many ways to get it, such as by fitting the pre–scission neutron multiplicities and fission probabilities[14, 16] or by the study of the proximity one–body dissipation or two–body viscosity as well as wall formula[17] and so on, which have been discussed in many papers. Since it is still not possible to reproduce with the same value of friction coefficient for neutron multiplicities and fission probabilities, therefore, in the present paper the general varying range of the friction coefficient used is chosen between zero and 300×10^{20} s^{-1}.

It is clear for Γ_f^{WSN} that when β goes to zero Γ_f^{WSN} is the exact Γ_f^{BW}, but for Γ_f^{KMBW} that when β goes to zero it is not the exact Γ_f^{BW}.

Fig. 1 shows the calculated results for $\beta=20\times10^{20}$ s^{-1}, $kT=0.5$ MeV, in which the solid line is for Γ_f^{WSN} or Γ_f^{BW}, the dashed line is for Γ_f^{KMBW}, the dotted line is for Γ_f^{KMBWR}. It is clear in this case that there is almost no difference between Γ_f^{WSN} and Γ_f^{BW}, and among them there are some differences but not much.

Fig. 2 shows the calculated results for $\beta=300\times10^{20}$ s^{-1}, $kT=3$ MeV, in which the solid line is for Γ_f^{BW}, the dashed line is for Γ_f^{WSN}, the dotted–dashed line is for Γ_f^{KMBW} or Γ_f^{KMBWR}.

It seems that in the varying range of friction from zero to $300\times$

10^{20} s^{-1} and kT from 0.5 to 3 MeV, Γ_f^{KMBW} or Γ_f^{KMBWR} and Γ_f^{WSN} present too much and too small differences from Γ_f^{BW}, respectively. It means that there is still some hard work to do in the way of consistent dynamical and statistical description of fission.

As far as we can see, it seems that the consistent dynamical and statistical description of fission introduced above with physical reasonable value of friction coefficient could be possible to be applied to understand the behaviors of fission cross section induced by neutron on actinides in high energy range (above 20 MeV to 1000 MeV) as analyzed in Ref [18].

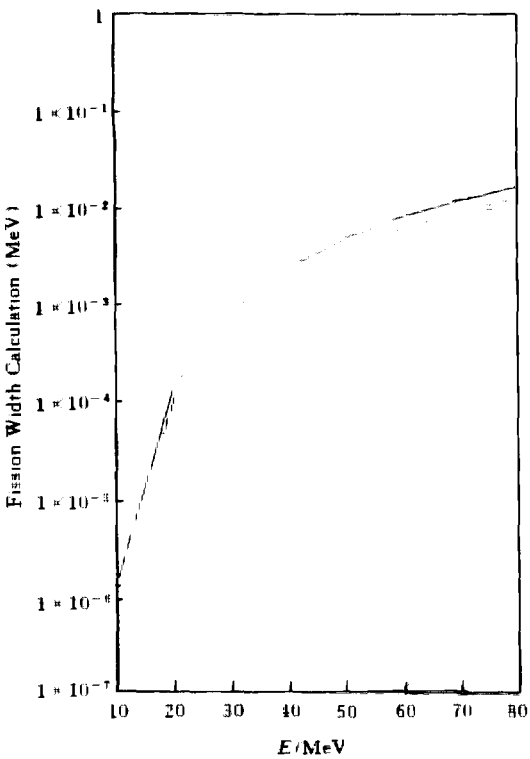

Fig. 1 Fission width (MeV)
$\beta = 20 * 10^{20}$ s^{-1}, $kT = 0.5$ MeV

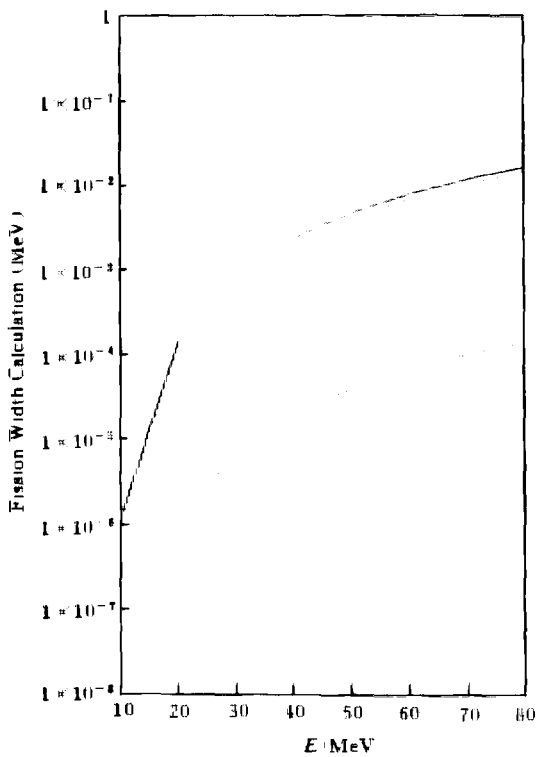

Fig. 2 Fission width (MeV)
$\beta = 300 * 10^{20}$ s^{-1}, $kT = 3$ MeV

References

[1] N. Bohr and J. A. Wheeler, Phys. Rev., 56, 426(1939)

[2] D. L. Hill, J. A. Wheeler, Phys. Rev., 89, 1102(1953)

[3] P. W. Lisowski et al., Nucl. Sci. and Eng., 106, 208(1990)

[4] A. D. Carlson et al., NEANDC-305 "U"

References

[5] J. P. Lestone et al., Phys. Rev. C, Vol. 49, 372(1994)
[6] Yan Shiwei et al., CNDP No. 12, p. 14(1994)
[7] J. O. Newton et al., Nucl. Phys. A, 483, 126(1988)
[8] J. O. Newton, Sov. J. Part. Nucl. 21, 349(1990)
[9] D. J. Hinde et al., Nucl. Phys. A502, 497c (1989)
[10] Wang Shunuan, IL NUOVO CIMENTO, 107, 299(1994)
[11] V. M. Strutinsky, Phys. Lett. B47, 121(1973)
[12] N. D. Mavlitov et al., Z. Phys. A, 342, 195～198 (1992)
[13] I. I. Gontchar et al., Phys. Rev. C, Vol. 47, No. 47, 2228(1993)
[14] P. Frobrich et al., Nucl. Phys. A556, 281～306(1993)
[15] D. Brink, Nucl. Phys., A519, 3c—16c(1990)
[16] P. Frobrich et al., Nucl. Phys. A563, 326(1993)
[17] G. D. Adeev et al., Sov. J. Part. Nucl. 19, 529(1988)
[18] J. P. Lestone et al., Phys. Rev. C, Vol. 49, 372(1994)

Calculation Methods in Program CCRMN

Cai Chonghai

(Department of Physics, Nankai University, Tianjin)

Shen Qingbiao

(China Nuclear Data Center, CIAE)

CCRMN is a program for calculating complex reactions of a medium—heavy nucleus with six light particles. In CCRMN, the incoming particles can be neutrons, protons, ^{4}He, deuterons, tritons, and ^{3}He. All reactions including the first, second, third, ···, up to tenth emitting processes can be calculated. CCRMN is valid in 1～100 MeV energy region, it can give correct results for optical model quantities and all kinds of reaction cross sections. The emitted particles are all the foregoing six kinds of particles in first, second and third emitting processes; neutrons, protons, ^{4}He and deuterons in fourth and fifth

processes; neutrons, protons and ^{4}He in sixth and seventh processes; and only neutrons and protons in eighth, ninth and tenth processes.

1 Function of CCRMN

The output data of CCRMN include total cross section; elastic scattering cross section and its angular distribution; total reaction (or nonelastic) cross section; radiative capture cross section[1,*]; (x,x′) reaction cross section and (x,x_1x_2) reaction cross section, where x, x_1 and x_2 can be neutron, proton, ^{4}He, deuteron, triton or ^{3}He, $\sigma_{x,2np}$, $\sigma_{x,3n}$, $\sigma_{x,4n}$, ···, $\sigma_{x,10n}$.

To compare with experimental data conveniently, the sum of the cross sections of all reactions that lead to the same residual nucleus is given, usually it is called as the isotope yields cross sections, for example, $\sigma_{2n1p} = \sigma_{x,2np} + \sigma_{x,nd} + \sigma_{x,t}$. The total cross section of emitted particle y is given in reactions (x,y), (x,yx'), (x,x'y), (x,yx_1x_2), (x,x_1yx_2), (x,x_1x_2y), ···, (x,yx_1 ··· x_9), (x,x_1yx_2 ··· x_9), ···, (x,x_1x_2 ··· x_9y) in the first, second, third, ···, up to tenth processes, no matter what particles x′, x_1, x_2, ···, x_9 are, where y can be neutron, proton, ^{4}He, deuteron, triton or ^{3}He. For example,

$$\sigma_{x,p\cdots} = \sigma_{x,p} + \sigma_{x,2p} + \sigma_{x,3p} + \cdots + \sigma_{x,10p} + \sigma_{x,px'} + \sigma_{x,x'p} + \cdots + \sigma_{x,px_1x_2\cdots x_9} + \sigma_{x,x_1px_2\cdots x_9} + \cdots + \sigma_{x,x_1x_2\cdots x_9p} + \sigma_{x,2px} + \sigma_{x,x'2p} + \cdots,$$

$$\sigma_{x,p\cdots tot} = \sigma_{x,p} + 2\sigma_{x,2p} + 3\sigma_{x,3p} + \cdots + 10\sigma_{x,10p} + \sigma_{x,px'} + \sigma_{x,x'p} + \cdots + \sigma_{x,px_1x_2\cdots x_9} + \sigma_{x,x_1px_2\cdots x_9} + \cdots + \sigma_{x,x_1x_2\cdots x_9p} + 2\sigma_{x,2px} + 2\sigma_{x,x'2p} + \cdots,$$

$$m_{x,p\cdots} = \sigma_{x,p\cdots tot} / \sigma_{x,p\cdots},$$

where x′, x_1, x_2, ··· , or x_9 is not equal to p. $\sigma_{x,p\cdots}$ is called as inclusive cross section, and $m_{x,p\cdots}$ as the multiplicity of $\sigma_{x,p\cdots}$ corresponding to emitted particle p. All nuclear data are given for the natural element as well as for its isotopes. In CCRMN, one element can consist of six isotopes at most, the difference of mass numbers between the heaviest and the lightest isotope should be equal to or less than ten.

2 Theoretical Framework

The CCRMN code is constructed within the framework of the optical model, pre–equilibrium statistical theory based on the exciton model[1], and the evaporation model. In the first, second, and third emitting processes, the pre–equilibrium emission and evaporation are considered, in the fourth to tenth emitting process, only evaporation is considered. For emission of composite particles, the pickup reaction mechanism introduced by Zhang et al [1] is included. In the calculation of state densities for the exciton model, the Pauli principle is considered. All nuclear level densities required in the evaporation model are calculated by the formula of Gilbert and Cameron[2]. The inverse reaction cross sections of the emitted particles used in statistical theory are calculated from the optical model. For gamma–ray emission, in addition to the evaporation, the pre–equilibrium emission is included; and the partial widths are calculated based on the giant dipole resonance model with one or two resonances.

In the optical model calculation, the phenomenological optical potential of Beccetti and Greenless[3] is frequently adopted (the parameters are usually given by a program for automatically searching the optimum optical model parameters). Using CCRMN code, the calculation can be done with microscopic optical potential based on Skyrme force[4] and the phenomenological optical potential calculation with CH89 or CH86 parameters[5] for the neutron and proton channels. The Neumanove methods to solve the radial equation are used. The step length is 0 1 fm, and there are 150 steps in solving the radial equation. The maximum number of fractional waves in the optical model calculation is 60. The Coulomb wave functions used in the optical model are calculated by the continued fraction method[6].

The CCRMN code does not calculate direct reactions, but it can accept direct reaction cross sections calculated by other programs as input for six outgoing channels in the first process. First, the input direct cross sections are subtracted from the total reaction cross section and then they are added to corresponding statistical cross sections.

In CCRMN, the Hauser–Feshbach calculation can not be done, but this program can accept the compound–nucleus elastic scattering cross section and its angular distribution calculated by another program as input data. At the same time, the lower limit of the integration of excited energy in the first emitted process at the emitting channel corresponding to the incoming channel is changed from zero to the first excited level energy.

3 Calculating Methods

The most important difference between CCRMN and other codes is the integral method in the pre-equilibrium and evaporation calculation. In CMUP2[7] and many other programs, arguments in integrand are always kinetic energies of emitted particles, one has to do the innerrest integration corresponding to the last emitted particle at first, and do the outerrest integration corresponding to the first emitted particle at last. So the multifold number of the integration in pre-equilibrium and evaporation calculation is equal to the number of emitted particles. Limited by the computer running time, usually one can do fourfold integration at most, so one can only consider up to fourth emitting process before. In CCRMN, along the approach in the GNASH code[8], through transforming the integral argument from the kinetic energy E_1, E_2, E_3, E_4, ···, of the emitted particle from the first, second, third, fourth, ···, emitting process to the excited energy u_1, u_2, u_3, u_4, ···, of the residual nucleus after the first, second, third, fourth, ···, emitting process, respectively, and inversing the integral sequence from

$$\int\cdots \mathrm{d}u_1\ \mathrm{d}u_2\ \mathrm{d}u_3\ \mathrm{d}u_4\cdots \text{ to } \int\cdots \mathrm{d}u_4\ \mathrm{d}u_3\ \mathrm{d}u_2\ \mathrm{d}u_1$$

one can find a method to change multifold (higher than twofold) integration to twofold integration, and then in principle can do the pre-equilibrium and evaporation calculation up to very high emitting process. To simplify expressions, here the index of channel is omitted at first and let :

E_0 being the kinetic energy of the projectile in the reference frame of centre of mass of the projectile and the target;

E being the excited energy of the compound nucleus formed from target nucleus absorbing the incoming particle;

Z_c, A_c being the charge and the mass number of the compound nucleus in the first emitting process, respectively;

Z_1, A_1 being the charge and the mass number of the compound nucleus in the second emitting process (or of the residual nucleus in the first emitting process), respectively;

Z_2, A_2 being the charge and the mass number of the compound nucleus in the third emitting process, respectively; and so on.

B_1, B_2, B_3, B_4, ··· being the combined energy of the residual nucleus and the outgoing particle in the first, second, third, fourth, ···, emitting processes, respectively;

x_1, x_2, x_3, x_4, ··· being the minimum kinetic energy of the emitted particle at

which the 'inverse cross section' is larger than $5 * 10^{-7}$ b in the first, second, third, fourth, ···, emitting processes, respectively,

n_0 being the initial exciton number; n, m, s being the exciton number at some steps, respectively,

l_1, l_2, l_3 being the nucleon number above the surface of the Fermi sea in the emitted composite particle x_1, x_2, x_3 in the first, second, third processes, respectively; and suppose

$$EB_1 = E - B_1,\ EB_2 = EB_1 - B_2,$$
$$EB_3 = EB_2 - B_3,\ EB_4 = EB_3 - B_4,\ \cdots$$
$$Bz_2 = B_2 + z_2,\ Bz_3 = B_3 + z_3,\ Bz_4 = B_4 + z_4,\cdots$$
$$z_{12} = z_1 + z_2,\ z_{123} = z_{12} + z_3,\ z_{1234} = z_{123} + z_4,\cdots$$

For the first emitting process,

$$\sigma_{x,x_1}(E_0) = \sigma_a(E_0) \int_{z_1}^{EB_1} dE_1 \left[\sum_{n=n_0}^{n} \sum_{l_1} P^{l_1}_{1,x_1} \right.$$
$$(Z_c, A_c, E, n_0, n, E_1)$$
$$D_2(Z_1, A_1, EB_1 - E_1, n - l_1) + D_1(Z_c, A_c, E, n_0)$$
$$\left. Q_{1,x_1}(Z_c, A_c, E, E_1) \right] Q_{2,l}(Z_1, A_1, EB_1 - E_1)$$

will change to ($u_1 = EB_1 - E_1$)

$$\sigma_{x,x_1}(E_0) = \sigma_a(E_0) \left[\int_0^{Bz_2} + \int_{Bz_2}^{EB_1 - z_1} \right] du_1$$
$$\left[\sum_{n=n_0}^{n} \sum_{l_1} P^{l_1}_{1,x_1} (Z_c, A_c, E, n_0, n, EB_1 - u_1) \right.$$
$$D_2(Z_1, A_1, u_1, n - l_1) + D_1(Z_c, A_c, E, n_0)$$
$$\left. Q_{1,x_1}(Z_c, A_c, E, EB_1 - u_1) \right] Q_{2,l}(Z_1, A_1, u_1)$$

where $\sigma_a(E_0)$ is the total reaction cross section at the incident energy E_0,

$\sum_{l_i} P^{l_i}_{i,x_i}(Z_{i-1}, A_{i-1}, U, ni, n, E_i)$ is the probability (in unit time and unit interval of energy) of the compound nucleus (Z_{i-1}, A_{i-1}) at excited energy U in the ith emitting process starting from initial exciton number ni, via λ_+, transitting to exciton number n and then emitting x_i particle with kinetic energy E_i,

$D_i(Z_{i-1}, A_{i-1}, U, ni)$ is the probability (in unit time and unit interval of energy) of the compound nucleus (Z_{i-1}, A_{i-1}) at excited energy U in the ith emitting process starting from initial exciton number ni, via λ_+, transitting to the equilibrium state (exciton number n) without any particles emitting;

$Q_{i,x_i}(Z_{i-1}, A_{i-1}, U, E_i)$ is the fraction of the compound nucleus (Z_{i-1}, A_{i-1}) at excited energy U in the ith emitting process at the equilibrium state evaporating x_i particle with kinetic energy E_i;

$Q_{i+1,\gamma}(Z_i, A_i, U-E_i)$ is the fraction of the compound nucleus (Z_i, A_i) at excited energy $U-E_i$ in the $(i+1)$th emitting process at the equilibrium state evaporating γ photon (with any energy).

For the second emitting process,

$$\sigma_{x,x_1x_2}(E_0)=\sigma_a(E_0)\int_{\cdot_1}^{EB_2-\cdot_2}dE_1\int_{\cdot_2}^{EB_1-E_1}dE_2$$
$$\Big[\sum_{\cdots_0}^{\bar{n}}\sum_{l_1}P^{l_1}_{1,x_1}(Z_c, A_c, E, n_0, n; E_1)$$
$$\Big(\sum_{\cdots-l_1}^{\bar{n}}\sum_{l_2}P^{l_2}_{2,x_2}(Z_1, A_1, EB_1-E_1, n-l_1, m; E_2)$$
$$D_3(Z_2, A_2, EB_2-E_1-E_2, m-l_2)$$
$$+D_2(Z_1, A_1, EB_1-E_1, n-l_1)$$
$$Q_{2x_1}(Z_1, A_1, EB_1-E_1, E_2))+D_1(Z_c, A_c, E, n_0)$$
$$Q_{1x_1}(Z_c, A_c, E; E_1)\,Q_{2x_2}(Z_1, A_1, EB_1-E_1;$$
$$E_2)\Big]\,Q_{3\gamma}(Z_2, A_2, EB_2-E_1-E_2).$$

Let us introduce the following notations,

$$PP_2(l_1, l_2, m, u_2)=\int_{u_2+Bx_2}^{EB_1-x_1}du_1$$
$$P^{l_2}_{2,x_2}(Z_1, A_1, u_1, m_0, m; u_1-B_2-u_2)$$
$$\sum_{\cdots_0}^{m+l_1}P^{l_1}_{1,x_1}(Z_c, A_c, E, n_0, n; EB_1-u_1)\ (m_0=n_0-l_1),$$

$$DQP_2(u_2)=\int_{u_2+Bx_2}^{EB_1-x_1}du_1\;Q_{2x_2}(Z_1, A_1, u_1; u_1-B_2-u_2)$$

$$\sum_{n=n_0}^{\bar{n}} \sum_{l_1} D_2 \left(Z_1, A_1, u_1, n-l_1 \right)$$

$$P_{1,x_1}^{l_1} \left(Z_c, A_c, E, n_0, n; EB_1 - u_1 \right),$$

$$DQQ_2(u_2) = \int_{u_2+Bx_2}^{EB_1-x_1} \mathrm{d}u_1 \; Q_{2,x_2} \left(Z_1, A_1, u_1, u_1 - B_2 - u_2 \right)$$

$$Q_{1,x_1} \left(Z_c, A_c, E; EB_1 - u_1 \right) D_1 \left(Z_c, A_c, E, n_0 \right)$$

And then the reaction cross section in the second process can be expressed as

$$\sigma_{x,x_1x_2}(E_0) = \sigma_a (E_0) \left[\int_0^{Bx_1} + \int_{Bx_3}^{EB_2-x_{12}} \right] \mathrm{d}u_2$$
$$\left[\sum_{l_1 l_2}^{\bar{n}} \sum_{n=n_0} PP_2 \left(l_1, l_2, m, u_2 \right) \right.$$

$$D_3 \left(Z_2, A_2, u_2, m-l_2 \right) + DQP_2 (u_2)$$
$$\left. + DQQ_2 (u_2) \right] Q_{3,x} \left(Z_2, A_2, u_2 \right).$$

To avoid the tedious expressions for reaction cross sections, next one will not give the original expressions, in which E_1, E_2, E_3, $\cdots$, are integral arguments, and directly give the expressions, in which u_1, u_2, u_3, $\cdots$ are integral arguments For the third emitting process, let

$$PP_3 \left(l_1, l_2, l_3, s, u_3 \right) = \int_{u_3+Bx_3}^{EB_2-x_{12}} \mathrm{d}u_2$$
$$P_{3,x_3}^{l_3} \left(Z_2, A_2, u_2, s_0, s; u_2 - B_3 - u_3 \right)$$

$$\sum_{n=n_0}^{s+l_2} PP_2 \left(l_1, l_2, m, u_2 \right) \left(s_0 = m_0 - l_2 \right),$$

$$DQP_3 (u_3) = \int_{u_3+Bx_3}^{EB_2-x_{12}} \mathrm{d}u_2 \; Q_{3,x_3} \left(Z_2, A_2, u_2, u_2 - B_3 - u_3 \right)$$

$$\sum_{l_1 l_2}^{\bar{n}} \sum_{n=n_0} D_3 \left(Z_2, A_2, u_2, m-l_2 \right) PP_2 \left(l_1, l_2, m, u_2 \right),$$

$$DQQ_3\ (u_3)=\int_{u_3+Bz_3}^{EB_2-z_{12}} du_2\ Q_{3,x_3}(\ Z_2,\ A_2,\ u_2,\ u_2-B_3-u_3\ )$$
$$[\ DQP_2\ (u_2\ )\ +\ DQQ_2\ (u_2\ )\ ]$$

$$PDQ_3\ (u_3)=[\ \sum_{l_1 l_2 l_3}\sum^{\bar{n}} PP_3\ (\ l_1,\ l_2,\ l_3,\ s,\ u_3\ )$$
$$+DQP_3\ (u_3)\ +\ DQQ_3\ (u_3)\ ]$$

then one can get

$$\sigma_{x,x_1x_2x_3}\ (E_0)=\sigma_a\ (E_0)\ [\ \int_0^{Bz_4}\ +\ \int_{Bz_4}^{EB_3-z_{123}}\ ]\ du_3$$
$$PDQ_3\ (u_3)\ Q_{47}\ (\ Z_3,\ A_3,\ u_3\ )$$

For the fourth emitting process, let

$$PDQ_4\ (u_4)=\int_{u_4+Bz_4}^{EB_3-z_{123}} du_3$$
$$Q_{4,x_4}(\ Z_3,\ A_3,\ u_3,\ u_3-B_4-u_4\ )\ PDQ_3\ (u_3)$$

and get

$$\sigma_{x,x_1x_2x_3x_4}\ (E_0)=\sigma_a\ (E_0)\ [\ \int_0^{Bz_5}\ +\int_{Bz_5}^{EB_4-z_{1234}}\ ]\ du_4$$
$$PDQ_4\ (u_4)\ Q_{57}\ (\ Z_4,\ A_4,\ u_4\ )$$

Repeating above treatments for the fifth, ···, tenth processes, all reaction cross sections expressed by twofold integrations can be obtained. Moreover, from above expressions, one can see that the only difference between the integral for u_1 in first and second processes is the lower limit of the integral. For the numerical integration to u_1 in the second integral interval (Bz_2 to EB_1-z_1) in first process, one can keep the values of relevant quantities in the integrand at all integral base points, and then one can get values of those quantities of u_1 in second process by linear interpolation. And the only difference between the integral to u_2 in second and third processes is also the lower limit of the integral. Therefore for the numerical integration to u_2 in the second integral interval (Bz_3 to EB_2-z_{12}) in second process, one can also keep the values of relevant quantities in the integrand at all integral base points, and then one can get values of those quantities of u_2 in the third process by linear interpolation. There-

fore, besides in the first process, one should always do twofold integration, and in the inner integral, one can get the values of some quantities in the integrand by linear interpolation to save the computing time. So in CCRMN, as the number of the emitting processes increases, only the number of channels increases, the multifold number of the integration in any emitting process is always two, does not increase. In this way one can easily finish the calculation and get the reaction cross section in any higher emitting process. This is the main character and a perfect advantage of CCRMN.

This program has been applied in practical calculations and got reasonable results.

* In CCRMN, the radiative capture cross section is defined as $\sigma_{\alpha,\gamma}$ (no other particles emit after (α,γ) photon emission) + $\sigma_{\alpha,\gamma\gamma}$ (after two γ photons emission, the third emitting particle can be anything), whereas $\sigma_{\alpha,\gamma\alpha'}$ will be added to $\sigma_{\alpha,\alpha'}$.

References

[1] Zhang Jingshang et al., Comm. Theor. Phys., 10, 33(1988)

[2] A. Gilbert et al., Can. J. Phys., 43, 1446(1965)

[3] F. D. Becchetti et al., Phys. Rev., 132, 1190(1969)

[4] Shen Qingbiao et al., Z. Phys., A, 303, 69(1981)

[5] R. L. Verner et al., Phys. report, 201, 57(1991); Phys. Lett., B, 185, 6(1987)

[6] A. R. Barnett et al., Computer Phys. Comm., 8, 377(1974)

[7] Cai Chonghai et al., Nucl. Sci. & Eng., 111, 317(1992)

[8] P. G. Young & E. D. Arthur, LA-6947

Progress on Calculation of Direct Inelastic Scattering Cross Section of Neutron

Chen Zhenpeng

(Dept. of Phys., Tsinghua Univ., Beijing)

For n+^{238}U inelastic scattering cross section, there exist discrepancies among the available evaluations in various libraries. This is partly due to the difference of Direct Inelastic Scattering (D. I. S.) cross section calculated with Coupled Channel Optical Model (CCOM). So some research work on this problem has been done in 1995.

1 Research on the Level Frame Used in CCOM Calculation

The level frame used in CCOM calculation is rather crucial. Fig. 1 shows that the discrepancy between calculated results by different level frame but with the same optical model parameters is notable. The D. I. S. angular distribution at 2^+ state of ^{238}U will get higher with the more and more levels be involved; and will become stable when the number of levels is more than 5.

The level frame used in CCOM calculations in some evaluations of n+^{238}U [1, 2] is 0^+, 2^+, 4^+. The DWBA was used for higher levels, so this will cause the discrepancies among them. In our work, the level frame is 0^+, 2^+, 4^+, 6^+, 8^+, 1^-, 3^-, 5^- with code EDIS88[3]. The levels 1^-, 3^-, 5^- belong to octupole bands, so the rotational–vibrational model is used.

2 Research on Used Parameters of SOM in Calculation of CCOM

The calculations of CCOM require optical model parameters of deformed nuclei, but the suitable parameters are not available. An effective way is to adjust few parameters with using the spherical optical model (SOM) ones as primary values and letting most of them unchanged. The criterion for changed range is that the calculated total cross section and elastic scattering differential cross sections of CCOM are agreement with that of SOM. The CCOM code ECIS88 was employed to fit these data which in fact were calculated by SOM code with the SOM parameters of Ref. [4]. A systematic search has been done

and shows that the depth of surface imaginary potential (W_s) and the radii of real potential (R_r) are the most sensitive. Fig. 2 shows the results of fitting for W_s and R_r. The linear formulas are :

$$W_s = 0.3916 + 0.2419\,E_n \ (\text{MeV})$$
$$R_r = 1.32047 - 0.001454\,E_n \ (\text{fm})$$

3 Research on the Amplitude of Octupole Phonon β_3

In calculation of CCOM with rotational–vibrational model, when the levels of octupole vibration bands are involved, the radii parameter R is :

$$R = R_0 \left| 1 + \beta_2 \ Y_{20}(\theta') + \beta_4 \ Y_{40}(\theta') + \frac{1}{\sqrt{7}} \left(b^{*}_{30} + b_{30} \right) \beta_3 \ Y_{30}(\theta') \right| \tag{1}$$

here the β_2 and β_4 are deformed parameters, usually they are available, the β_3 is the amplitude of octupole phonon, usually it is not available We manage to get it by this way as follows.

The electric octupole operation up to the second order in $\alpha^{[2]}$ and $\alpha^{[3]}$ is[5] :

$$Q^{\text{coll}}_{3\mu} = \frac{3ZR_0^3}{4\pi} \left[\alpha^{*}_{3\mu} - \frac{5}{\sqrt{3\pi}} \left(\alpha^{[2]} * \alpha^{[3]} \right)_{3\mu} \right] \tag{2}$$

usually the contribution of second term is small, so Eq. (2) can be written as

$$Q^{\text{coll}}_{3\mu} \approx \frac{3ZR_0^3}{4\pi} \alpha^{*}_{3\mu} \tag{3}$$

The reduced E3 transition probability is defined as

$$B(E_3, I_i \to I_f) = \frac{2I_f + 1}{2I_i + 1} \left| \langle \psi_f \,/\!/\, Q^{\text{coll}}_3 \,/\!/\, \psi_i \rangle \right|^2 \tag{4}$$

For coulomb excitation, ψ_i is the wave function of ground–state, ψ_f is the final state of E_3 transition.

For octupole deformation operator there exists a transformation relation from Lab. system to intrinsic system as :

$$\alpha^{*}_{3\mu} = \sum_{\nu} D^{3^{+}}_{\mu\nu} (\theta_i) a_{3\nu} \tag{5}$$

So, for the octupole vibration state with $\lambda = 3$, $\mu = 0$ there is :

$$\alpha^{*}_{30} = D^{3*}_{00} (\theta_i) a_{30} \tag{6}$$

By using Wigner–Eckart formula we get :

$$(I_f \; // \; Q_3^{\text{coll}} \; // \; I_i) = \frac{(I_f \; 0 \mid Q_{30} \mid I_i \; 0)}{(I_i \; 0 \; 3 \; 0 \mid I_f \; 0)} \tag{7}$$

$$(I_f \; 0 \mid Q_3^{\text{coll}} \mid I_i \; 0) = \frac{3ZR_0^3}{4\pi} (I_f \; 0 \mid D^{3*}_{00} \; a_{30} \mid I_i \; 0) \tag{8}$$

here

$$\mid I_f \; 0) = \sqrt{\frac{2I_f + 1}{8\pi^2}} D^{I_f *}_{00} \chi_{00} (\eta) \mid 1) \tag{9}$$

$$\mid I_i \; 0) = \sqrt{\frac{2I_i + 1}{8\pi^2}} D^{I_i *}_{00} \chi_{00} (\eta) \mid 0) \tag{10}$$

$$a_{30} = \frac{\beta_3}{\sqrt{7}} (b^{*}_{30} + b_{30}) \tag{11}$$

The b^{*}_{30} and b_{30} are the phonon creation and annihilation operators, respectively. Putting Eqs. (9), (10) and (11) in Eq. (8) and by using the integrated formula of 3–D functions[6], we get

$$(I_f \; 0 \mid Q_{30} \mid I_i \; 0) = \frac{3ZR_0^3}{4\pi} \cdot$$

$$\sqrt{\frac{2I_i + 1}{2I_f + 1}} \beta_3 \mid (3 \; 0 \; I_i \; 0 \mid I_f \; 0) \mid^2 \tag{12}$$

Now from Eq. (4) we get the relation formula for $B(E_3;\ I_i \to I_f)$ and β_3

$$B(E_3; I_i \to I_f) = \frac{2I_f + 1}{1I_i + 1} \left| \frac{(I_f\ 0 \mid Q_{30} \mid I_i\ 0)}{(I_i\ 0\ 3\ 0 \mid I_f\ 0)} \right|^2$$

$$= \frac{1}{\sqrt{7}} \left(\frac{3ZR_0^3}{4\pi} \right)^2 \beta_3^2 \left| (I_i\ 0\ 3\ 0 \mid I_f\ 0) \right|^2 \tag{13}$$

There are some experimental values of $B(E_3)$[7, 8], finally we get

$$\beta_3 \approx 0.221 \pm 0.003 \tag{14}$$

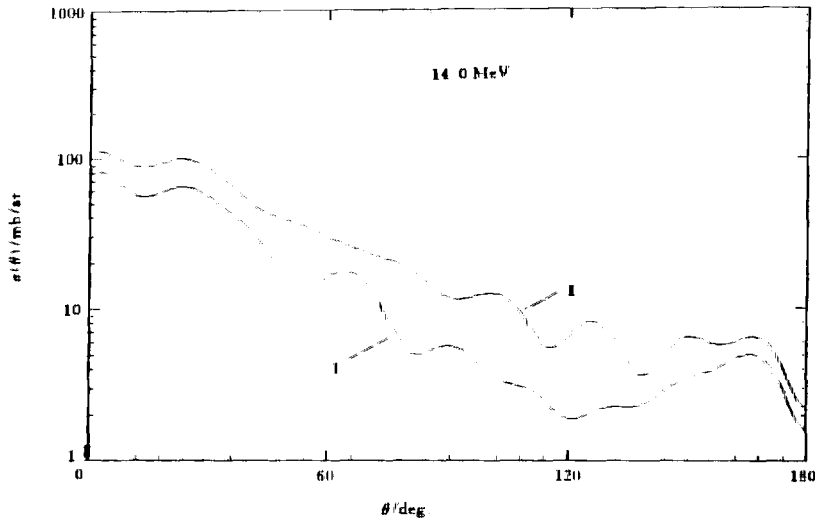

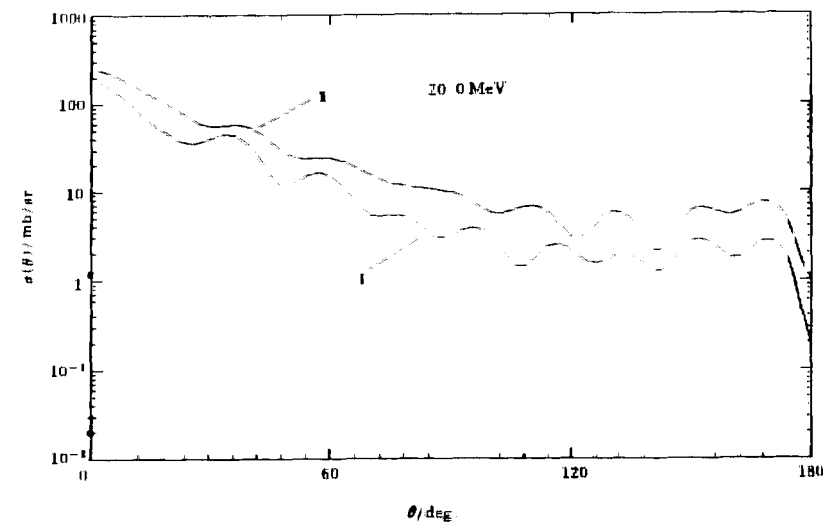

Fig 1 The angular distribution of $^{238}U(n,n')$ at 2^+ state calculated by CCOM with different coupled levels

I for 0^+, 2^+, 4^+ II for 0^+, 2^+, 4^+, 6^+, 8^+, 1^-, 3^-, 5^-

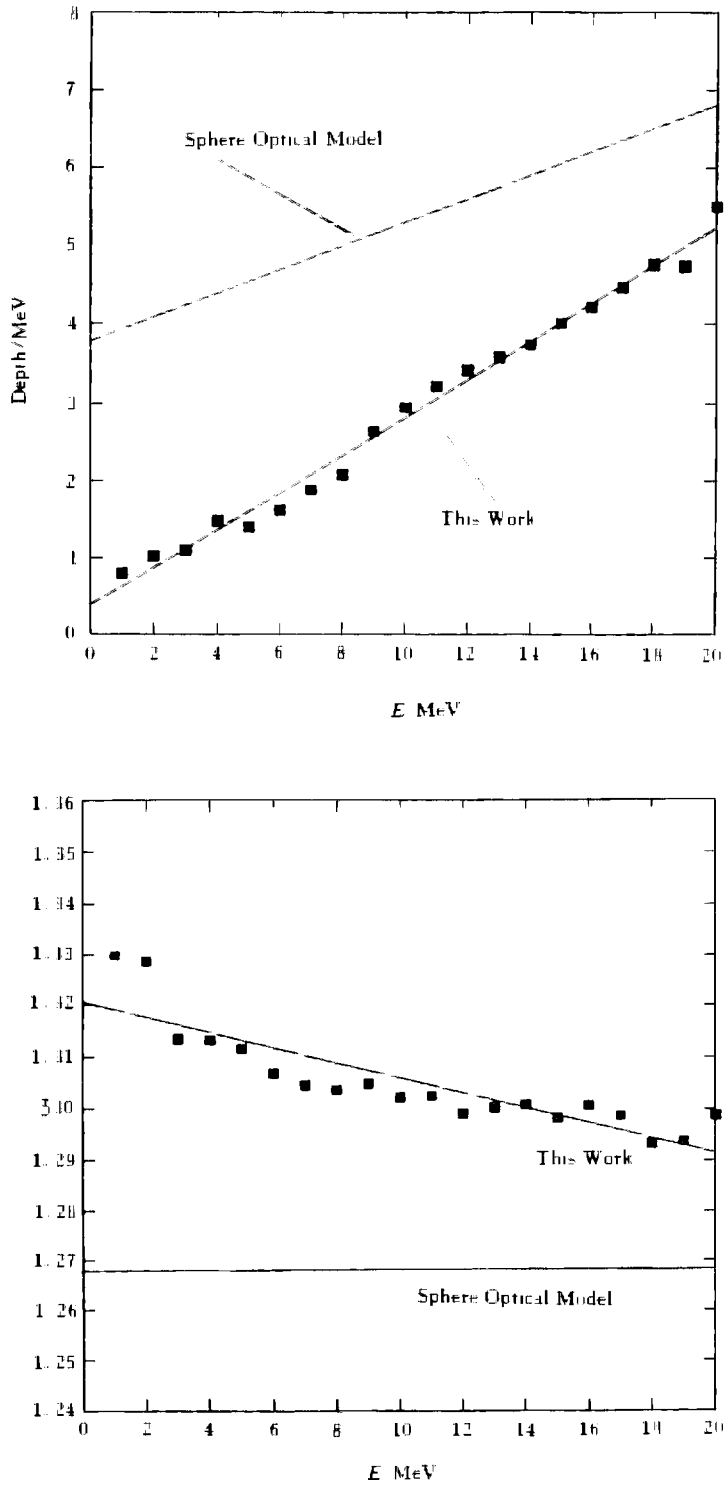

Fig 2 The results of fitting by CCOM for W_s and R_r

References

[1] Y. Kanda, JAERI 1319, 417(1990)

[2] Tang Guoyou et al., "Atomic Energy Sci. & Tech.", Vol. 29(4), 348(1995)

[3] J. Rayal, ECIS88, NEA 0850

[4] Tang Guoyou, private communication

[5] G. Stanislan et al., J. Phys. G Nucl. Phys., 8, 787(1982)

[6] Liao Jizhi, Modern Nuclear Model, 348(1989)

[7] F. K. McGowan et al., Nucl. Phys., A571, 569～587 (1994)

[8] J. G. Alessi et al., Phys. Rev., C23, 79(1981)

Calculation of Neutron Monitor Reaction Cross Sections of ^{90}Zr in Energy Region up to 100 MeV

Shen Qingbiao Yu Baosheng Cai Dunjiu

(China Nuclear Data Center, CIAE)

Introduction

The activation products ^{89}Zr (half life is 78.41 h) and ^{88}Zr (half life is 83.4 d) can be produced from n+^{90}Zr reaction through (n,2n) and (n,3n) reactions, respectively ^{88}Y (half life is 106.65 d) can be produced through (n,2np), (n,nd), and (n,t) reactions; ^{87}Y (half life is 79.8 h) through (n,3np), (n,2nd), and (n,nt) reactions; ^{86}Y(half life is 14.74 h) through (n,4np), (n,3nd), and (n,2nt) reactions.

In order to determine the neutron optical potential parameters for n+^{90}Zr reaction in the energy region up to 100 MeV, more neutron experimental data of ^{90}Zr and some nonelastic scattering cross sections of neighboring nucleus Cd above 20 MeV were used. Then various cross sections of n+^{59}Co reaction were calculated.

1 Theories and Parameters

The program SPEC[1], including the first to the sixth particle emission processes, was used in our calculations. The optical model, evaporation model, and exciton model[2] are included in this program. The preequilibrium and direct reaction mechanisms of γ emission[3] are taken into account. The direct inelastic scattering cross sections are obtained by the collective excitation distorted-wave Born approximation[4] The compound-nucleus elastic scattering contributions are calculated by Hauser-Feshbach model.

The pick-up mechanism of cluster formation[5~7] for composite particle emissions is included in the first and second particle emission processes.

Based on various neutron experimental data of ^{90}Zr and neighboring nucleus Cd from EXFOR library, a set of optimum neutron optical potential

parameters in energy region 2~100 MeV obtained is as follows :

$$V = 51.8987 - 0.22839E - 0.0004102E^2 - 24.0\ (N-Z)/A \quad (1)$$

$$W'_S = \max\{0,\ 10.5113 - 0.10563E - 12.0\ (N-Z)/A\} \quad (2)$$

$$W'_V = \max\{0,\ -2.16355 + 0.24183E - 0.0009475E^2\} \quad (3)$$

$$U_{SO} = 6.2 \quad (4)$$

$$r_r = 1.21685,\ r_S = 1.22357,\ r_V = 1.26899,\ r_{SO} = 1.21685 \quad (5)$$

$$a_r = 0.71296,\ a_S = 0.48916,\ a_V = 0.70376,\ a_{SO} = 0.71296 \quad (6)$$

The Gilbert–Cameron level density formula[8] is applied in our calculations, and the exciton model constant K is taken as 3900 MeV^3.

2 Calculated Results and Analyses

Fig. 1 shows the comparison of the calculated neutron total cross sections with the experimental data in the energy region 2~100 MeV for n+^{90}Zr reaction. The theoretical values are in good agreement with the experimental data. Fig. 2 shows that the calculated neutron nonelastic cross sections agree better with the experimental data. Fig. 3 gives the comparison of the calculated with the experimental (n,2n) cross sections of ^{90}Zr. The calculated values are basically agreement with the experimental data.

The experimental data and the calculated results show that the larger (n,2n) cross sections producing ^{89}Zr are lying in 13~30 MeV energy region; (n,3n) reaction producing ^{88}Zr in 25~45 MeV energy region.

Fig. 4 shows the calculated $^{88,\ 87,\ 86}$Y production cross sections for up to 100 MeV. From Fig. 4 one can see that ^{88}Y production reaction can be a promising neutron monitor reaction in the energy region from 25 to 50 MeV.

3 Summary

Many nuclear data for n+^{90}Zr reaction were calculated by using optical model, evaporation model, and exciton model. The calculated results show that the activation products $^{89,\ 88}$Zr and $^{88,\ 87}$Y are important neutron monitor reaction products for n+^{90}Zr reaction in energy range up to 100 MeV. Especially, ^{88}Y production reaction can be a promising neutron monitor reaction in the energy region from 25 to 50 MeV.

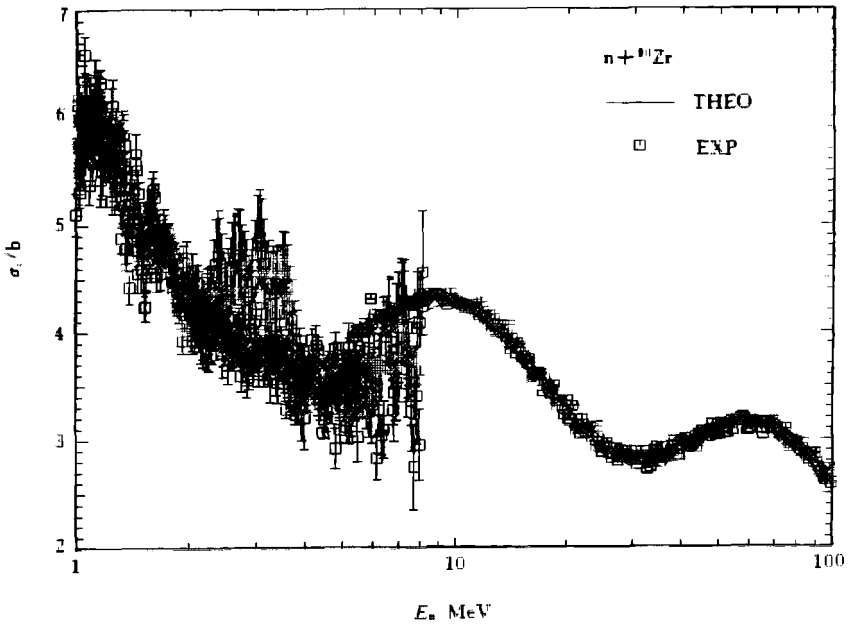

Fig 1 Neutron total cross sections of ^{90}Zr

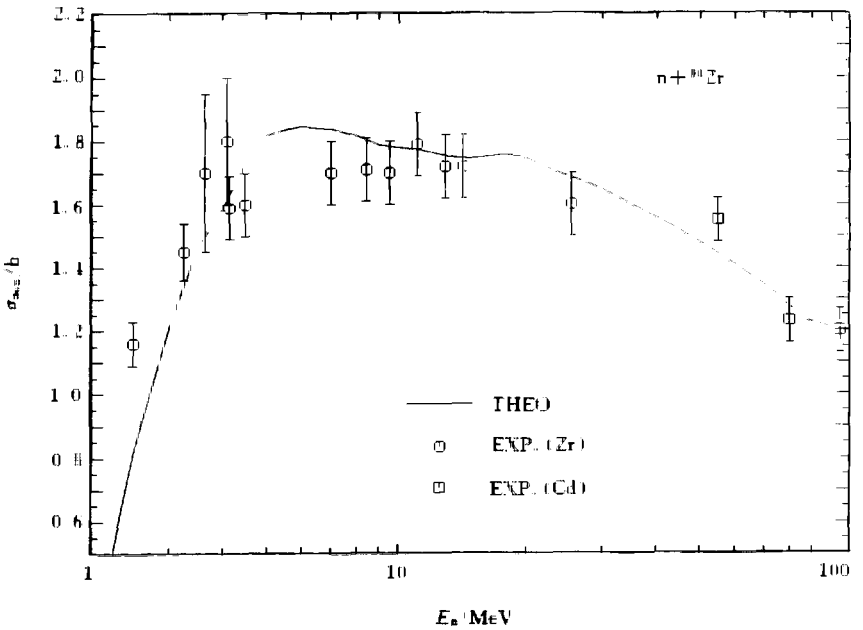

Fig. 2 Neutron nonelastic scattering cross sections of ^{90}Zr

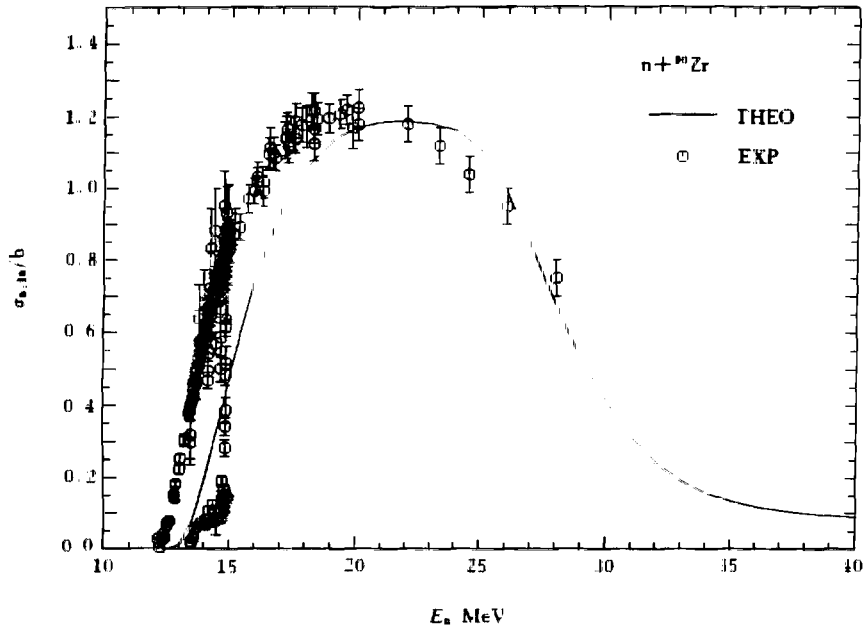

Fig. 3 (n,2n) cross sections of ^{90}Zr

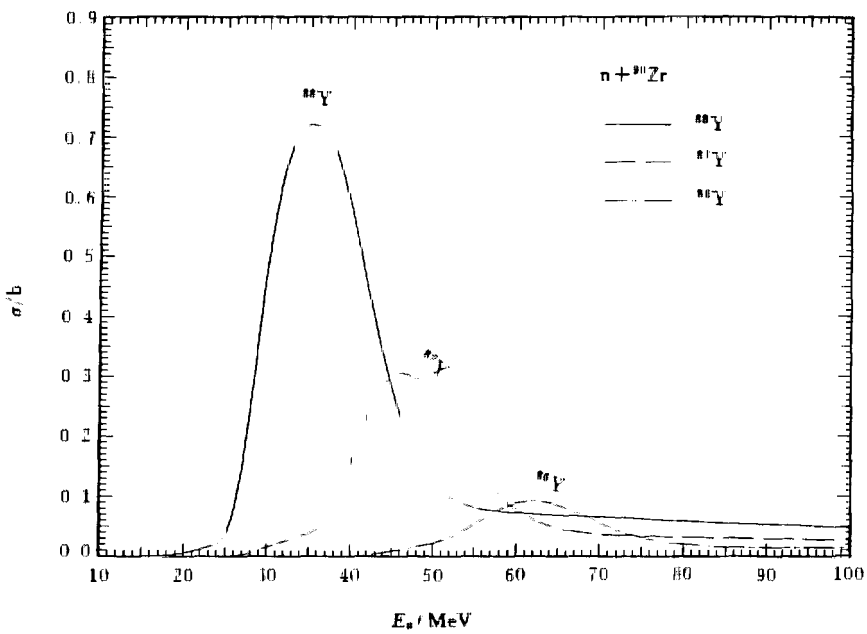

Fig. 4 The calculated $^{88,87,86}Y$ production cross sections for n+^{90}Zr reaction

References

[1] Shen Qingbiao et al., CNDP, 11, 28(1994)

[2] M. Blann, Ann. Rev. Nucl Sci., 25, 123(1975)

[3] J. M Akkermans et al., Phys. Let., 157B, 95(1985)

[4] P. D Kunz, "Distorted Wave Code DWUCK4", University of Colorado, unpublished

[5] A. Iwamoto et al., Phys. Rev., C26, 1821(1982)

[6] K. Sato et al., Phys. Rev., C28, 1527(1983)

[7] Zhang Jingshang et al., Commun. in Theor Phys., (Beijing, China), 10, 33(1988)

[8] A. Gilbert et al , Can. J. Phys., 43, 1446(1965)

III DATA EVALUATION

The Method and Program System CABEI for Adjusting Consistency between Natural Element and Its Isotopes Data

Liu Tingjin Sun Zhengjun

(China Nuclear Data Center, CIAE)

To meet the requirement of nuclear engineering , especially nuclear fusion reactor, now the data in the major evaluated libraries, such as ENDF / B-6, JENDL-3.2, JEF-2.2, BROND-2.1 and CENDL-2.1, are given not only for natural element, but also for its isotopes. It is clear that these data must be consistent in physics. Unfortunately, some data in the libraries, for example Fe in CENDL-2.1, do not satisfy consistent relationship. Inconsistence between element and its isotopes data is one of the main problems in present evaluated neutron libraries[1]

As well known, the data of each nuclide must satisfy itself consistence (for example, total cross section equals the sum of all partial cross sections, nonelastic cross section equals the sum of all partial cross sections except elastic cross section, and total inelastic cross section equals the sum of cross sections of inelastic scattering to discrete and continuous states etc.). The consistence between natural element and its isotopes data makes the data must satisfy another kinds of consistent relationships at the same time, this is the key point and main difficulty for this kind of adjustment

The formulas for adjusting to satisfy simultaneously the two kinds of consistent relationships were derived by means of least square method, the program system CABEI were developed, which includes programs EPOIN for selecting and arranging energy point in order, INTER for data interpolation, ADJUS for data adjusting, DIFFE for calculating the difference between the data of natural element and its isotopes, and RECOV for rewrite the data into the file in ENDF / B-6 format.

The correctness and reliability of the programs were tested by calculating

the typical examples, the effects of the given weight were studied. The results show that adjusted values satisfy the two kinds of consistent relationships, and changes are in reasonable ranges.

As an example, the Fe data in CENDL-2.1 were adjusted, the problems in the practical adjustment were investigated, including adjusting for complete data, defining the energy region for adjustment, treating the reaction channels which are not same one by one, selecting the effects of the adjustment weight and output energy points etc.

Reference

[1] J. J. Schmidt, Proc. of Intern. Symp. on Nuclear Data Evaluation Methodology, p. 1, BNL, U. S. A. (1992)

CN9700489

The Evaluation and Calculation of Production Cross Sections of ^{18}F, ^{77}Br and ^{186}Re Medical Radioisotopes from ^{18}O, ^{77}Se and $^{186}W(p,n)$ Reactions up to 80 MeV

Zhuang Youxiang

(China Nuclear Data Center, CIAE)

Introduction

The medical radioisotopes are used for diagnostic and therapeutic purposes, as well as metabolism and physiological function researches in modern medicine. If a short-lived radioisotope emits a predominant or single γ-ray of 60 ~ 300 keV, it is of greater advantage since single photon emission computed tomograph (SPECT) can be performed; similarly β^+ emitters are also of great significance since three dimensional high resolution scans can be obtained via positron emission tomography (PET). Some of the radioisotopes find therapeutic applications, especially if they emit α or high energy

β^- particles, or Auger electrons[1]

The major applications are of functional imaging using PET agents for ^{18}F, various therapeutic pharmaceuticals via Auger electrons for ^{77}Br, cancer's diagnosis and therapy for ^{186}Re

Nuclear data relevant to medically important radioisotopes can be divided into two major categories: the decay data and nuclear reaction cross sections. The former is of prime importance in deciding upon the suitability of a radioisotope for medical application, and the latter is of great significance regarding the production and radionuclidic quality control of the desired radioisotope. In general, the decay data are known with sufficient accuracies, but the reaction cross section need more attention, especially charged particle nuclear data (CPND) because they are scarce and scattered.

1 The Evaluations of Experimental Data and Theoretical Calculations for ^{18}O, ^{77}Se, $^{186}W(p,n)$ Reactions up to 80 MeV

1.1 General Analysis

The related experimental data were collected up to 1995. The bibliographies and index to CPND are as follows:

Nuclear Science Abstracts; Nuclear Data Table, Atomic Data and Nuclear Data Table; INIS Atomindex, UCRL-50400, BNL-NCS-50640, 51771, EXFOR Master-File Index.

The excitation functions of ^{18}O, ^{77}Se, $^{186}W(p,n)$ reactions were measured with the aid of either residual nucleus activity or outgoing neutron methods. Enriched samples, stacked target irradiation or energy degradation by foils, beam current integration, chemical separation, separate monitor-foil, coincidence technique, NaI(Tl) crystal, plastic scintillator, Ge-Li detector, BF_3 neutron counter etc. were used in these measurements.

In general, there are some experimental data in energy range from threshold to 30 MeV, thus it is necessary for each reaction to do theoretical calculation for interpolation or / and extrapolation of experimental data up to 80 MeV.

(1) $^{18}O(p,n)^{18}F$ reaction cross section

The main 6 measurements are listed in Table 1.

Table 1 The main measurements of $^{18}O(p,n)^{18}F$ reaction cross section

Author (y)	Lab	Energy range (MeV)
Bloom et al (1965)[2]	1USAORL	6～13
Anderson(1969)[3]	1USALRL	7.0～13.5
Bair(1973)[4]	1USALRL	2.5～3.9
Ruth et al.(1979)[5]	1USABNL	2.3～15.0
Kitwanga et al.(1990)[6]	2BLGLVN	11.2～30.0
Marquez(1952)[7]	1USACHI	420

The data measured by Bloom[2], Anderson[3] and Bair et al.[4] were not adopted because of no numeral data. It may be seen in Fig. 1 that the recommend values from threshold to 30 MeV can be obtained by fitting experimental data of Ruth[5] and Kitwanga et al[6].

(2) $^{77}Se(p,n)^{77}Br$ reaction cross section

There are 4 measurements, see Table 2.

Table 2 The main measurements of $^{77}Se(p,n)^{77}Br$ reaction cross section

Author(y)	Lab	Energy range (MeV)
Janssen et al (1980)[8]	2NEDENT	9.9～24.6
Levkovskij et al.(1991)[9]	4KASKAZ	7.7～30
Johnson et al (1958)[10]	1USACRL	2.2～2.7
Reuland et al (1969)[11]	1USACHI	400

Since the data measured by Janssen et al.[8] are $^{18}O(p,n_0)^{18}F$ reaction cross sections, therefore the data measured by Levkovskij et al.[9] with activation method and Johnson et al.[10] by means of neutron measurement were accepted. It is necessary for this reaction to do theoretical calculation for interpolating the data between 2.7～7.7 MeV and extrapolating the data from 30 to 80 MeV (see Fig. 2)

(3) $^{186}W(p,n)^{186}Re$ reaction cross section

Altogether 2 measurements collected up to 1995 are shown in Table 3

Table 3 The measurements of $^{186}W(p,n)^{186}Re$ reaction cross section

Author(y)	Lab	Energy range (MeV)
Shigeta et al.(1994)[12]	2JPNJAE	5.47～19.80
Treytl et al (1966)[13]	1USAPEN	130～396

They are shown in Fig. 3. It is need theoretical calculation to get the recommended values from 20 to 80 MeV.

1.2 Theoretical Calculation

The excitation functions of ^{18}O, ^{77}S, $^{186}W(p,n)$ reactions were calculated by the code ALICE95[14] up to 80 MeV. The evaporation calculations were performed according to Weisskopf and Ewing. The nuclear masses were calculated from the Meyers and Swiatecki mass formula, including shell corrections and pairing effects. The level density parameters were taken from the work of Ignatyuk. The inverse cross sections were calculated by using the optical model. The hybrid model was chosen for the pre-equilibrium reactions. The nucleon-nucleon mean free paths were used in these calculations.

The comparison between calculated cross sections and experimental data from threshold to 80 MeV are given in Figs. 4~6.

It can be seen that the agreements of calculated results with the higher energy parts of measured data are good for ^{18}O, ^{77}Se, $^{186}W(p,n)$ reactions, and with the low energy part of $^{77}Se(p,n)$ reaction is excellent, the theoretical trends at 25~80 MeV are also right.

2 Recommended Values and Its Errors

The recommended values for $^{18}O(p,n)^{18}F$ reaction cross section were based on experimental data from 2.574 to 30 MeV (see Fig. 1), and taken from the smoothed calculated value from 30 to 80 MeV (see Fig. 4).

The recommended values for $^{77}Se(p,n)^{77}Br$ reaction cross section were based on experimental data between 2.176~2.7 MeV and 7.7~30 MeV, and taken from the calculated results between 2.7~7.7 MeV and the shape of theoretical calculation between 30~80 MeV.

The recommended values for $^{186}W(p,n)^{186}Re$ reaction cross section were based on experimental data between threshold~19.8 MeV, and taken from the shape of theoretical calculation between 19.8~80 MeV.

The smallest cited errors for $^{18}O(p,n)^{18}F$, $^{77}Se(p,n)^{77}Br$ and $^{186}W(p,n)^{186}Re$ reaction cross sections based on experiments are adopted 10% by us, because almost all measurements with accuracies of 7%~12%; and the theoretical calculations are about 20%~30%.

This project is supported by the International Atomic Energy Agency (IAEA).

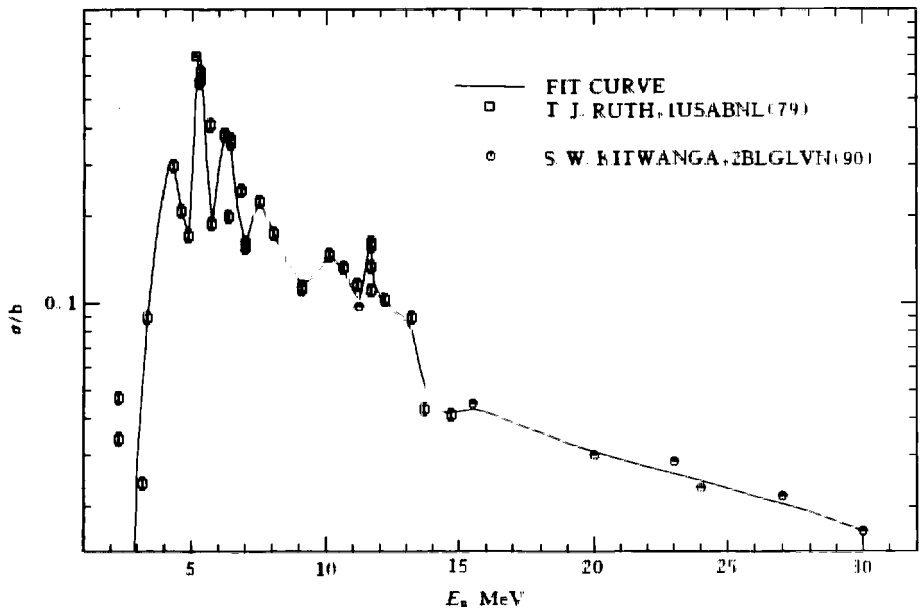

Fig 1 $^{18}O(p,n)$ cross section

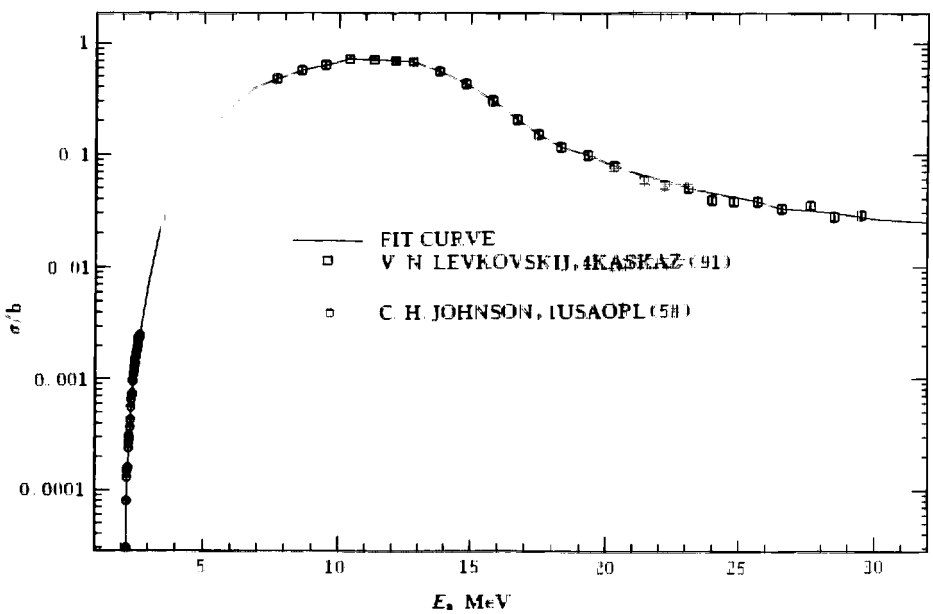

Fig 2 $^{77}Se(p,n)$ cross section

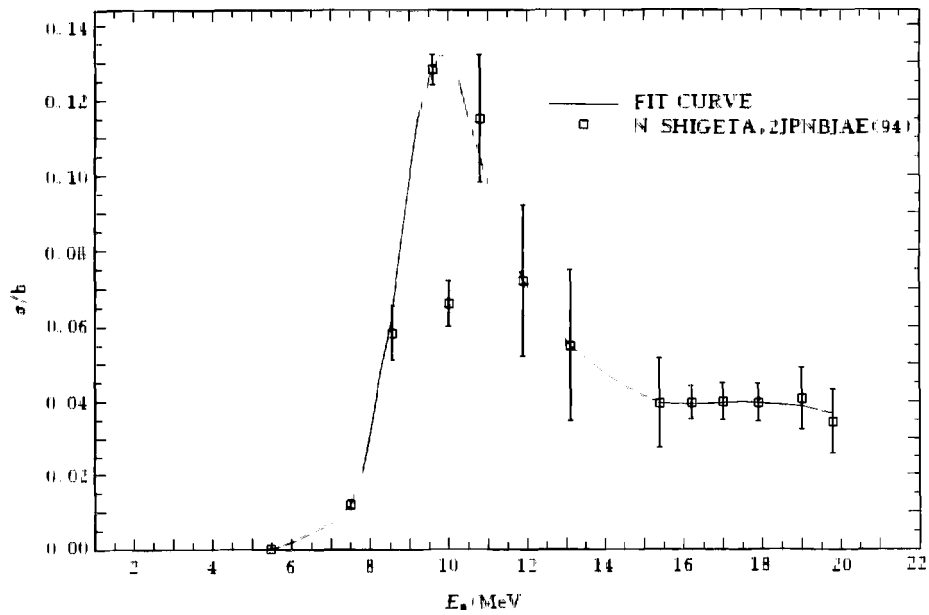

Fig. 3 $^{186}W(p,n)$ cross section

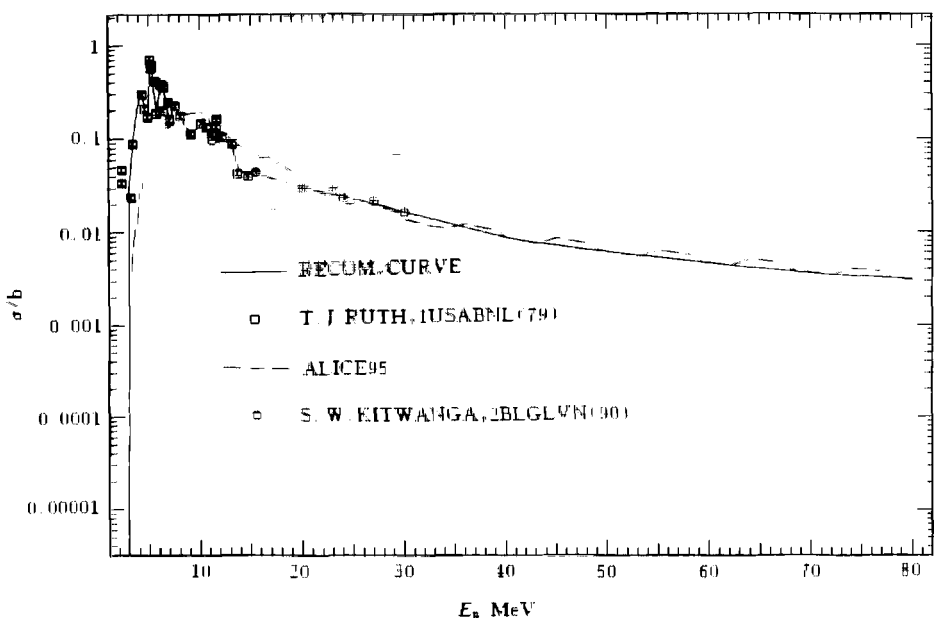

Fig 4 Comparison of calculated $^{18}O(p,n)$ cross section with exp data

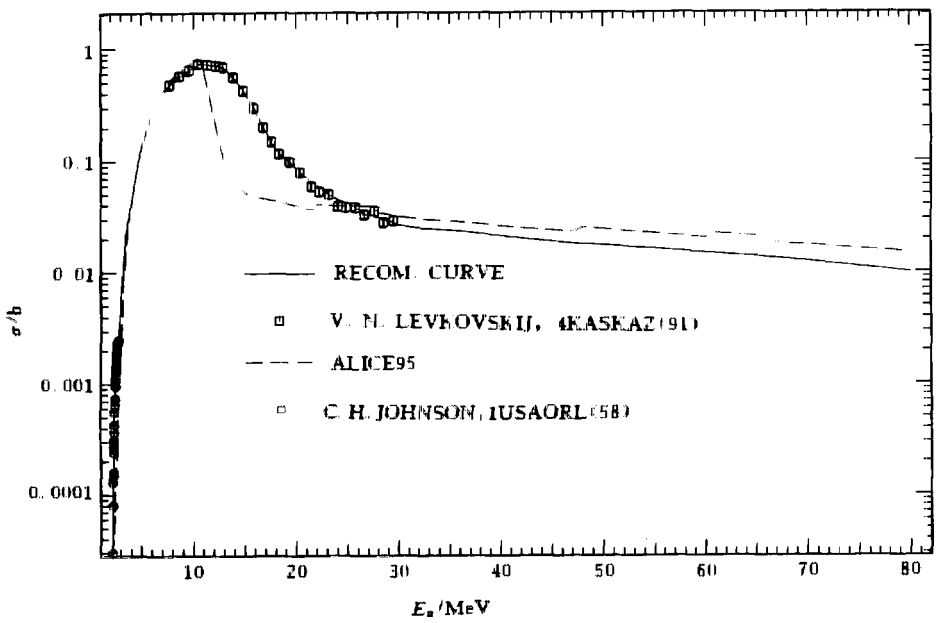

Fig. 5 Comparison of calculated ^{77}Se(p,n) cross section with exp. data

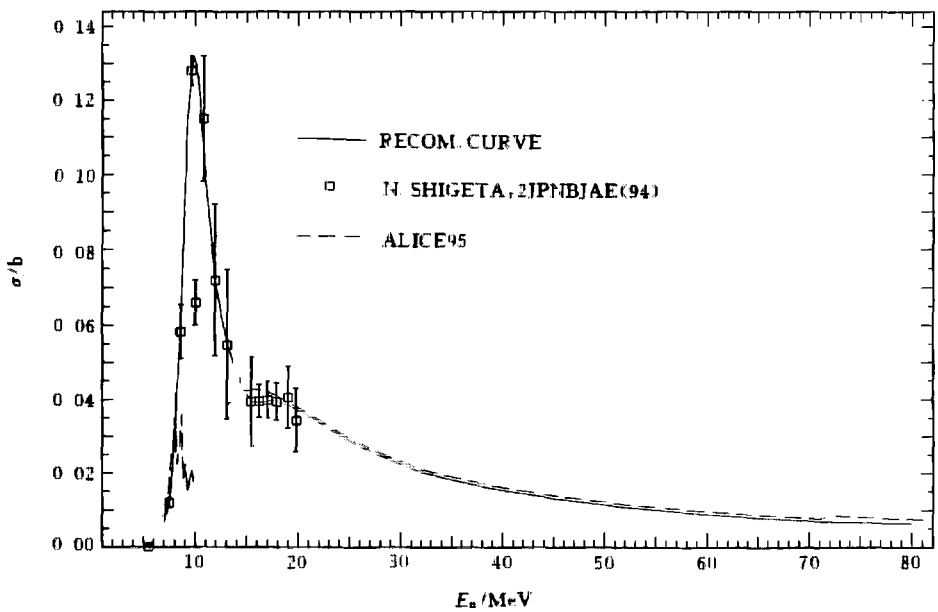

Fig. 6 Comparison of calculated ^{186}W(p,n) cross section with exp data

References

[1] S. M. Qaim, INDC(NDS)-195 / GZ, p. 25~32(1987)
[2] S. D. Bloom et al., Phys. Rev. Lett., 15, 264(1965)
[3] J. D. Anderson et al., Phys. Rev., 177, 1416(1969)
[4] J. K. Bair, Phys. Rev., C8, 120(1973)
[5] T. J. Ruth et al., Radiochim. Acta, 26, 21(1979)
[6] S. W. Kitwanga et al., Phys. Rev., C42, 748(1990)
[7] L. Marquez, Phys. Rev., 86, 405(1952)
[8] A. G. M. Janssen et al., Int. J. Appl. Radiat. Isot., 31, 405(1980)
[9] A. N. Levrovskij et al., EXFOR A0510, 136 (1991)
[10] C. H. Johuson et al., ORNL-2910, 25(1960), Phys. Rev., 109, 1243(1958)
[11] D. J. Reuland et al., Inorg. Nucl. Chem., 31, 1915(1969)
[12] N. Shigeta et al., Private Communication (1994)
[13] N. J. Treytl et al., Phys. Rev., 146, 836(1966)
[14] M. Blann et al., CODE ALICE / LIERMORE95

Evaluation of Neutron Monitor Cross Sections for $^{59}Co(n,x)^{56,57,58}Co$, $^{52,54,56}Mn$, ^{59}Fe Reactions

Yu Baosheng Shen Qingbiao Cai Dunjiu

(China Nuclear Data Center, CIAE)

Abstract

The neutron monitor cross sections for $^{59}Co(n,x)^{56,57,58}Co$, $^{52,54,56}Mn$, ^{59}Fe reactions were evaluated based on recent experimental data and theoretical calculations from threshold energy to 100 MeV.

Introduction

Cobalt is a constituent of structural materials in fusion reactor and an adequate material of threshold activation detector for monitoring high energy

neutron field. So the accurate knowledge of cross sections for $^{59}Co(n,x)^{56,57,58}Co$, $^{52,54,56}Mn$, ^{59}Fe reactions is of importance as the reactions through which radioactive products can be produced in fusion and neutron monitoring reaction in intermediate energy application. The measured cross sections exist below 40 MeV for $^{59}Co(n,x)^{56,57,58}Co$ reactions and below 20 MeV for $^{59}Co(n,x)^{56}Mn$, ^{59}Fe reactions, the experimental data are scarce in higher energy region. In order to recommend the cross sections, the experimental data availably were evaluated so as to guide the theory calculation for higher energy region. The theory model parameters in the calculation were adjusted to fit the measured data. The cross section of $^{59}Co(n,x)^{56,57,58}Co$, $^{52,54,56}Mn$, ^{59}Fe reactions were evaluated and calculated from threshold energy to 100 MeV. All of recommended cross sections were determined based on the evaluated experimental data and improved theoretical calculations.

1 $^{59}Co(n,x)^{56,57,58}Co$ Reactions

The $^{56,57,58}Co$ products come from $^{59}Co(n,4n)$, (n,3n), (n,2n) reactions. Due to ^{59}Co is the sole isotope of the element, no other reactions lead to $^{56,57,58}Co$ productions. For $^{59}Co(n,2n)^{58}Co$ reaction, the measured data are available [1~41] from threshold energy to 40 MeV and shown in Fig. 1. The measured data were mainly carried out by activation method, some data by large liquid scintillation method. The evaluation at 14.7 MeV is carried out firstly based on the data measured by Frehaut[21], Greenwood[27], Garlea[28], Meadows[32], Ikeda[35], Kobayashi[36], Zhao Wenrong[37], Li Tingyan[38] and Mannhart[39] around 14 MeV. The recommended cross section is 770 ± 10 mb. The present result is consistent with recent evaluated values of Zhao Wenrong [37], Cai Dunjiu [42] from CIAE and higher than the cross section from ENDF/B-6. The experimental data of Vesser[17], Frehaut[21], Ikeda[35], Zhao Wenrong[37] and Mannhart[39] are normalized to the recommended value at 14.7 MeV. The comparisons among this evaluated values and the data of ENDF/B-6, JENDL-3, CENDL-2 are shown in Fig. 2.

At present evaluation, the measured data of Frehaut[21], Li Tingyan[38] and Mannhart[39] below 12 MeV and the measured data of Bormann[12], Veeser[17], Ghoran[20] Provoper[22], Huang Jianzhou[33] above 12 MeV were adopted. Recently activation cross section for the $^{59}Co(n,x)^{56,57,58}Co$ reactions have been measured above 28 MeV energy range by Uno[40] with p+Li neutron source using activation technique. Therefore, the recommended data for $^{59}Co(n,2n)^{58}Co$ reaction were obtained between threshold and 40 MeV based on experimental data. The recommended cross sections for $^{59}Co(n,x)^{58}Co$ reaction from thresh-

old to 100 MeV were obtained based on experimental data and calculated theoretical results[41] and shown in Fig. 3.

The measured data for $^{59}Co(n,x)^{56,57}Co$ reactions were carried out based on the activation cross section of Uwamino[41] using p + Be and of Uno[40] using p + Li neutron source with activation technique at higher energy range. The recommended data for $^{59}Co(n,x)^{57}Co$ reaction were obtained based on the experimental data mentioned above and our theoretical results. The calculated data for $^{59}Co(n,x)^{56}Co$ reaction are recommended after normalizing to only measured value at 38.3 MeV. The cross sections mentioned above are also shown in Fig. 3.

2 $^{59}Co(n,x)^{52,54,56}Mn$

For $^{59}Co(n,x)^{52,54,56}Mn$ reactions, the experimental data exist for $^{59}Co(n,\alpha)^{56}Mn$ reaction from threshold to 20 MeV. Our evaluated value at 14.7 MeV is 31.15 ± 0.65 mb which is consistent with ones of Zhao Wenrong[37]. The evaluated data for $^{59}Co(n,x)^{52,54,56}Mn$ reactions were obtained based on the experimental data of Bahal[25], Garlea[28], Berrada[30], Ikeda[35], Li Tingyan[38], Mannhart[39], Liskien[52], Huang Jianzhou[56], Agrawal[57], and Meadows[59] below 20 MeV and calculated theoretically data above 20 MeV. Both of experimental and calculated data are consistent each other within experimental errors between 18 to 20 MeV.

For $^{59}Co(n,x)^{52,54}Mn$ reactions, no experimental data are available. By using the model parameters adjusted based on the evaluated data for $^{59}Co(n,\alpha)^{56}Mn$ reaction below 20 MeV, the cross sections for the $^{59}Co(n,x)^{52,54,56}Mn$ reaction were calculated. The recommended results for $^{59}Co(n,x)^{52,54,56}Mn$ reactions are shown in Figs. 4~6.

3 $^{59}Co(n,x)^{59}Fe$ Reaction

The ^{59}Fe product come from $^{59}Co(n,p)^{59}Fe$ reaction. The measured data available exist from threshold energy to 20 MeV. The cross sections were evaluated by Zhao Wenrong[37] from threshold to 20 MeV. Present evaluation improved greatly the previous evaluation by supplementing the accuracy measured data of Mannhart[39], especially in the energy region 8 to 15 MeV where experimental data had been very scarce. The evaluated data for $^{59}Co(n,x)^{59}Fe$ reaction were obtained based on the experimental data of Li Tingyan[38], Mannhart[39], and Smith[64,65] below 20 MeV and calculated theoretically values are consistent with experimental data between 17 to 20

MeV The recommended data for $^{59}Co(n,x)^{59}Fe$ reaction are shown in Figs 7~8.

4 Summary

At present work, the evaluated cross section around 14 MeV are in good agreement with other evaluated data as shown in the following table:

The comparison of cross sections (in mb) at 14.32 MeV

Reactions	Present work	Other work
$^{59}Co(n,2n)^{58}Co$	732.16±11	740.3 ±27.1 [39]
		745.8 ± 9.00[42]
		734.4 ±12.0 [37]
$^{59}Co(n,\alpha)^{56}Mn$	31.76± 0.8	31.46± 1.16[39]
		31.34± 0.80[37]
		31.50± 0.60[42]
$^{59}Co(n,p)^{59}Fe$	50.6 ± 1.4	50.63± 2.34[37]
		48.90± 1.40[42]

The cross sections of $^{59}Co(n,x)^{56,\ 57,\ 58}Co$ reactions were recommended based on the measured data of Vesser[17] using large liquid scintillation method and recently measured data using activation method of Uno[40] between 20 and 40.0 MeV. Therefore, the evaluated data are very useful for guiding the theoretical calculation in higher energy

The present evaluated data of $^{59}Co(n,x)^{56}Mn$ and $^{59}Co(n,p)^{59}Fe$ reactions are higher than the previous evaluated data below 12 MeV and reproduce the new experimental data very well. The inconsistency of evaluated values below 15 MeV has been improved. For $^{59}Co(n,\alpha)$ and $^{59}Co(n,p)$ reactions, each measured data of Mannhart[39] were accompanied with a "gas-out" data in order to subtract parasitic neutron produced in the gas cell structure and breakup neutrons from D(n,np) reaction. The new measured data of Mannhart[39] for $^{59}Co(n,\alpha)$ and $^{59}Co(n,p)$ reaction are higher than those evaluated previously. Therefore, present evaluated data improved the previous evaluated results below 14 MeV and extended energy range up to 100 MeV.

Acknowledgements

The authors are indebted to IAEA (International Atomic Energy Agency),

CNNC (China National Nuclear Corporation) and CIAE for their supports, and thank to Drs. A. B. Pashchenko, T. Benson, O. Schwerer, Lu Hanlin, Zhao Wenrong for their kind help and suggestions.

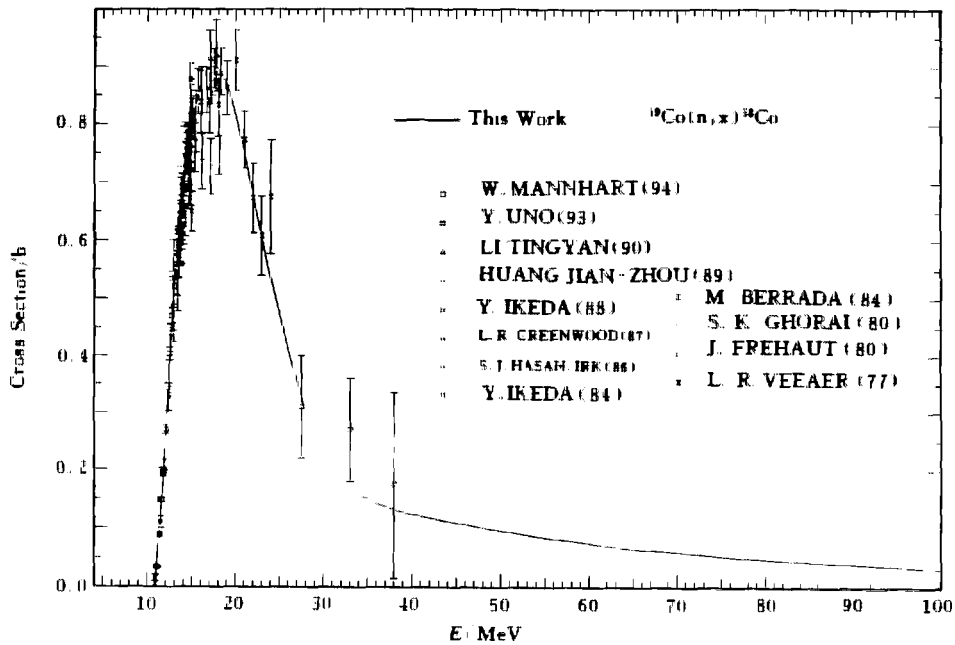

Fig. 1 Comparison of evaluated & measured data for ^{59}Co(n,x)^{58}Co reactions

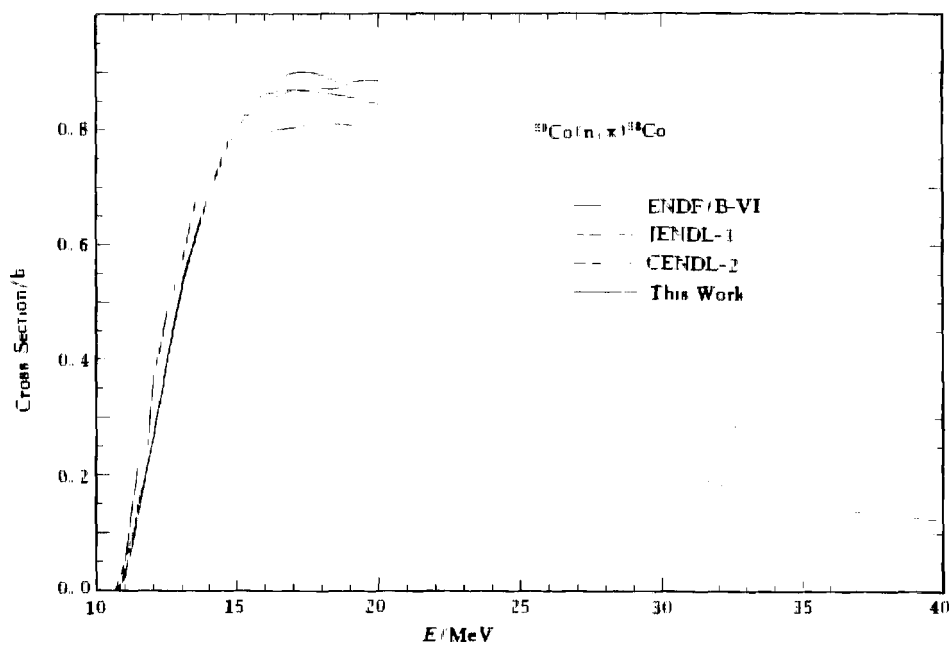

Fig 2 Comparison of evaluated data for ^{59}Co(n,x)^{58}Co reactions

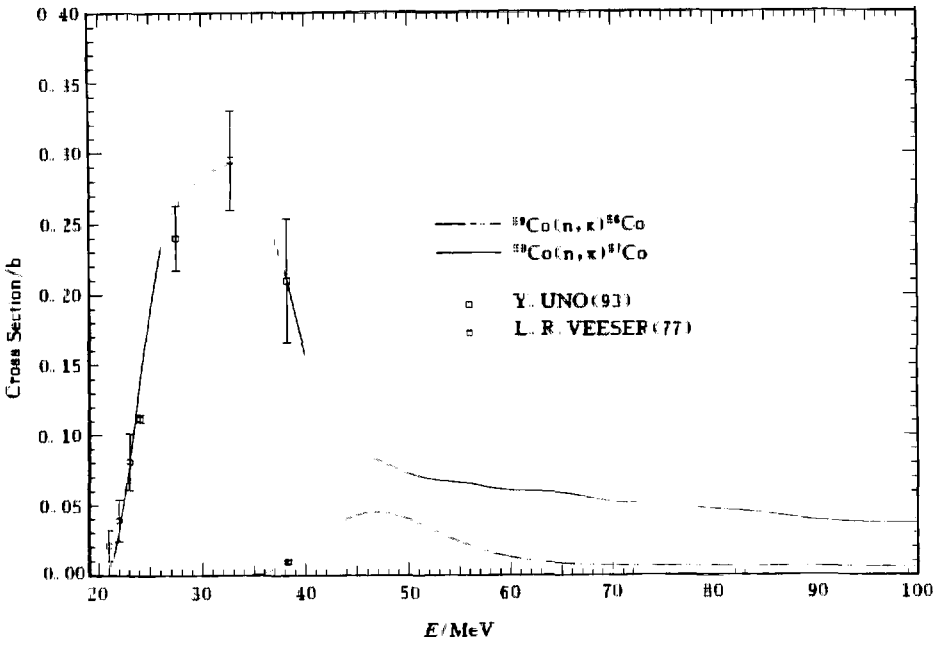

Fig. 3 Evaluated & measured data for $^{59}Co(n,x)^{57,56}Co$ reactions

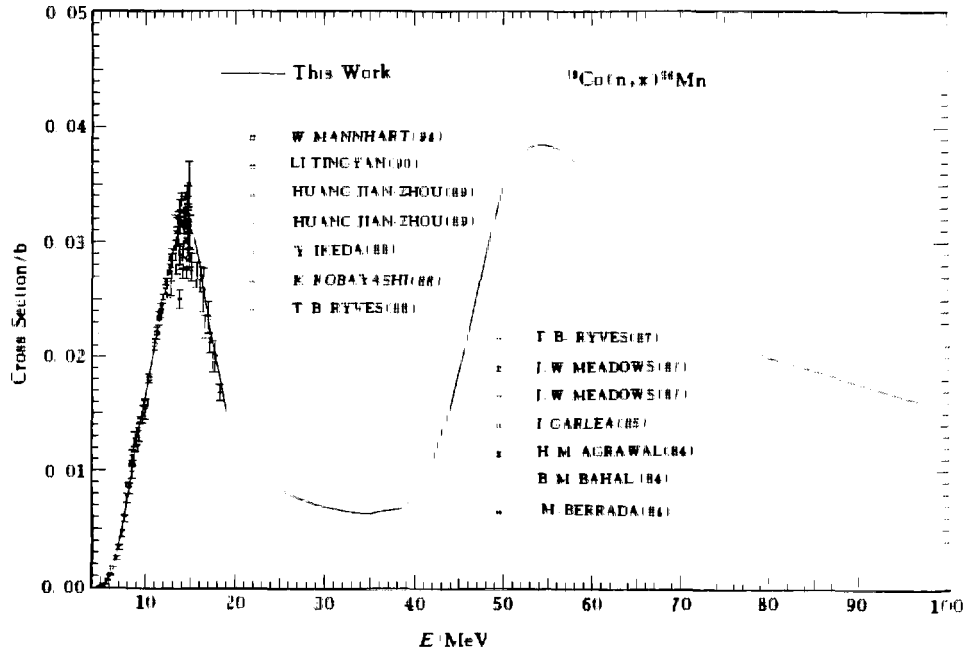

Fig. 4 Comparison of evaluated & measured data for $^{59}Co(n,x)^{56}Mn$ reactions

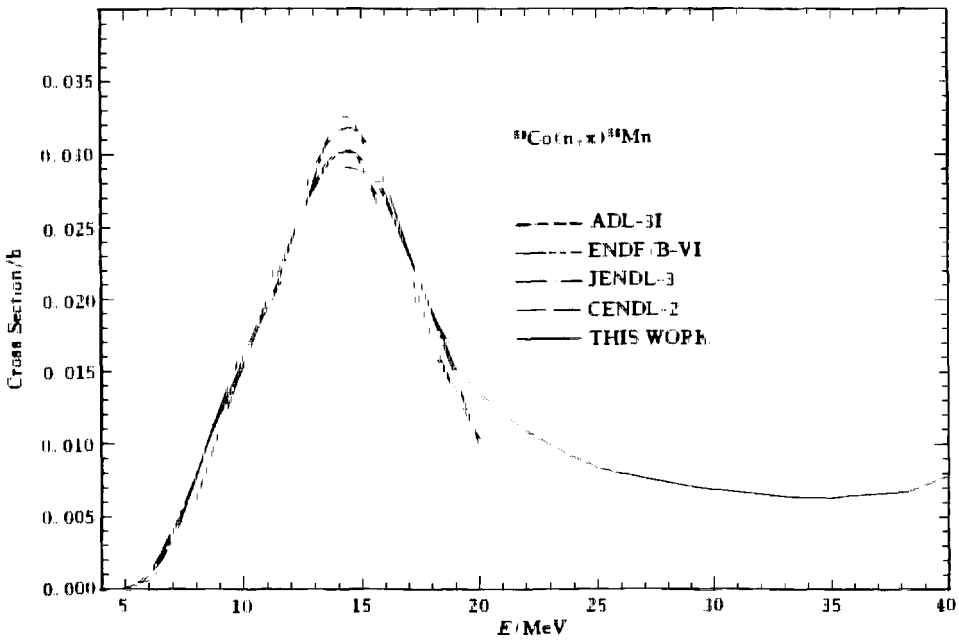

Fig. 5 Comparison of evaluated data for $^{59}Co(n,x)^{56}Mn$ reactions

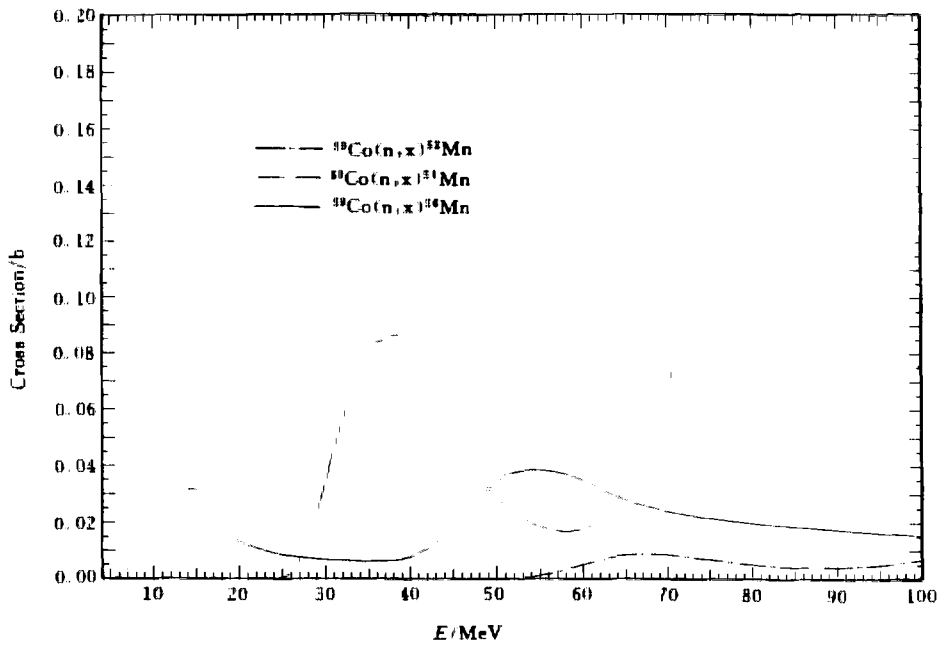

Fig. 6 Evaluated data for $^{59}Co(n,x)^{56,54,52}Mn$ reactions

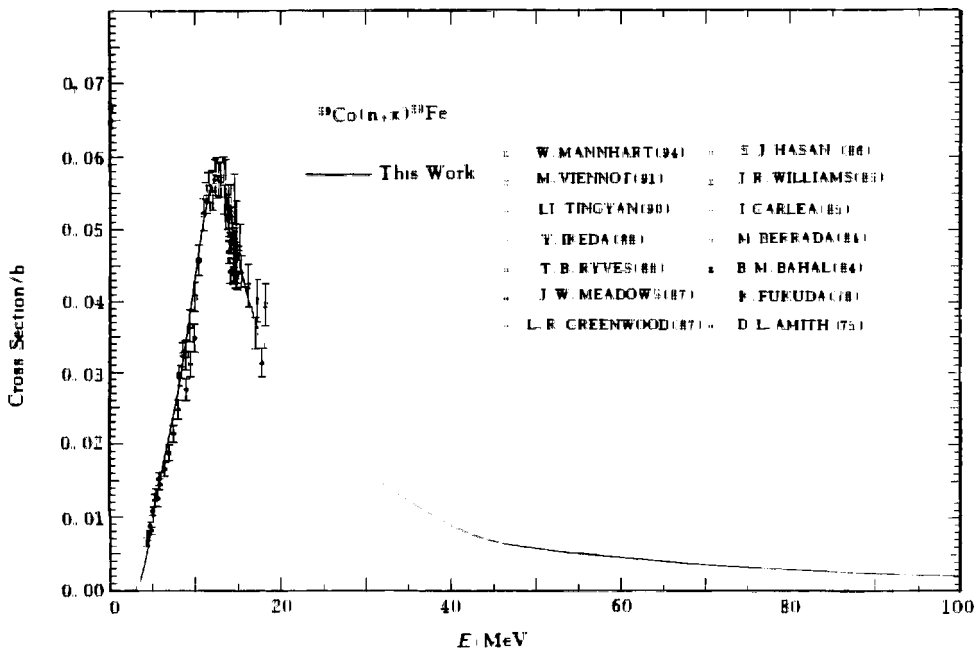

Fig. 7 Comparison of evaluated & measured data for ^{59}Co(n,x)^{59}Fe reactions

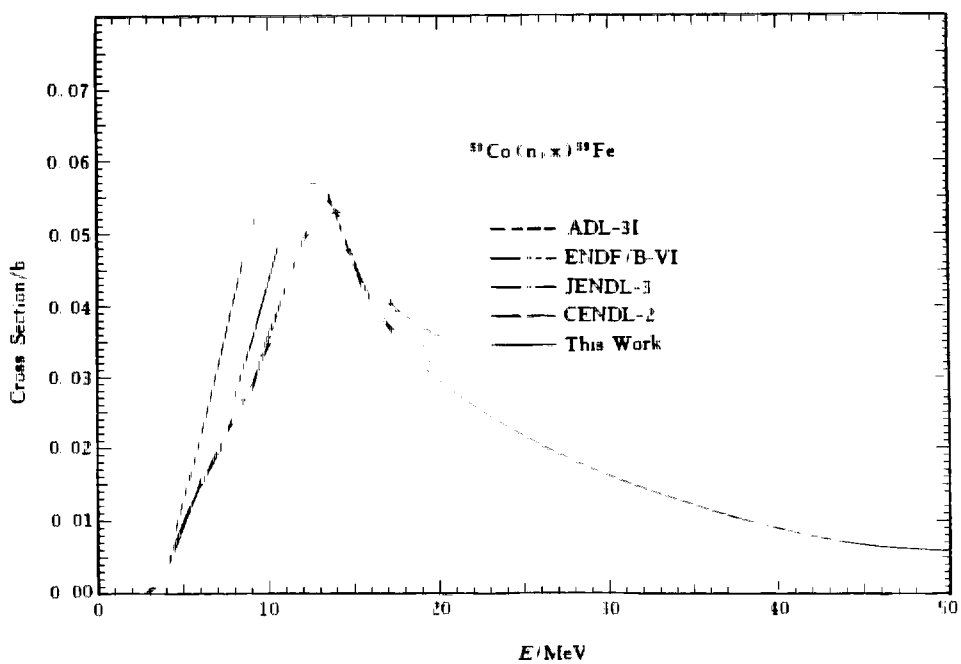

Fig 8 Comparison of evaluated data for ^{59}Co(n,x)^{59}Fe reactions

References

[1] V. J. Ashby et al , EXFOR 11632004(1958)

[2] E. Weigold, Austra. J Phys. 13, 186(1960)

[3] B. D Kern et al., A-KTY-59 / 60. 3(1960)

[4] M Bormann et al , J. Phys RAD. 22, 602(1961)

[5] R. Wenusch et al., OAWA, 99, 1(1962)

[6] E. Weigold et al., Nucl Phys., 32, 106(1962)

[7] J Cabe et al , EAND(E)-49L, 82(1963)

[8] B. Granger et al., EANDC(E)-49L, 83(1963)

[9] J M F Jeronymo et al., Nucl. Phys., 47, 157(1963)

[10] J E. Strain et al., ORNL-3672(1965)

[11] A. Paulsen et al., J. Nucl. Energy-AB, 19, 907(1965)

[12] M Bormann et al , J. ZN, A21, 988(1966); EANDC(E)-66, 42(1966)

[13] S. Okumura, Nucl. Phys., A93, 74(1967)

[14] P. Decowski et al., Nucl Phys., A112, 513(1968)

[15] O. A Salnikov et al., YK-7, 102(1972)

[16] J Araminowicz, INR-1464, 14(1973)

[17] L. R. Veeser et al., Phys Rev C16, 1792(1977)

[18] JU. E. Kozyr et al., EXFOR 40596020(1977)

[19] K. Fukuda et al., NEANDC(J)-56U, 44(1978)

[20] S. K. Ghorai et al , J. Ann. Nucl. Energy, 7, 41(1980)

[21] J. Frehaut et al , BNL-NCS-51245, 399(1980)

[22] G. A. Prokopets et al , EXFOR 41102023

[23] A. Reggoug et al., MOH-5, 14(1982)

[24] N T Molla et al., INDC(BAN)-002, 1(1983)

[25] B. M. Bahal et al., GKSS-84-E(84); NEANDC(E) 252U, 28(1984)

[26] Y. Ikeda et al., Proc. Conf. on Nucl Data for Scie. and Tech , 1, 175(1985) Santa Fe USA

[27] L. R Greenwood, DOE-ER-0046-21, 15(1985)

[28] I Garlea et al , INDC(GDR)-34 / GI(1985)

[29] J. Rev. Roum. Phys 30, 673(1985), ZFK-562, 126(1985)

[30] M. Berrada et al , INDC(MOR)-003 / GI(1985)

[31] S. J. Hasan., J. Phys G12, 389(1986)

[32] J. W Meadows et al., J. ANE, 14, 489(1987)

[33] Huang Jianzhou et al , Chin. J Nucl. Methods, A225, 103(1987)

[34] T. B. Ryves, J. Ann. Nucl. Energy, 15, 561(1988)

[35] Y. Ikeda et al., JAERI-1312(1988)
[36] K. Kobayashi et al., Proc. Conf. on Nucl. Data for Scie. and Tech., p. 261(1988) Mitto, Japan
[37] Zhao Wenrong et al., INDC(CPR)-16(1989)
[38] Li Tingyan et al., High Energy Phys. and Nucl. Phys., 14, 542(1990) in Chinese
[39] W. Mannhart, Conf. on Nucl. Data for Scie. and Tech., p. 258 (1994) Gathinburg, USA
[40] Yu Baosheng and Yoshitomo Uno, Private Communication(1995)
[41] Uwamino et al., Nucl. Sci. and Tech., 31, 1(1994)
[42] Cai Dunjiu et al., INDC(CPR)-024(1991)
[43] Shen Qingbiao et al., CRP Report (1995)
[44] E. B. Paul et al., Can. J. Phys., 31, 267(1953)
[45] H. G. Blosser et al., PR, 110, 531(1958)
[46] E. Weigold et al., Austr. J. Phys., 13, 186(1960)
[47] I. L. Preiss et al., Nucl. Phys., 15, 326(1960)
[48] F. Gabbard et al., Phys. Rev., 128, 1276(1962)
[49] R. C. Barrall et al., AFWL-TR-68-134(1969)
[50] D. C. Santry et al., Can. J. Phys., 42, 1030(1964)
[51] C. S. Khurana et al., Nucl. Phys., 69, 153(1965)
[52] H. Liskien et al., JNE, A / B 19, 73(1965)
[53] E. Frevert et al., Acta. Phys. Austr., 20, 304(1965)
[54] V. N. Levkovskil et al., YF, 8, 7(1968)
[55] J. C. Robertson et al., JEN, 27, 531(1973)
[56] Huang Jianzhou et al., Chinese J. Nucl. Phys., 3, 59(1981)
[57] H. M. Agrawal, Trans. Amer. Nucl. Soc., 47, 431(1984)
[58] R. Fischer et al., Phys. Rev., C34, 460(1986)
[59] J. W. Meadows et al., Annual Nucl. Energy, 14, 489(1987)
[60] F. L. Hassler et al., Phys. Rev., 125, 1011(1962)
[61] H. K. Vonach et al., Nucl. Phys., 68, 445(1965)
[62] G. N. Maslov et al., YK-9, 50(1972)
[63] J. Dresler et al., INR-1464, 12(1973)
[64] D. L. Smith et al., Nucl. Sci. Eng., 58, 314(1975)
[65] D. L. Smith et al., Nucl. Sci. Eng., 60, 187(1976)
[66] M. Viennot et al., Nucl. Sci. Eng., 108, 289(1991)

Evaluation of the (n,p) Cross Sections for Natural Ni and Its Isotopes ^{58,60,61,62,64}Ni

Ma Gonggui Wang Shiming Zhang Kun

(Institute of Nuclear Science and
Technology, Sichuan University, Chengdu)

Introduction

Nickel is a very important structure material in nuclear engineering. The neutron activation cross section of the (n,p) reaction is very important for fusion reactor from the view point of monitoring neutron field in the context of radiation damage, radiation safety, neutron dosimetry, etc. The cross sections ^{58,60,61,62,64}Ni(n,p)^{58,60,61,62,64}Co were evaluated based on measured data and theoretical calculation from threshold to 20 MeV.

The natural nickel consists of five stable isotopes. Their abundances and threshold energies are listed in Table 1.

Table 1 Isotopic abundances and reaction threshold energies of nickel

Isotope	58	60	61	62	64
Abun. / %	68.27	26.1	1.13	3.59	0.91
Thre. / MeV	0.0	2.076	0.549	4.532	6.627

1 Evaluation of Cross Sections

1.1 ^{58}Ni(n,p)^{58}Co Reaction

There are 14 sets of experimental data[1-14] in the energy range from 4.0 to 17.8 MeV. The evaluated datum at 14.1 MeV was taken from Ref. [15]. Below 17.8 MeV, the (n,p) cross sections were obtained by fitting experimental data. Above 17.8 MeV, the recommended data were obtained by extrapolating the fitting experimental data to 20 MeV. The comparison of experimental data with evaluated ones is shown in Fig. 1.

1.2 $^{60}Ni(n,p)^{60}Co$ Reaction

There are 9 sets of experimental data[1, 3, 8, 10, 16~20] in the energy range from 4.0 MeV to 20.0 MeV. The evaluated datum was taken from Ref. [15] at 14.1 MeV. Above 4.0 MeV, the (n,p) cross sections were obtained by fitting experimental data. Below 4.0 MeV, the recommended data were obtained by extrapolating the fitting experimental data to threshold. The comparison of experimental data with evaluated ones is shown in Fig. 2.

1.3 $^{61}Ni(n,p)^{61}Co$ Reaction

There are 3 sets of experimental data[1, 21, 22] in the energy range from 5.3 to 9.5 MeV and around 14.0 MeV. The evaluated datum was taken from Ref. [15] at 14.1 MeV. Below 14.0 MeV, the (n,p) cross sections were given by fitting experimental data. Above 14.0 MeV, the recommended data were taken from calculated result, and normalized to the fitted data (85 mb) at 14.0 MeV. The comparison of experimental data with evaluated ones is shown in Fig. 3.

1.4 $^{62}Ni(n,p)^{62}Co$ Reaction

There are 8 sets of experimental data[1, 5, 20, 21, 23~26] around 14.0 MeV. The evaluated datum at 14.1MeV was taken from Ref. [15]. The recommended data were taken from calculated results with code UNF[27], and normalized to the fitted data (29 mb) at 14.0 MeV. The comparison of experimental data with evaluated ones is shown in Fig. 4.

1.5 $^{64}Ni(n,p)^{64}Co$ Reactions

Due to no experimental data for ^{64}Ni, the (n,p) cross sections were theoretically calculated with code UNF[27]. At 14.1 MeV, the evaluated datum 4.3 mb of Ref. [15] was used to normalize corresponding model calculated results (see Fig. 5).

1.6 The (n,p) Reaction for Natural Nickel

For natural Ni, there are only two sets of experimental data[28, 29] around 14.1 MeV. The evaluated datum at 14.1 MeV was taken from Ref. [15]. The (n,p) cross sections of natural Ni were obtained by summing the isotopic data

weighted by the abundance. The comparison of experimental data with evaluated ones is shown in Fig. 6. It is found that the present evaluation is in agreement with the experimental data.

2 Summary

Based on experimental data and theoretical calculation, the (n,p) cross sections for natural nickel and its isotopes were recommended in the neutron energy region up to 20.0 MeV. The present evaluated data were compared with ENDF/B-6, JENDL-3, BROND-2 and EFF-2. It is shown that the present evaluations agree with the measured data of Ni isotopes well.

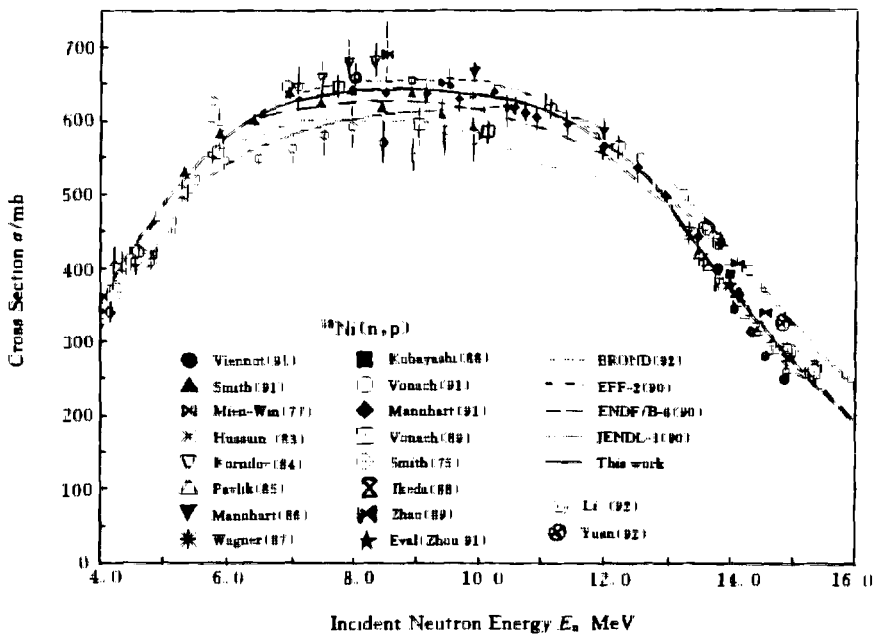

Fig. 1 (n,p) cross section for ^{58}Ni

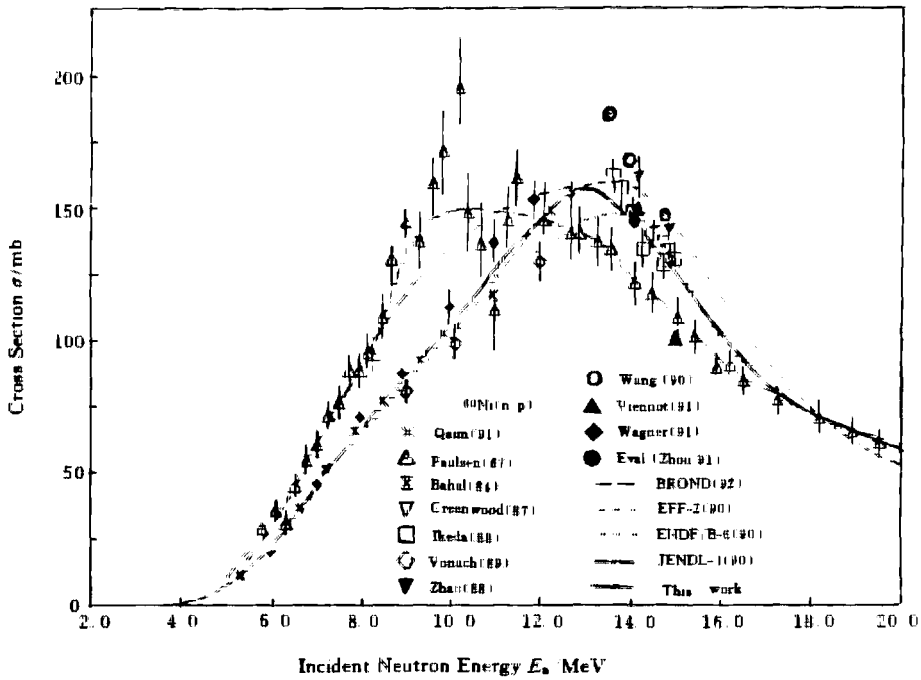

Fig. 2 (n,p) cross section for ^{60}Ni

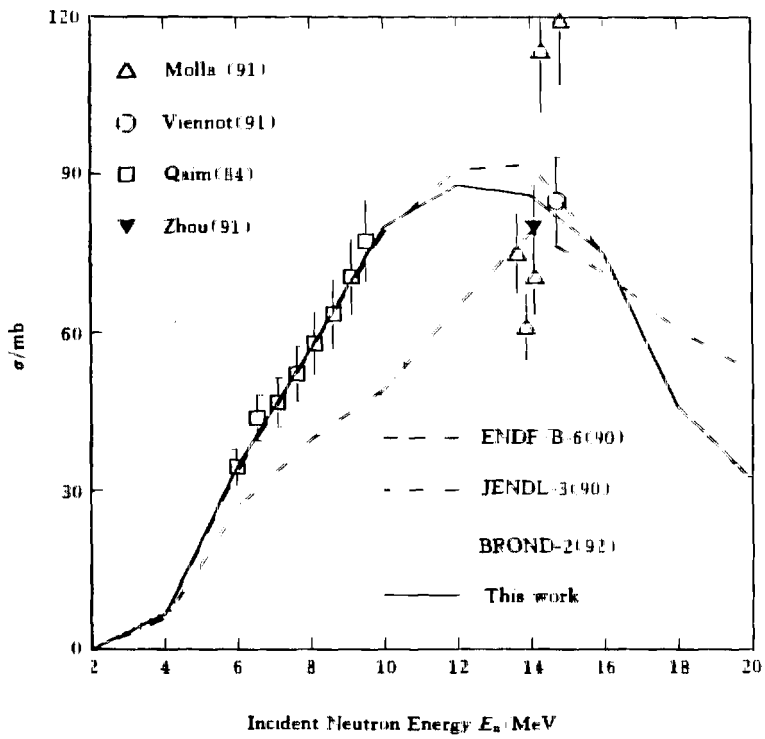

Fig. 3 (n,p) cross section for ^{61}Ni

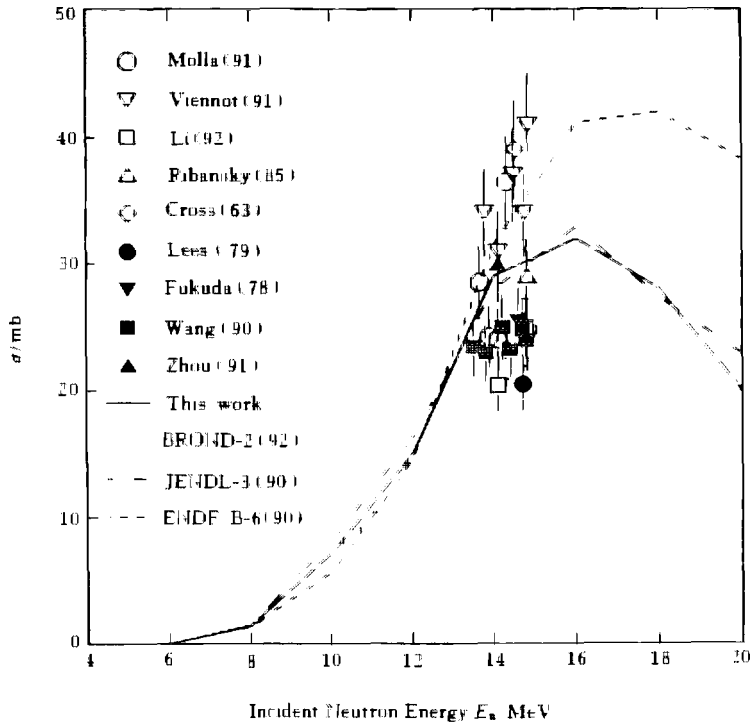

Fig. 4 (n,p) cross section for ^{62}Ni

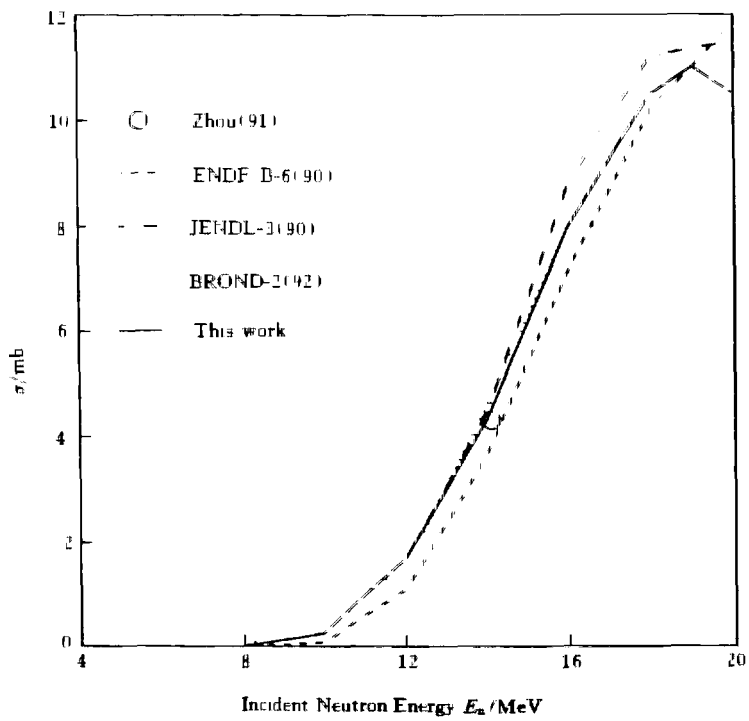

Fig. 5 (n,p) cross section for ^{64}Ni

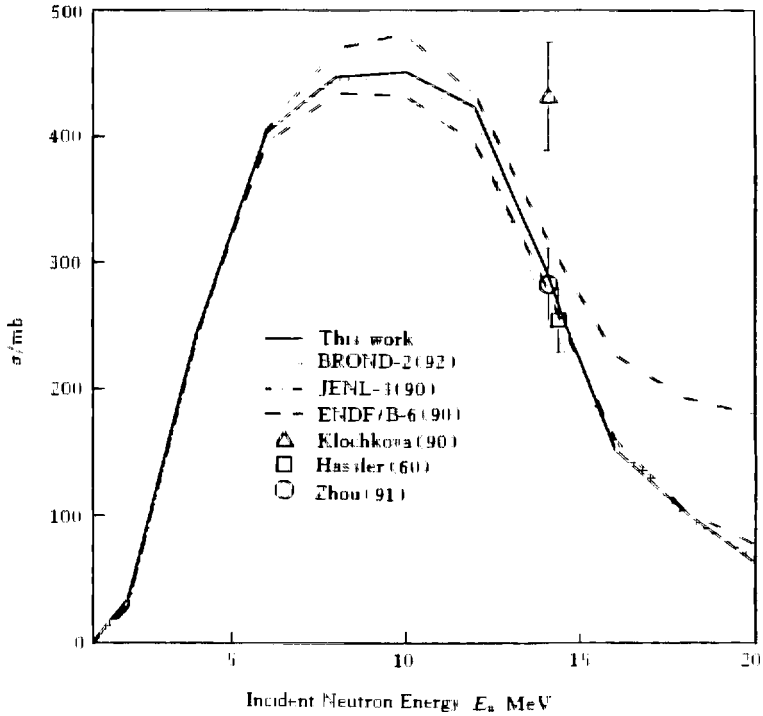

Fig. 6 (n,p) cross section for Ni

References

[1] M. Viennot et al., Nucl. Sci. Eng., 108, 289(1991)

[2] D. L. Smith et al., Proc. of Conf. on Nucl. Data for Science and Technology, Juelich, 282(1991)

[3] H. Vonach et al., Specialists Meeting on Neutron Act. Cross Sections for Fission and Fusion Eng. App., Argonne, 1989, 91Juelich, 282(1991)

[4] W. Mannhart et al., Proc. of Conf. on Nucl. Data for Science and Technology, Juelich, 282(1991)

[5] Li Tingyan et al., High Energy Physics and Nuclear Physics, 16(1), 151(1992)

[6] Yuan Junqian et al., High Energy Physics and Nuclear Physics, 16(1), 57(1992)

[7] A. Pavlik et al., Nucl. Sci. Eng., 90, 186(1985)

[8] Y. Ikeda et al., Report JAERI-1312, Japan Atomic Energy Research Inst., Tokai-mura (1988)

[9] K. Kobayashi et al., Proc. of Conf. on Nuclear Data for Science and Technology, Mito, 261(1988)

[10] Zhao Wenrong et al., Report CNDC-89014,Inst. of Atomic Energy, Beijing, (1989)

[11] M. Wagner et al., Ann. Nucl. Eng., 15, 363(1987)

[12] N. M. Kornilov et al., Atomnaya Energiya, 59, 128(1985)
[13] H. A. Hussain et al., Int. J. Appl. Radiat. Isot., 34, 731(1983)
[14] Wu Mienwin et al., Nucl. Sci. Eng., 63, 268(1977)
[15] Zhou Delin et al., A Progress Report to FENDL Meeting, (1991)
[16] S. M. Qaim et al., Proc. of Conf. on Nucl. Data for Science and Technology, Juelich, 291 (1991)
[17] M. Wagner et al., Proc. of Conf. on Nucl. Data for Science and Technology, Juelich, 358 (1991)
[18] L. R. Greenwood et al., ASTM-STP-956, 743(1987)
[19] B. M. Bahal et al., Report GKSS-84-E, Germany, (1984)
[20] Wang Yongchang et al., High Energy Physics and Nuclear Physics, 14, 923(1990)
[21] N. I. Molla et al., Proc. of Conf. on Nucl. Data for Science and Technology, Juelich, 355(1991)
[22] S. M. Qaim et al., Nucl. Sci. Eng., 88(2), 143(1984)
[23] I. Ribansky et al., INDC(CSR)-7, (1985)
[24] K. Fukuda et al., NEANDC(J)-56/U, 44(1978)
[25] E. W. Lees et al., AERE-R-9390, (1979)
[26] M. G. Cross et al., EANDC (CAN)-16, 1(1963)
[27] Zhang Jingshang., Nucl. Sci. Eng., 114, 55~63 (1993)
[28] F. L. Hassler et al., Phys. Rev., 125, 1011(1962)
[29] Klochkova et al., 40th All-Union Conf. on Nucl. Spec. and Nucl. Struc., Leningrad, USSR, 276(1990)

The Evaluation of H Total Cross Section from 20 MeV to 2 GeV

Liu Tingjin

(China Nuclear Data Center, CIAE)

The H total cross section was evaluated in the neutron energy region from 20 to 2000 MeV. 39 sets of experimental data were collected from EXFOR experimental data library, CINDA, INIS index and recent reports. The measured data were analyzed, evaluated, compared and processed, and as a result, 11 sets

of data[1~11] were selected.

The recommended experimental data were fitted by using spline fit program with knot optimization[12], the fit values are taken as recommended ones.

Both the statistical and systematical errors were analyzed and given out carefully for each set of data. The differences among the data measured by different laboratories were determined quantitatively. The covariance matrix of the recommended values was constructed by taking into account of statistical, systematical uncertainties of each set of data and the differences among them. The uncertainty of the recommended values and the correlation coefficients among the different energy points are given (they are 0.55% ~ 1.5% and 0.70 ~ 0.95, respectively).

The data are compared with those from ENDF/B-6 (<100 MeV), the differences are 0.5% ~ 2.0% from 20 to 40 MeV, and almost the same in the energy region 40 ~ 100 MeV. The data also compared with other experimental data, they are in agreement within the data errors.

H total cross section has been widely used as standard cross section in low energy region (< 20 MeV), it also can be used in intermediate and high energy region for the nuclear data measurement and evaluation.

References

[1] J. C. Davis et al., PR/C, 3, 1798(1971)

[2] F. P. Brady et al., PRL, 25, 1628(1970)

[3] T. J. Devlin et al., PR/D, 8, 136(1973)

[4] M. N. Kreisler et al., PRL, 20, 468(1968)

[5] D. F. Measday et al., NP, 85, 142(1966)

[6] P. W. Lisowski et al., PRL, 49, 255(1982)

[7] R. K. Keeler et al., NP/A, 377, 529(1982)

[8] S. Cierjacks et al., PRL, 23, 866(1969)

[9] P. H. Bowen et al., NP, 22, 640(1961)

[10] D. L. Larson et al., ORNL-5787, 174(1980)

[11] A. Bol et al., PR/C, 32, 623(1985)

[12] Liu Tingjin et al., CNDP, 11, 116(1994)

Evaluation of Cross Sections for Neutron Monitor Reactions $^{90}Zr(n,x)^{89,88}Zr$, $^{88,87,86}Y$ from Threshold to 100 MeV

Yu Baosheng Shen Qingbiao Cai Dunjiu

(China Nuclear Data Center, CIEA)

The cross sections for $^{90}Zr(n,x)^{89,88}Zr$ and $^{90}Zr(n,x)^{88,87,86}Y$ reactions in intermediate energy region are useful in neutron field monitor, safety and material damage research Below 20 MeV, the evaluated cross sections for $^{90}Zr(n,2n)^{89}Zr$ reaction are recommended based on the recent experimental data, including the new measured results in CIAE (Above 20 MeV) The measured cross sections are still insufficient to do evaluation So the evaluation for $^{90}Zr(n,x)^{89,88}Zr$ and $^{90}Zr(n,x)^{88,87,86}Y$ reactions from threshold to 100 MeV are based on experimental and calculated data

1 For $^{90}Zr(n,x)^{89,88}Zr$ Reactions

In order to eliminate the discrepancies in the existing data, the background neutron effects need to be corrected and subtracted For 6~ 13 MeV neutron energy range, the background neutron of low energy comes mainly from D(d,np) break-up reactions and D(d,n) reaction It is noted that these effects increase with the neutron energy and strongly depend on the threshold of the specific reaction Recently, some accurate experimental data have been obtained

The cross sections for $^{90}Zr(n,2n)^{89}Zr$ reaction, many new experimental data were available The evaluation is based on these new measured data of Csicki[1], Ikeda[2], Kobayashi[3], Palvik[4] around threshold and above 18 MeV and Zhao Wenrong[5] from 13 to 19 MeV These new measured data make the evaluated data to be modified much more

The measured cross sections of Bayhurst[6] for $^{90}Zr(n,x)^{89,88}Zr$ reactions extend to 30 MeV The calculated data are close to the experimental data for $^{90}Zr(n,2n)^{89}Zr$ reaction around 25 MeV Therefore, the recommended cross sections for this reaction were obtained based on the evaluated experimental da-

ta below 25 MeV and theoretical calculated data[7] above 25 MeV

Only one measured datum exists at 28 MeV for $^{90}Zr(n,3n)^{88}Zr$ reaction[6], the theoretical calculated data are normalized to it as recommended one.

The recommended data are shown in Fig. 1

2 For $^{90}Zr(n,x)^{88,87,86}Y$ Reactions

The cross sections for $^{90}Zr(n,x)^{88,87,86}Y$ reactions were calculated, shown in Fig. 2 and recommended. The cross sections for $^{90}Zr(n,x)^{88}Y$ reaction can be used for the neutron field monitor as a proposed candidate reaction in the energy range between 30 to 50 MeV, for the decay data of ^{88}Y are very well known and the cross section is large enough.

Acknowledgements

The authors are indebted to IAEA (International Atomic Energy Agency), CNNC (China National Nuclear Corporation) and CIAE for their supports, and thank to Drs. A. B. Pashchenko, T. Benson, O. Schwerer, Lu Hanlin and Zhao Wenrong for their kind help and suggestions.

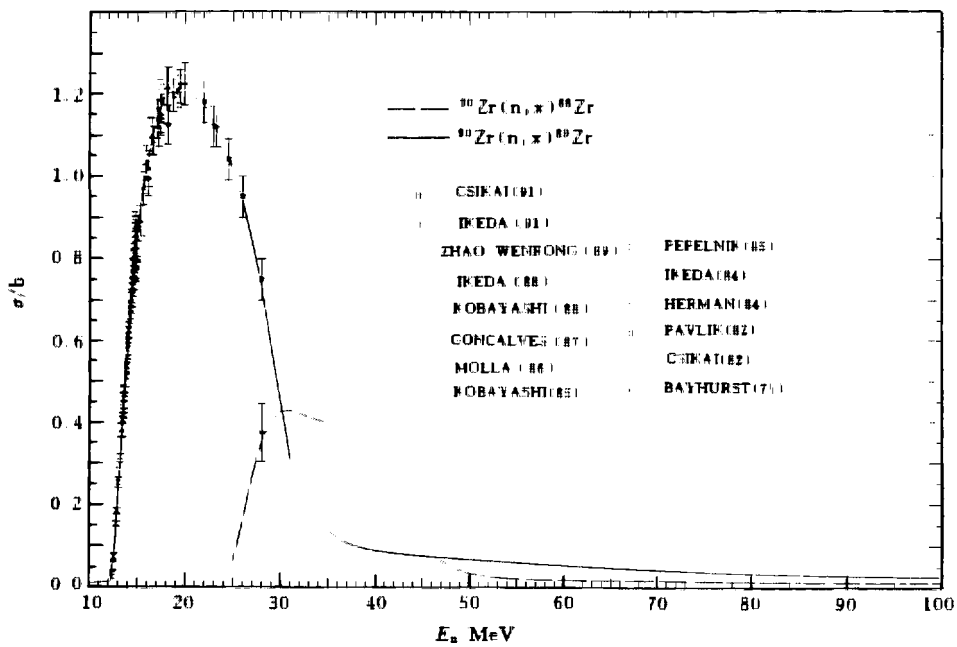

Fig. 1 Evaluated & measured data for $^{90}Zr(n,x)^{89,88}Zr$ reactions

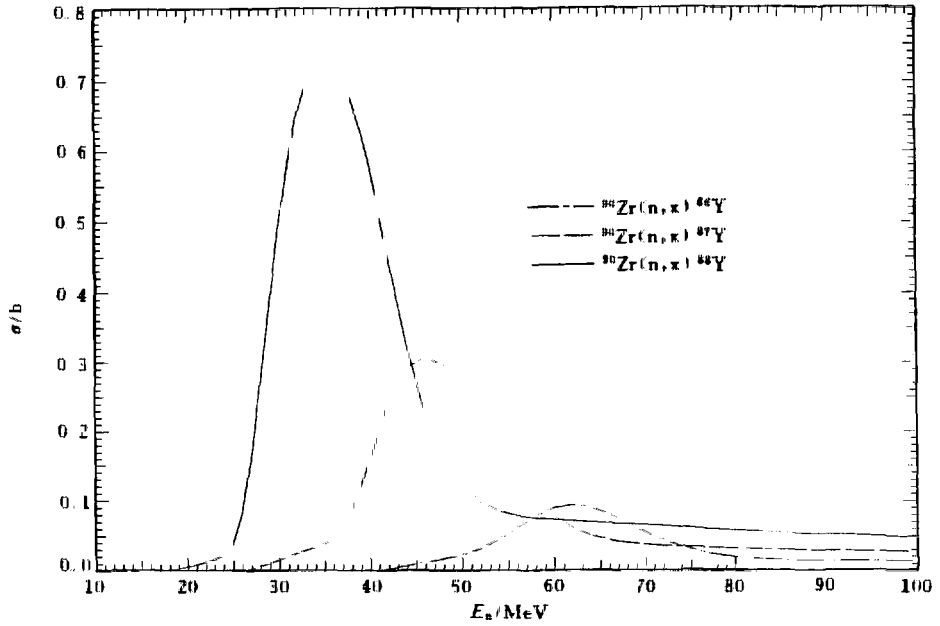

Fig 2 Recommended data for ^{90}Zr(n,x)$^{88, 87, 86}$Y reactions

References

[1] J. Csikai et al , Annual Nuclear Energy, 18, 1(1991)

[2] Y Ikeda et al , JAERI-M-91-032 (1991)

[3] K Kobayashi et al , NEANDC(J)-155, 52(1990)

[4] A Pavlik et al., EXFOR 21807002 (1988)

[5] Zhao Wenrong et al , INDC(CPR)-16 (1989)

[6] B A Bayhaurst et al., Phys Rev , C, 12, 451(1975)

[7] Shen Qingbiao et al , this CPR work report (1995)

Comparison of A Semi-empirical Method With Some Model Codes for Gamma-ray Spectrum Calculation

Fan Sheng Zhao Zhixiang

(China Nuclear Data Center, CIAE)

Abstract

Gamma-ray spectra calculated by a semi-empirical method are compared with those calculated by the model codes such as GNASH, TNG, UNF and NDCP-1. The results of the calculations are discussed

Introduction

The gamma-ray production data such as gamma-ray spectrum from neutron induced reactions is very important for nuclear engineering application. Some model programs such as TNG[1], GNASH[2], UNF[3] and NDCP-1[4] are able to be used to calculate the gamma-ray spectrum However these codes need to input and adjust a lot of parameters, such as optical model potential, level density and giant dipole resonance parameters as well as gamma-ray branching ratios etc. to fit the measured data. It is difficult and complex to adjust those parameters for the nuclei which are deficient in the measured data.

A semi-empirical method[5] based on evaporation model and exciton model has been developed to calculate continuum gamma-ray spectrum and multiplicity from neutron induced reactions In this method, constant temperature level density is adopted to simplify the calculation, and only one parameter R need to be adjusted to fit all measured data However the contribution of discrete level is not considered, and it can not be used to fissile nuclides. Using this method, the calculations for 12 targets, including Ti, V, Cr, Fe, Zn, Ni, Nb, Mo, Ta, W, Au and Pb, were performed. The parameter R was adjusted for each nuclei to fit the measured total gamma-ray spectra, and the systematics of the parameter R was studied

1 Model Parameter Used and Comparison

Gamma-ray spectra for ^{56}Fe, ^{93}Nb in JENDL-3 were calculated with GNASH, optical model parameters and level density parameters are given in the documents concerned respectively.

Gamma-ray spectrum of ^{93}Nb was calculated by TNG code, to fit the measured data the optical model parameters were adjusted (see Table 1). The results calculated with TNG and GNASH codes as well as the semi-empirical model are shown in Fig. 1, and all the calculations reproduce the measured data (see Fig. 1).

Table 1 Neutron optical model parameters for n+^{93}Nb

V_0(MeV)	V_1(MeV)	W'	W'_0(MeV)	W'_1(MeV)	a_v (fm)	R_v (fm)	R_D (fm)	a_d (fm)
48.0	−0.293	0	9.6	0	0.47	1.27	1.27	0.66

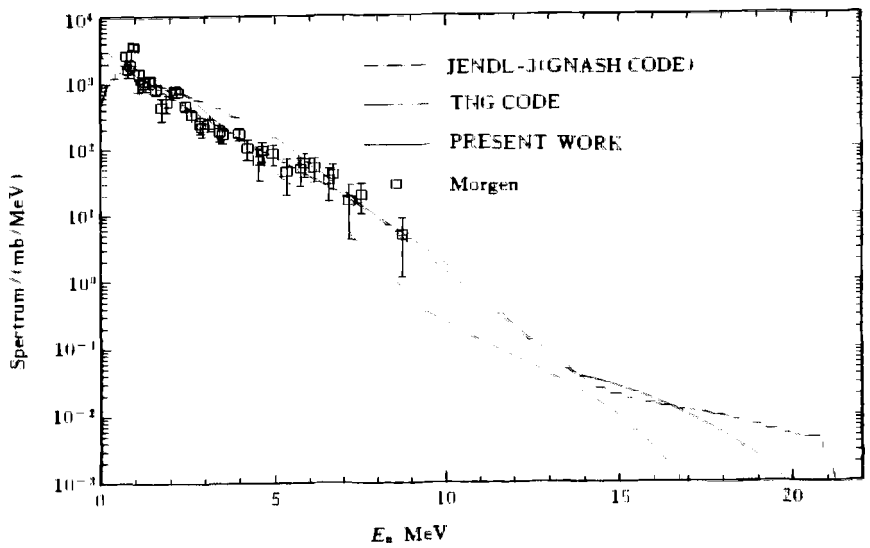

Fig. 1 The comparison of gamma-ray spectrum of ^{93}Nb at $E_n = 14$ MeV

Gamma-ray spectrum of ^{89}Y calculated by NDCP-1[6] code is in agreement with that calculated by using a semi-empirical model and systematics (see Fig. 2).

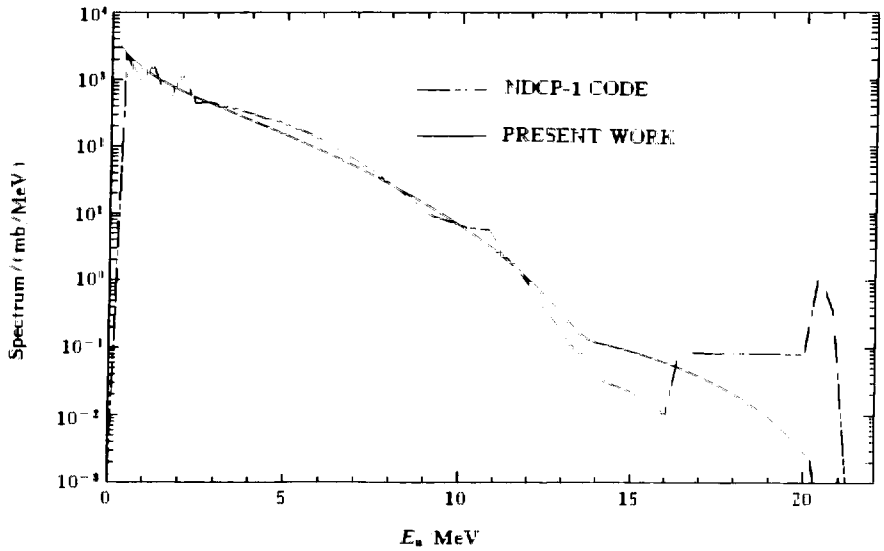

Fig. 2 The comparison of gamma-ray spectrum of ^{93}Y at $E_n = 14$ MeV

Gamma-ray spectrum of ^{56}Fe was calculated by UNF to fit the measured data, the optical model parameters were adjusted. (see Table 2). The comparison of the gamma-ray spectrum calculated by using a semi-empirical model with those calculated by using UNF and GNASH codes is shown in Fig. 3

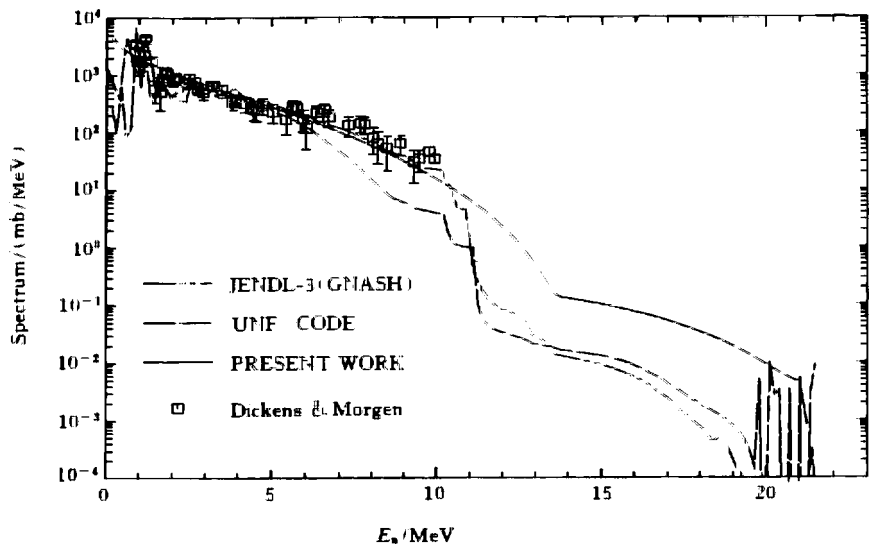

Fig. 3 The comparison of gamma-ray spectrum of ^{56}Fe at $E_n = 14$ MeV

Table 2 Neutron optical model parameters for n+^{56}Fe

A_R (fm)	A_S (fm)	A_{VV} (fm)	A_{SO} (fm)	X_R (fm)	X_S (fm)
0.55	0.45	0.45	0.55	1.25	1.25
X_V (fm)	X_{SO} (fm)	X_C (fm)	U_0 (MeV)	U_1 (MeV)	V_0 (MeV)
1.25	1.25	1.25	−2.70	0.32	58.00
V_1 (MeV)	V_{SO} (MeV)	W_0 (MeV)	W_1 (MeV)		
−0.32	6.20	16.80	0.70		

2 Conclusion and Discussion

There are some available measured data at low energy part of the gamma-ray spectrum ($E_\gamma \lesssim 10$ MeV), the results calculated by using the semi-empirical model and the model codes TNG, GNASH, UNF and NDCP-1 reproduced them well, but a big difference exists in the hard part of spectrum ($E_\gamma > 10$ MeV). This is a troublesome problem, for lack of experimental data.

The codes of TNG, GNASH, UNF and NDCP-1 can be used to calculate not only spectrum, but also cross sections, double-differential cross section etc. However, the semi-empirical method is can be used only to calculate gamma-ray spectrum, and need to input the cross sections of all reaction channels. The work to study a systematics formulas, which does not depend on the cross sections and only on the incident neutron energy and nuclear properties including mass number, atomic number, binding energy and separation energy, is very significant and will be performed in the future

Acknowledgements

The author would like to thank Dr C. Y. Fu (ORNL, USA) for providing the explanation of input data for TNG code, and Drs. Zhou Delin, Zhang Jinshang, Zhou Chunmei and Han Yinlu for helpful discussions.

References

[1] C. Y. Fu, A consistent Nuclear Model for Compound and Pre-equilibrium Reactions with Conservation of Angular Momentum. ORNL / TM-7402, (1980)

[2] P. G. Young, E. D. Arthur. GNASH: A Pre-equilibrium, Statistical Nuclear Model Code for Calculation of Cross Section and Emission Spectra. LA-6947, (1977)

[3] Zhang Jingshang, A Unified H-F and Exciton Model for Calculation DDX of Neutron Induced Reactions Below 20 MeV, Nucl. Sci. and Eng, 114, 55 (1993)

[4] Liu Jiangfeng et al., Program NDCP-1 and Theoretical Calculations on $n+^{16}O$, CNDP, No. 10, p. 28 (1993)

[5] Fan Sheng et al., A Semi-empirical Model for Calculation of Continuum Gamma-ray Spectrum and Multiplicity from Neutron Induced Reactions (to be Published)

[6] Liu Jiangfeng et al., CNDP, 14, 8(1995)

CN9700495

Nuclear Data Sheets Update for $A = 197$

Zhou Chunmei

(China Nuclear Data Center, CIAE)

The 1991 version of the Nuclear Data Sheets for $A = 197$ was evaluated in 1990. In present paper the Nuclear Data Sheets for $A = 197$ has been carried out on the basis of the nuclear reaction and decay experiments leading to all the nuclei with mass number $A = 197$ since cutoff date of the last evaluation, December 1989. Most evaluation data have been updated, or revised. The nuclei of updated data mainly are ^{197}Hg, ^{197}Pb, ^{197}Bi, and ^{197}Po. The level properties and their gamma radiations from reaction and decay experiments are presented by means of schemes or tables. The data set of HIGH SPIN LEVELS, GAMMAS for ^{197}Pb was added to. The adopted levels and adopted gamma radiations for all nuclei are shown in the tables. The experimental methods, references and necessary comments are given in the text.

The updated version of Nuclear Data Sheets for $A = 197$ has been put into the Evaluated Nuclear Structure Data File, ENSDF, at National Nuclear Data Center, Brookhaven National Laboratory, USA, and will be published in Data Sheets.

The Re-evaluation of ^{84}Rb Decay Data

Huang Xiaolong Zhou Chunmei

(China Nuclear Data Center, CIAE)

The decay data for ^{84}Rb were re-evaluated. The comprehensive analysis and theoretical calculations were done. The energies and intensities of γ rays and their internal conversion coefficients, energies and intensities of Auger electrons, conversion electrons and x-rays, were recommended. The decay scheme was also given. Finally the balance of radiation rays intensities and energies was checked.

Introduction

The ^{84}Rb is an important radionuclide and its decay data are fundamental data in nuclear applications. For recent ten years it has been evaluated by some authors [1, 2]. But the radiation energies and ray intensities of these evaluated data are not balanced. Obviously it is necessary to revise these evaluated data. In this paper, the decay data of ^{84}Rb were re-evaluated using the decay data evaluation system, and a complete set of decay data is given.

1 Half-life

Since 1955, the half-life of ^{84}Rb has been measured in four laboratories[3~6], shown in Table 1. The results are in agreement except Gehrling's [5] measurements, which is higher than other three measurements. So in present work, the weighted mean value, i. e. 32.85 ± 11 d, which was calculated by using three sets of measurements 33.0 ± 0.2, 33 ± 1 and 32.77 ± 0.14, is adopted.

Table 1 Half-life of ^{84}Rb

Year	$T_{1/2}$ / d	Ref.
1955	33.0 ± 0.2	3
1964	33 ± 1	4
1971	34.5 ± 0.2	5
1976	32.77 ± 0.14	6
1995	32.85 ± 0.11	present evaluation

2 Evaluation of Transition Energies and Intensities of ^{84}Rb

2.1 β^+ / ε Transition Energies and Intensities of ^{84}Rb

The experimental data on the β^+ / ε transition energies and intensities of ^{84}Rb have been reported since 1955. Analysis of the transition intensity balance for the levels of ^{84}Kr leads to two measurements, Gehrling's[5] results, i. e. I_ε(1.91 MeV) / I_ε(0.88 MeV) = 0.0217 ± 0.0002, I_ε(0.88 MeV) / $I_{\beta+}$(0.88 MeV) = 5.57 ± 0.07, $I_{\beta+}$(0.88 MeV) / $I_{\beta+}$(0 MeV) = 1.008 ± 0.012, and Goedbloed's[7] results, i. e. P_L(0.88 MeV) / P_K(0.88 MeV) = 0.119 ± 0.002, $I_{\varepsilon K}$(0.88 MeV) / $I_{\beta+}$(0.88 MeV) = 3.96, are partially taken into account. The other measurements, Booij's[8] results, i. e. $E_{\beta+}$(881.6 keV) = 780.6 ± 1.3 keV, $E_{\beta+}$(0 MeV) = 1657.8 ± 0.8 keV, Schulz's[9] results, i. e. P_L(0.88 MeV) / P_K (0.88 MeV) = 0.116 ± 0.002, and Welker's[3] results, i. e. P_L(0.89 MeV) / P_K (0.89 MeV) = 0.12 ± 0.05, I_ε(0.89 MeV) / $I_{\beta+}$(0.89 MeV) = 5.15 ± 0.38, I_ε(0 MeV) / $I_{\beta+}$(0 MeV) = 2.06 ± 0.36, are not adopted because they are probably too high due to summation and pileup effects.

As a result, the present evaluated transition energies are obtained by subtracting level energies from Q value (2681.3 ± 2.3 keV), while the evaluated transition intensities are calculated by the following quantities $I_{\beta+}$(881.4 keV) / $I_{\beta+}$(0 keV) = 0.96 ± 0.05, I_ε(0 keV) / $I_{\beta+}$(0 keV) = 1.028 ± 0.012 (theory), I_ε(881.4 keV) / $I_{\beta+}$(881.4 keV) = 3.9 ± 0.2 (theory), I_ε(1910 keV) / I_ε (881.4 keV) = 0.0217 ± 0.0002. They are presented in Table 2, and the associated $logf\ T_{1/2}$ values calculated by LOGFT computer program is also given.

Table 2 Transition intensities and $logf\ T_{1/2}$ values in the $\varepsilon+\beta^+$ decay of ^{84}Rb

E_i / keV *	I_ε / %	I_{β^+} / %	$I_{\varepsilon+\beta^+}$ / %	$logf\ T_{1/2}$
1897.784 ± 0.010	1.10 ± 0.04	0	1.10 ± 0.04	8.076 ± 0.017
881.615 ± 0.003	54.6 ± 1.3	14.0 ± 0.4	68.6 ± 1.4	7.111 ± 0.010
0	13.4 ± 0.6	13.1 ± 0.5	26.5 ± 0.8	9.505 ± 0.014

* — From E_γ and decay scheme using least-squares fitting.

2.2 β^- Transition Energies and Intensities of ^{84}Rb

In 1958, Benczer[10] measured $I_{\beta-}$(0 keV) / $I_{\beta+}$(0 keV) ≤ 0.29. If $I_{\beta+}$(0 keV) = 13.1 ± 0.5 (see ^{84}Rb ε decay), the calculated intensities of β^- is about

3.8%. Having no γ-rays in this decay, the evaluated energies is Q value (894 ± 4 keV) and intensities is 3.8 ± 0.5 (per 100 decays) because this decay branch to intensity per 100 decays of the parent nucleus is 3.8%. The final results are listed in Table 3, and the $logf T_{1/2}$ value is also given.

Table 3 Transition intensities and $logf T_{1/2}$ values in the β^- decay of ^{84}Rb

E_i / keV	I_{β^-} / %	$logf T_{1/2}$
0	3.8 ± 0.5	9.41 ± 0.09

3 Evaluation of the γ Energies and Intensities of ^{84}Rb

All measurements of γ energies and relative intensities of ^{84}Rb are listed in Table 4. After checking their measured methods and analysing error, the γ energies measured by Greenwood's[11] and relative intensities measured by Grutter[12] are directly adopted as the recommended values, shown in Table 5.

If the absolute γ intensities are required, the normalization factor N for converting relative intensities to absolute intensities is calculated. As mentioned above, the transition intensities of $\varepsilon+\beta^+$ decay to ground state is 26.5 ± 1.1, while the $\varepsilon+\beta^+$ decay branch to intensity per 100 decays of the parent nucleus is 96.2 ± 0.5, it is easy to deduce that $N = 0.689 \pm 0.009$

In addition, values of energies and intensities of x-ray, Auger electron and internal conversion electron in the $\varepsilon+\beta^+$ decay of ^{84}Rb are also calculated by RADLST computer program (see Table 6).

Table 4 Experimental values of energies and relative intensities of γ rays in the $\varepsilon+\beta^+$ decay of ^{84}Rb

Year	Author	E_γ / keV	I_γ	Ref.
1982	Grutter	881.65±0.10 1016.18±0.10 1897.84±0.15	100 0.506±0.015 1.07±0.03	12
1979	Greenwood	881.610±0.003 1016.162±0.013 1897.761±0.014		11
1972	Hill	881.6±0.1 1015.9 1897.6±0.2		13
1971	Gehrling		100 0.47±0.03 1.37±0.01	5
1967	Heath	881.46±0.20 1015.86±0.30 1897.02±0.30		14
1967	Vrzal		100 0.61±0.07 1.10±0.07	15

Table 5 Recommended values of energies, intensities and multipolarity of γ rays in the $\varepsilon+\beta^+$ decay of ^{84}Rb

E_γ / keV	multi. *	I_γ^*	I_γ^* / %
881.610±0.003	[$E2$]	100	68.9±0.9
1016.162±0.013	($M1+E2$)	0.506±0.015	0.35±0.01
1897.761±0.014	[$E2$]	1.07±0.03	0.74±0.03

* — Taken from Ref. [1].

Table 6 Recommended values of energies and intensities of x-ray, Auger electron and internal conversion electron in the $\varepsilon+\beta^+$ decay of ^{84}Rb

KX_i	E_{KX_i} / keV	I_{KX_i} / %
$K_{\alpha 2}$	12.598±0.002	11.4 ±0.3
$K_{\alpha 1}$	12.649±0.002	22.1 ±0.5
K_β	14.1	5.64±0.16
AE	E_{AE} / keV	I_{AE} / %
L	1.500	76.0±0.4
K	10.80	21.5±0.4
CE_i	E_{CE_i} / keV	I_{CE_i} / %
K (881.61 γ)	867.284±0.004	0.039±0.008

4 Q Value

In 1993 Gudi, et al.[16], recommended a new set of data. In present work Q values are taken from their results. They are 2681.3± 2.3 keV and 894± 4 keV for ε / β^+ and β^- decay of ^{84}Rb, respectively.

5 Decay Scheme

The decay schemes of ε / β^+ and β^- decay of ^{84}Rb corresponding to the evaluated data are given in this work, shown in Fig. 1 and Fig. 2 respectively. It is noted that the γ intensities is γ transition intensities.

6 Checking in Physics

To ensure the balance of ray transition intensities and radiation energies, the balance calculations have been done. The results are listed in Tables 7, 8 and Table 9. It shows that the transition intensities and radiation energies are balanced.

Table 7 Comparison of the calculated balance of radiation intensities in the $\varepsilon+\beta^+$ decay of ^{84}Rb

Level / keV	RI* / (out)	RI* / (in)	RI* / (net)	Net / (calc.)	Net / (input)
0	0	101.07±0.03	−101.07±0.03	26.6±0.09	26.5±0.8
881.615±0.003	100.0	0.506±0.015	99.494±0.015	68.6±0.9	68.6±0.14
1897.784±0.010	1.58±0.04	0.000	1.58±0.04	1.09±0.03	1.10±0.04

RI* — Relative intensity (includes intenal conversion electrons)

Table 8 Comparison of the calculated balance of radiation energies in the $\varepsilon+\beta^+$ decay of ^{84}Rb

	E_β	E_{CE}	E_γ	E_{Recoil}	$E_{Neutron}$	E_{Total}	E_{QR}
Q_i	146.614	3.795	883.226	0.009	1521.338	2554.994	2579.411
ΔQ_i	±3.201	±0.095	±9.685	±0.003	±23.524	±25.641	±13.604

Table 9 Comparison of the calculated balance of radiation energies in the β^- decay of ^{84}Rb

	E_β	E_{CE}	E_γ	E_{Recoil}	$E_{Neutron}$	E_{Total}	E_{QR}
Q_i	12.647	0.0	0.0	0.0	21.325	33.972	33.972
ΔQ_i	±1.665	0.0	0.0	0.0	±2.807	±3.264	±4.473

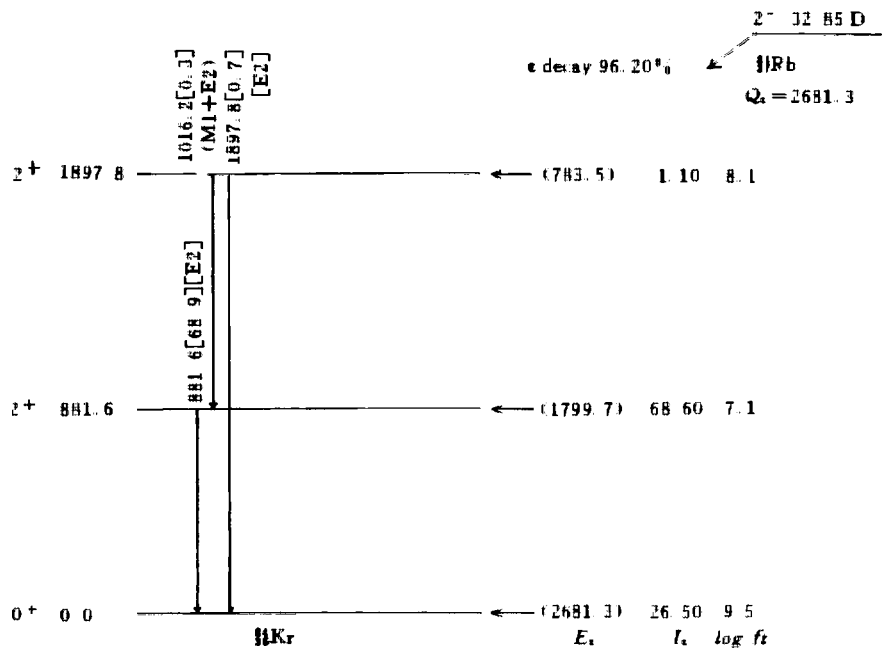

Fig. 1 The decay scheme of ^{84}Rb $\varepsilon+\beta^+$ decay

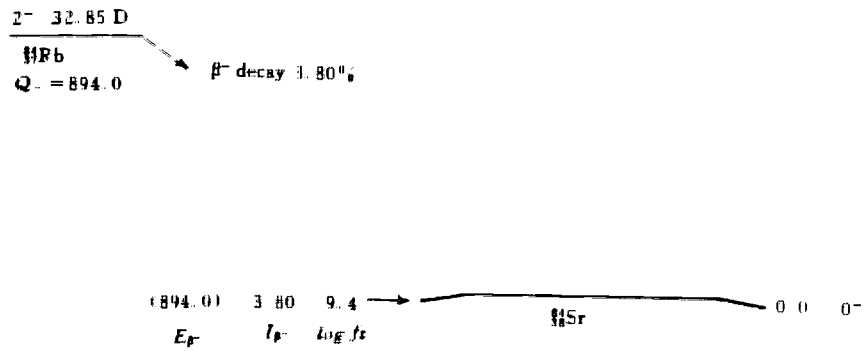

Fig 2 The decay scheme of ^{84}Rb β^- decay

References

[1] H. W. Muller et al., Nuclear Data Sheets, Vol. 27, 339(1979)

[2] H. W. Muller, Nuclear Data Sheets, Vol. 56, No 4, 551(1989)

[3] J. P. Welker et al., Phys. Rev., 100, 74(1955)

[4] L. M. Langer et al., Phys. Rev., 133, B1145(1964)

[5] V. Gehrling et al., Z. Phys., 246, 376(1971)

[6] J. E. Gindler, Inorg. Nucl. Chem. Lett, 12, 931(1976)

[7] W. Goedbloed et al., Nucl. Phys., A159, 409(1970)

[8] H. M. W. Booij et al., Nucl. Phys., A160, 337(1971)

[9] G. Schulz, Nucl. Phys., A101, 177(1967)

[10] N. Benczer, CU-177(1958)

[11] R. C Greenwood et al., Nucl. Instrum. Methods, 159, 465(1979)

[12] A. Grutter, Int Appl. Radiat Isotop, 33, 456(1982)

[13] J. C. Hill, Phys Rev, C5, 805(1972)

[14] R. L Heath, IDO-17222(1967)

[15] J. Vrzal, Bull. Acad. Sci. USSR Phys Ser., 31, 170(1967)

[16] A. Gudi et al., The 1993 Atomic Mass Evaluation (II), Nuclear Reaction and Separation Energies, Nucl. Phys, A565, 66(1993)

CN9700497

Nuclear High-Spin Data for $A = 174$, 176, and 184

Huo Junde

(Department of Physics, Jilin University)

Nuclear high-spin data are important in the frontier areas of nuclear structure physics. Nearly all nuclear physics groups active in high-spin research maintain a computerized data file of the level schemes deduced from their own experiments. Furthermore, several of those groups have also made an effort to produce data files for specific mass regions that address the needs of their own research program. While some of these files may have had a common origin in the Niels Bohr Institute data file, each laboratory produced a separate data file which then evolved on its own. Attempts to standardize the diverging data files have not been successful, due mainly to the lack of an organizer devoted to this

task. Furthermore, the recent explosion of data on high-spin states, associated with the advent of sizable arrays of Compton-suppressed germanium detectors, has made it nearly impossible for any of the individual groups to maintain a comprehensive file for even a limited number of nuclides in the deformed region. In order to keep abreast of such developments it is essential that a high-spin data file be in place as soon as possible.

At U. S. Nuclear Data Network (USNDN) meeting held at Asilomar in October 1993, Sub-task force on high-spin data evaluation was set up in order to evaluate and compile the gamma-ray data from heavy-ion reaction.[1] It was determined that a high-spin evaluation activity will be started at IAEA Advisory Group meeting held by the Lawrence Berkeley Laboratory, USA, in May 1994[2].

High-spin data for $A = 174$, 176, and 184 mass chains were evaluated during I visited Oak Ridge National Laboratory, USA in 1995

1 $A = 174$ High-Spin Data

The nuclear high-spin data for $A = 174$ has been evaluated using experimental nuclear high-spin data up to June 1995. The information for ^{174}Yb, ^{174}Lu, ^{174}Hf, ^{174}Ta, ^{174}W, ^{174}Re, ^{174}Os, and ^{174}Pt from various reaction experiments together with their adopted high-spin levels and gamma transition properties presented.

There is a coulomb excitation data file in which 4 rational bands exist in ^{174}Yb high-spin data.

High-spin levels, gammas, ^{170}Er(^{7}Li, 3nγ), and ^{176}Yb(p,3nγ) data files exist in ^{174}Lu high-spin data, where are 16 bands.

There are high-spin levels, gammas, ^{130}Te (^{48}Ca,4nγ), ^{172}Yb (α,2nγ), ^{160}Gd(^{18}O,4nγ), ^{175}Lu(p,2nγ), (d,3nγ) in ^{174}Hf high-spin data, where are 17 bands.

High-spin levels, gammas, ^{160}Gd(^{19}F,5nγ), ^{169}Tm(^{9}Be,4nγ) data files exist in ^{174}Ta high-spin data, where are 4 bands.

High-spin levels, gammas, ^{159}Tb(^{19}F,4nγ), ^{165}Ho(^{14}N,5nγ), ^{162}Dy(^{16}O,4nγ), ^{169}Tm(^{11}B,6nγ) exist in ^{174}W high-spin data files, where are 3 bands.

There is a ^{159}Tb(^{20}Ne,5nγ) data file in which rotational bands exist in ^{175}Re high-spin data.

High-spin levels, gammas, ^{51}V(^{127}I,4nγ), ^{146}Nd(^{32}S,4nγ), ^{150}Sm(^{28}Si, 4nγ), ^{150}Sm(^{29}Si,5nγ) exist in ^{174}Os high-spin data, where are 4 rotational bands.

^{107}Ag(^{70}Ge,p2nγ), ^{144}Sm(^{33}S,3nγ) exist in ^{174}Pt high-spin data, where is

only gs band.

2 $A = 176$ High–Spin Data

There is coulomb excitation data file in ^{176}YB and ^{176}Lu high–spin data, respectively.

^{174}Yb(α,2nγ), ^{176}Yb(α,4nγ) data file included ^{181}Ta(π^-,5nγ) exists in ^{176}Hf high–spin data, where are 15 bands.

There are high–spin levels, gammas, ^{170}Er(^{11}B,5nγ), ^{170}Er(^{10}B,4nγ), ^{173}Yb(^{7}Li,4nγ), and ^{175}Lu(α,3nγ) in ^{176}Ta high–spin data files, where are 4 bands.

High–spin levels, gammas, ^{150}Nd(^{30}Si,4nγ), ^{164}Dy(^{16}O,4nγ), ^{169}Tm(^{11}B, 4nγ), ^{176}Hf(α,4nγ), ^{154}Sm(^{26}Mg,4nγ) data files exist in ^{176}W high–spin data, where are 6 bands.

High–spin levels, gammas, ^{159}Tb(^{22}Ne,5nγ), ^{165}Ho(^{16}O,5nγ), and ^{169}Tm(^{12}C,5nγ) exist in ^{176}Re high–spin data, where are 3 bands.

There are high–spin levels, gammas, ^{164}Er(^{16}O,4nγ), ^{152}Sm(^{28}Si,4nγ), and ^{162}Dy(^{20}Ne,6nγ) in ^{176}Os high–spin data, where are 4 bands.

^{144}Sm(^{35}Cl,p2nγ) data file exists in ^{176}Pt high–spin data, where are 3 bands.

3 $A = 184$ High–Spin Data

There is coulomb excitation data file in which two bands exist in ^{184}W high–spin data.

High–spin levels, gammas, ^{170}Er(^{18}O,4nγ), ^{182}W(α,2nγ), ^{184}W(α,4nγ), ^{185}Re(p,2nγ), ^{186}W(α,6nγ), and ^{187}Re(p,4nγ) data files exist in ^{184}Os high–spin data, where are 5 bands.

There are ^{174}Yb(^{14}N,4nγ), ^{175}Lu(^{13}C,4nγ), ^{176}Yb(^{14}N,6nγ), ^{176}Lu(^{12}C, 4nγ) (HI,xnγ) data file of ^{184}Ir, where are 3 bands.

High–spin levels, gammas, ^{154}Sm(^{34}S,4nγ), ^{175}Lu(^{14}N,5nγ), and ^{177}Hf(^{12}C,5nγ) exist in ^{184}Pt high–spin data, where are 9 bands.

^{161}Dy(^{27}Al,4nγ) and ^{165}Ho(^{24}Mg,5nγ) exist in (HI,xnγ) data file of ^{184}Au, where are 2 bands.

There is ^{156}Gd(^{32}S,4nγ) data file in which two hands exist in ^{184}Hg high–spin data.

The evaluator would like to thank Dr. Murray Martin for his review, interest and useful discussions, and Ms Mary Ruth Lay for help with computer and references during the evaluators's stay at Nuclear Data Project, Oak Ridge Na-

tional Laboratory (May ~ August, 1995).

References

[1] J Dairiki, private communication, April 15, 1994

[2] C. L. Dunford and H. D. Lemmel, INDC(NDS)–307, 1994

IV BENCHMARK TESTING

Thermal Reactor Benchmark Testing of CENDL-2 and ENDF / B-6

Liu Guisheng

(China Nuclear Data Center, CIAE)

Abstract

In order to test of CENDL-2, ten homogeneous and eight heterogeneous thermal assemblies were used. Both of 123 group cross section libraries based on CENDL-2 and ENDF / B-6 were generated by a nuclear data processing systemNSLINK, respectively. The calculations of resonance self-shielding, cell spectra, cell reaction rate ratios and effective multiplication factors (K_{eff}) of these assemblies have been performed by the modified PASC-1 code system

The calculated results using CENDL-2 show an excellent agreement with corresponding experimental values. However, for some assemblies the K_{eff} values calculated by ENDF / B-6 data are underestimated.

Introduction

For the validation of the CENDL-2 for thermal reactor applications, 18 thermal reactor benchmark assemblies, which are recommended by CSEWG, have been selected. These benchmarks cover light and heavy water moderated uranium metal and uranium oxide as well as homogeneous solutions of uranyl and plutonium nitrate[1, 2].

For generation of 123 group cross section libraries based on CENDL-2 and ENDF / B-6, NJOY / NSLINK code system [3] was used. In CENDL-2 and ENDF / B-6, there are some nuclides (^{235}U, ^{238}U, ^{239}Pu and ^{240}Pu) with Reich-Moore resonance parameters. Currently, the module XLACSR in the NJOY / NSLINK processing system can only use SLBW (Single-Level Breit Wigner) or MLBW (Multi-Level Breit Wigner) resonance parameters. It can not treat R-M resonance parameters at all. Therefore, Dr. Cai Chonghai has

written a code RMTOMLBW to convert R–M parameters into MLBW parameters in the resolved–resonance region[4]. When he compared the pointwise cross sections calculated from the converted MLBW parameters with that calculated from original R–M parameters, it is found that the satisfying results are obtained. So the RMTOMLBW has been used for this work.

The modified code system PASC–1[5] has been applied to the calculations of the thermal reactor benchmark assemblies. Our calculated values are comparable with corresponding experimental values, the calculated values from ENDF / B–6 by ORNL[6] and LANL[7] and that from JEF–1 by IKE[8].

1 Description of Benchmark Assemblies

Eighteen thermal reactor benchmark assemblies have been used in this study. They can be divided into two kinds of homogeneous and heterogeneous assemblies. Their main characteristics are shown in the Table 1 and 2, respectively.

1.1 Homogeneous Critical Assemblies

Five simple unreflected spheres of ^{235}U (as uranyl nitrate) in water, which are called ORNL–1, 2, 3 ,4 and 10, are selected for the benchmark testing. Three of them are poisoned with boron. These benchmarks are quite sensitive to fast scattering data of hydrogen and oxygen, the thermal capture cross sections of ^{235}U and hydrogen and the thermal fission cross–sections of ^{235}U.

Table 1 Homogeneous critical assembly characteristics

Assembly	H / ^{235}U	H / ^{239}Pu	Radius	Exp. K_{eff}
ORNL–1	1378		34 595	1 00026
ORNL–2	1177		34 595	0 99975
ORNL–3	1033		34 595	0 99994
ORNL–4	972		34 595	0 99924
ORNL–10	1835		61 011	1 00031
PNL–1		700	19 509	1 00000
PNL–2		131	19 509	1 00000
PNL–3		1204	22 700	1 00000
PNL–4		911	22 700	1 00000
PNL–5		578	20 1265	1 00000

There are another five unreflected spheres of homogeneous aqueous plutonium nitrate assemblies with different H / ^{239}Pu ratios. They are PNL−1 through 5 The PNL−assemblies are useful for testing H_2O scattering data, cross sections of resonance and thermal fission of ^{239}Pu and the ^{239}Pu fission spectrum.

1.2 Heterogeneous Critical Assemblies

Eight cylinder lattice reactors are considered for the calculations. Five of them are light water moderated lattice−cell assemblies and the others are heavy water moderated The fuel rods are arranged in a triangular lattice having different pitches. The important lattice−cell characteristic parameters are listed in the Table 2.

Table 2 Characteristic parameters of lattice−cell assemblies

Lattice Assembly	Radius / cm	Fuel Material	Rod Enriched	Moderator	Pitch / cm	Vol. Ratio M / F
TRX−1	0.4915	U metal	1.3 %	H_2O	1.8060	2.35
TRX−2	0.4915	U metal	1.3 %	H_2O	2.1740	4.02
BAPL−UO_2−1	0.4864	UO_2	1.311 %	H_2O	1.5578	1.43
BAPL−UO_2−2	0.4864	UO_2	1.311 %	H_2O	1.6523	1.78
BAPL−UO_2−3	0.4864	UO_2	1.311 %	H_2O	1.8057	2.40
ZEEP−1	1.6285	Nat U	0.75 %	D_2O	20.000	40.42
ZEEP−2	1.6285	Nat U	0.75 %	D_2O	13.970	19.13
ZEEP−3	1.6285	Nat U	0.75 %	D_2O	12.060	13.96

The measured integral parameters for these assemblies include K_{eff} and the following lattice−cell reaction rate ratios, $\rho 28$, ratio of epithermal to thermal ^{238}U capture, $\delta 25$, ratio of epithermal to thermal ^{235}U fission, $\delta 28$, ratio of ^{238}U fission to ^{235}U fission, C^*, ratio of ^{238}U capture to ^{235}U fission.

These experiments can be used for testing the ^{238}U self−shielding resonance cross sections, inelastic scattering, fast fission, and capture cross sections, the ^{235}U thermal fission cross sections and fission spectrum, H_2O and D_2O fast scattering data.

2 Theory Method

2.1 Generation of Multigroup Constants

The code system NSLINK was applied to processing nuclear data and generating 123 group cross section libraries in AMPX master library format from CENDL-2 and ENDF/B-6, respectively. NSLINK is composed of NJOY, MILER, XLACSR and UNITABR.

The NJOY-91.91 is applied to processing ENDF/B evaluated nuclear data. It makes the following calculations : resonance reconstruction, Doppler broadening, resonance self-shielding for unresolved energy region, neutron thermalization and generating multigroup constants of 123 groups. Finally, the GENDF data file in ENDF/B format is obtained.

The MILER reads both of GENDF files independent and dependent on temperature and converts them to a multigroup cross section data file with the Bondarenko self-shielding factors in the AMPX master library format.

The XLACSR reads an evaluated nuclear data file with SLBW or MLBW resonance parameters and produces necessary resonance data in AMPX format for the Nordheim resonance treatment

The UNITABR merges the data file in AMPX format from MILER with another from XLACSR. The output data file in AMPX master library format can be used for fast reactor calculations as well as for thermal reactor calculations

2.2 Benchmark Calculations

First of all, the BONAMI-C, which is a modified version of the BONAMI-S in the PASC-1 code system, performs resonance self-shielding calculation by using the Bondarenko method and produces a problem-dependent AMPX master data set And then, the NITAWL-S performs a Nordheim resonance integral treatment for the resolved resonance region and produces a problem-dependent AMPX working library.

The XSDRNPM-C is a modified version of one dimensional transport code XSDRNPM-S in the PASC-1 code system. The modified XSDRNPM-C can calculate epithermal and thermal lattice-cell reaction rates The code is run twice. The first, it makes lattice-cell spectrum calculation of 123 groups in P_3S_8 for a heterogeneous assembly or infinite medium spectrum calculation for a homogeneous assembly and produces spectrum averaged cross section set of 48 groups. The second, it is used for critical calculations. For heterogeneous assembly, the experimental total buckling is used to account for leakage correction. The calculated integral parameters include K_{eff} and lattice-cell reaction

rate ratios $\rho 28$, $\delta 25$, $\delta 28$ and C^*.

3 Calculated Results of Integral Parameters

3.1 Effective Multiplication Factors

Table 1 presents the calculated results of K_{eff} values of ten homogeneous and eight heterogeneous assemblies for CENDL-2 and ENDF/B-6 by CNDC and the values of K_{eff} published for benchmark testing of ENDF/B-6 [6, 7], JEF-1[8] and ENDF/B-5[9].

Table 3 Results of K_{eff} calculations

	CNDC		ORNL	LANL	CSEWG	IKE
Assembly	CENDL-2	ENDF/B-6	ENDF/B-6	ENDF/B-6	ENDF/B-5	JEF-1
ORNL-1	0.9995	0.9971	0.9965	0.9969	1.0025	1.0013
ORNL-2	0.9990	0.9968	0.9964	0.9967	1.0006	1.0015
ORNL-3	0.9959	0.9938	0.9935		0.9970	0.9985
ORNL-4	0.9973	0.9952	0.9950		0.9982	0.9997
ORNL-10	0.9944	0.9928	0.9961	0.9972	0.9964	0.9986
PNL-1	1.0244	1.0076	1.0089	1.0087	1.0211	1.0176
PNL-2	1.0180	1.0025		1.0037		1.0167
PNl-3	1.0031	0.9897	0.9942	0.9904	1.0003	0.9978
PNL-4	1.0073	0.9962	1.0013	0.9971	1.0072	1.0060
PNL-5	1.0145	1.0000	1.0065		1.0110	1.0117
TRX-1	0.9968	0.9909	0.9894	0.9869	0.9961	0.9961
TRX-2	0.9993	0.9939	0.9915	0.9891	0.9984	0.9973
BAPL-UO_2-1	0.9998	0.9949	0.9975	0.9949	1.0030	1.0001
BAPL-UO_2-2	1.0007	0.9957	0.9971	0.9959	1.0033	0.9999
BAPL-UO_2-3	1.0027	0.9979	0.9972	0.9974	1.0045	0.9988
ZEEP-1	1.0019	0.9998			1.0036	
ZEEP-2	1.0001	0.9981			1.0016	
ZEEP-3	0.9987	0.9969			1.0009	

Considering the results of ENDF/B-6, the K_{eff} values calculated by CNDC are agreeable to that by ORNL and LANL except that our K_{eff} value of assembly ORNL-10 was underestimated by 0.4% and the K_{eff} values of both TRX were overestimated by 0.48% and 0.15%, respectively. It is obvious that our results are reliable. There are some differences between the calculated

K_{eff} values of the same assembly by ORNL and LANL. For example, the differences for TRX−1 and BAPL−UO_2−1 are 0.0025 and 0.0026, respectively.

For CENDL−2 the K_{eff} values calculated of the U−fueled assemblies are satisfactory and they range from 0.9944 to 1.0027. For ENDF/B−6, however, the calculated K_{eff} values range from 0.9869 to 0.9975. That is to say, the K_{eff} values predicted with CENDL−2 are better than those obtained with ENDF/B−6.

Using CENDL−2, the calculated K_{eff} results for BAPL−UO_2−1, −2, −3, ZEEP−1, −2 and −3 are best. With ENDF/B−6 the K_{eff} values of these assemblies were underestimated, whereas with ENDF/B−5 they were overestimated slightly.

With CENDL−2 for calculating Pu−fueled assemblies, the K_{eff} were considerably overestimated like ENDF/B−5 and JEF−1. With ENDF/B−6, the predicted K_{eff} values are the best.

3.2 Lattice Cell Reaction Rate Ratios

The lattice cell reaction rate ratios $\rho 28$, $\delta 25$, $\delta 28$ and C^* of five assemblies with light water moderated lattice cell were calculated for CENDL−2 and ENDF/B−6, respectively. The results calculated by CNDC−L (NSLINK/PASC−1) and CNDC−Z (NJOY−WIMSR/WIMS−D4)[10] based on CENDL−2 together with ENDF/B−6 from Ref. [11] (NJOY/WIMS−D4), ENDF/B−5 from Ref. [9] and JEF−1 from Ref. [8] are given in Table 4 ~ 7. The C/E represents the ratio of calculated to experimental value.

Table 4 $\rho 28$ epithermal/thermal ^{238}U Captures (C/E)

	CENDL−2		ENDF/B−6		ENDF/B−5	JEF−1
Assembly	CNDC−L	CNDC−Z	CNDC−L	KAERI	CSEWG	IKE
TRX−1	1.0533	1.0309	1.0448	1.0490	1.0295	1.0280
TRX−2	1.0342	1.0191	1.0248	1.0390	1.0108	1.0005
BAPL−UO_2−1	1.0475	1.0017	1.0373	1.0360	1.0173	1.0213
BAPL−UO_2−2	1.0813	1.0359	1.0704	1.0710	1.0473	1.0510
BAPL−UO_2−3	1.0451	1.0077	1.0374	1.0350	1.0088	1.0156

Table 5 $\delta 25$ epithermal / thermal ^{235}U fissions (C / E)

	CENDL-2		ENDF / B-6		ENDF / B-5	JEF-1
Assembly	CNDC-L	CNDC-Z	CNDC-L	KAERI	CSEWG	IKE
TRX-1	1.0049	0.9932	1.0102	0.9660	1.0162	1.0051
TRX-2	0.9899	0.9806	0.9945	0.9530	1.0000	0.9902
BAPL-UO_2-1	0.9957	0.9761	1.0000	0.9640	1.0026	1.0012
BAPL-UO_2-2	1.0021	0.9846	1.0065	0.9710	1.0000	1.0074
BAPL-UO_2-3	1.0054	0.9904	1.0094	0.9810	1.0096	1.0115

Table 6 $\delta 28$ ^{238}U fissions / ^{235}U fissions (C / E)

	CENDL-2		ENDF / B-6		ENDF / B-5	JEF-1
Assembly	CNDC-L	CNDC-Z	CNDC-L	KAERI	CSEWG	IKE
TRX-1	1.0148	1.0171	1.0433	1.0610	1.0455	1.0581
TRX-2	0.9812	0.9828	1.0025	1.0026	1.0087	1.0678
BAPL-UO_2-1	0.9577	0.9438	0.9782	1.0000	1.0026	0.9936
BAPL-UO_2-2	0.9174	0.9039	0.9353	0.9570	0.9329	0.9543
BAPL-UO_2-3	0.9223	0.9095	0.9381	0.9650	0.9351	0.9632

Table 7 C^* ^{238}U captures / ^{235}U fissions (C/E)

	CENDL-2		ENDF / B-6		ENDF / B-5	JEF-1
Assembly	CNDC-L	CNDC-Z	CNDC-L	KAERI	CSEWG	IKE
TRX-1	1.0039	0.9940	1.0113	1.0150	1.0013	1.0018
TRX-2	0.9919	0.9872	0.9998	1.0050	0.9923	0.9881

Table 5 and 7 show that $\delta 25$ and C^* are in good agreement with experimental values, respectively. There is an exception to $\delta 25$ for ENDF / B-6. The KAERI calculations are overpredicted by 1.9 %～4.7 %.

From Table 4, generally speaking, $\rho 28$ is overpredicted significantly for H_2O-moderated lattices. For the ENDF / B-6, the values calculated by the CNDC-L are in good agreement with that by KAERI. Using CENDL-2, the CNDC-L calculations for $\rho 28$ are 4% higher than the CNDC-Z calculations for the UO_2 lattices and 2% higher than the CNDC-Z calculations for the metal uranium lattices. From Table 6, in general, $\delta 28$ is underpredicted significantly for the UO_2 lattices. With CENDL-2, the calculated $\delta 28$ for TRX lattices are in good agreement with measurement. But the $\delta 28$ for TRX-1 is overestimated by about 4.5 %～6 % with other evaluated libraries.

The calculated results from Tables 4 and 6 show a tendency to make $\rho 28$ increase and $\delta 28$ decrease with the increase of lattices pitch. That is to say, the capability moderated high energy neutron is overestimated, therefore the calculated spectrum of system softened.

4 Conclusion

CENDL–2 predictions of K_{eff} for five homogeneous and eight heterogeneous thermal benchmark assemblies with U–fueled are in very good agreement with experiments. The average K_{eff} for three H_2O–moderated lattices of uranium oxide rods and three D_2O–moderated lattices of natural uranium rods are 1.0011 and 1.0002, respectively. It is understood that for CENDL–2 the calculated K_{eff} for three Pu–fueled assemblies with the lower values of H/^{239}Pu were overestimated by 1.45~2.44 %. The re–evaluations of the cross section data for plutonium nuclides should be needed.

ENDF/B–6 predictions of K_{eff} for thermal reactor benchmark assemblies are less than other data libraries.

Several evaluated nuclear data libraries including CENDL–2 overpredict $\rho 28$ of all of lattices and underpredict $\delta 28$ for three uranium oxide lattices. Since all benchmark testing results from different data sources yielded nearly the same discrepancies, it may be thought that not only data uncertainties but also systematic errors in the benchmark experiments cause the deviations between experiment and calculation.

References

[1] D. S. Craig, AECL–7690 Rev. 1 (1984)

[2] CSEWG, ENDF–202 (1974)

[3] P. F. A. de Leege, IRI–131–091–003, (1991)

[4] Cai Chonghai et al., NFA–ACT–92–15 (1992)

[5] Liu Guisheng et al., Chin. Jour. of Nucl. Sci. and Eng., 13, 13, 9(1993)

[6] R. Q. Wright et al., Proceedings Inter. Conf. on Nucl. Data for Sci. and Tech., Vol. 2, p. 815, Gatlinburg, Tennessee, May 9~13, 1994

[7] R. E. MacFalane, ibid, p. 786, 1994

[8] W. Bernnat et al., IKE–6–157, 1986

[9] CSEWG, ENDF–311, BNL–NCS–31531 (1982)

[10] Zhang Baocheng et al., CNDP, 13, 116 (1995)

[11] Jung–do Kim et al., (KAERI), INDC(JPN)–157/L, p. 394 (1992)

V DATA AND PARAMETER LIBRARY

The Status of CENDL-2.1

Liang Qichang Liu Tingjin Zhao Zhixiang
Yu Baosheng Liu Tong Sun Zhengjun

(China Nuclear Data Center, CIAE)

A modified version of CENDL-2, i e CENDL-2.1 was completed and released in 1995.

The library contains evaluations of neutron reaction data for 68 elements or isotopes from ^{1}H to ^{249}Cf in the neutron energy range from 10^{-5} eV to 20 MeV.

Compared to CENDL-2, the size of the library has been increased significantly, the modifications have been made to most materials, so the accuracy of the data have been improved :

1. 14 new evaluations completed by Chinese or Chinese / Japanese cooperation have been added, they are Cl, $^{50, 52, 53, 54}Cr$, $^{54, 56, 57, 58}Fe$, $^{63, 65}Cu$, Lu, Hg, and Tl.
2. 9 evaluations have been updated or re-evaluated, which were done by Chinese or Chinese / Japanese cooperation. They are ^{27}Al, ^{nat}Ca, ^{nat}Cr, ^{55}Mn, ^{nat}Fe, ^{nat}Cu, ^{93}Nb, ^{nat}Ag and ^{238}U.
3. The secondary neutron energy spectra have been modified for 20 nuclides They are ^{16}O, ^{23}Na, Mg, Si, P, S, K, Ti, ^{51}V, Ni, Zr, Cd, In, Sb, Hf, W, ^{197}Au, Pb, ^{237}Np and ^{239}Pu.
4. The total cross section and elastic scattering cross section have been updated for 8 elements. They are S, K, Ti, Ni, Zr, Sb, Hf, and Pb.
5. The double differential cross section, gamma production data and covariance data have been added for many nuclides.

The comparison of the CENDL-2 and CENDL-2.1 are given as follows

	Nuclides	MF6	MF12~15	MF31~33
CENDL-2	54	4	10	7
CENDL-2.1	68	25	38	10
Increasing	14	21	28	3

Improvement and Supplements for CENDL-2

Yu Baosheng

(China Nuclear Data Center, CIAE)

In order to provide more double differential cross sections of secondary neutrons and charged particles in CENDL-2.1, the evaluated data of 15 nuclides were adopted, which were performed by Yu Baosheng of CNDC and Chiba of JAERI / NDC for JENDL-3 Fusion File. The data were checked and slightly corrected for CENDL-2.1 in 1995. The data include file 1 ~ 4, 6, 12 ~ 15, which reproduce the trend of measured data very well in general.

The nuclides are ^{27}Al, ^{50,52,53,54,Nat}Cr, ^{55}Mn, ^{93}Nb, ^{54,57,58,Nat}Fe and ^{63,65,Nat}Cu, which were added in CENDL-2.1 or replaced the old ones in CENDL-2. In this work, the DDX is expressed by Kumabe's or Kalbach's systematics for neutron, depending on the target nucleus, and by the Kalbach's systematics for charged particles. The composite energy spectrum and the precompound fraction (f_{MSD}) required in the systematics were calculated by model code SINCROS-II.

The author would like to thank Drs Liang Qichang and Sun Zhengjun for their kind help.

Progress on Chinese Evaluated Nuclear Parameter Library (V)

Su Zongdi Huang Zhongfu Liu Jianfeng Ge Zhigang
Zhang Limin Sun Zhengjun Yu Ziqiang Zuo Yixin
Ma Gonggui Chen Zhenpeng Wang Baojin

1 Progress on Six Sub-Libraries

1.1 The MCC Sub-library

A new edition of MCC-1.1 (1995 Version) sub-library has been completed. It contains the atomic mass data for 4771 nuclides ranging from $Z=0$, $A=1$ to $Z=122$, $A=328$, including the measured and systematics mass excesses, atomic masses and total binding energies for 2650 nuclides compiled and recommended by Audi and Wapstra in 1993[1] and mass excesses of 2121 nuclides calculated by Moller et al. in 1994[2]. A few of them (181 nuclides) were calculated by Moller et al. in 1991[3] and collected, recommended by us.

MCC-1.1 data file also contains the half-life and abundance spin and parity of nuclear ground state. Most of these data were taken from Refs. [4] and [5], a few were collected and compiled by us.

The format of MCC-1.1 data file, the functions and routine procedure of the management-retrieval code are just the same as the MCC-1 sub-library[6, 7].

1.2 The DLS Sub-library

The data of the DLS data file were translated from the Evaluated Nuclear Structure Data File (ENSDF)[4]. In consideration of the demands for different kinds of research fields, such as the compound nucleus reaction theory, nuclear level density, nuclear structure and so on, most of the evaluated experimental levels and gamma rays in ENSDF were kept, except the levels with undetermined energies and their gamma rays. These data have further been checked and corrected, and its format has further been refined. The DLS data file contains the data of 79461 levels and 93177 gamma-rays for 1908 nuclides up to now. They are energy, spin, parity and half-life of each measured level, as well as the order numbers to the final levels, branching ratios and multipolarities for gamma-rays of the levels, if they existed.

The DLS management-retrieval code has basically been finished at CNDC. It contains SN and NR two kinds of retrieval ways, can cut off and select the levels and gamma rays required from whole discrete level scheme according to user's demand.

1.3 The NLD Sub-library

The NLD sub-library consists of two data files for the data related to level density (LRD) and level density parameters (LDP) , and its management retrieval code.

A. The LRD data file

The LRD data file contains the S-wave average resonance spacing D_0,

strength function S_0 and cumulative number N_0 of low-lying levels for about 300 nuclides recommended by us in 1993[8], as well as the radioactive capture width[9].

In order to update the D_0 and S_0 values, the program AVRPES to estimate D_0 values, which contains the moment method[10], maximum likelihood method[11], Bayesian approach[12] and so on, has been refined, the resolved resonance parameters from BNL-325[11], ENDF / B-6, JEF-2 and JENDL-3 are being collected and analysed, a set of the resolved resonance parameters will be evaluated and recommended.

B. The level density parameters (LDP)

Generalized superfluid model of the nuclear level density and relevant parameters have been studied. A new set of asymptotic values of level density parameter a at high excitation energy and supplementary shift values of excitation energy for 249 nuclides ranging from ^{41}Ca to ^{250}Cf was obtained by fitting the D_0 and N_0 values mentioned above. Shell correction in nuclear binding energy, energy of the first 2^+ level, deformation parameter of nucleus were taken from those of Ignatyuk et al[15]. Since the two sets of GSM level density parameters were estimated by fitting the different D_0 and N_0 values, their parameter values are different. And they should be further analysed and compared.

The LDP data file contains eight sets of level density parameters for three popular level density formulae. They are three sets of parameters for the composite four-parameter formula (GC) (i. e. Gilbert and Cameron[14], Cook et al.[15] and ours[16]), three sets of parameters for back-shifted Fermi gas formula (BS) (i. e. parameters of the rigid and half-rigid body of Dilg et al.[17] and ours[18]), as well as two sets of parameters for the generalized superfluid model (GSM) (Ignatyuk et al.[13] and ours[19]). The LDP data file was set up and submitted to the IAEA.

The management-retrieval code of the NLD sub-library including two retrieval ways SN and NR, has been completed. It not only can retrieve the data from LRD and LDP files, and also can calculate the D_0 and N_0 values with the different sets of level density parameters and compare the calculated results with the relevant data in LRD file to help users to choose the required level density parameters.

In addition, an intercomparison of three kinds of popular level density formulae mentioned above has been made. As the first step, the ability describing the low lying levels was compared. The D_0 values of 54 nuclides ranging from ^{46}Sc to ^{246}Cm were selected from our recommended D_0 values, which are consistent within the errors with the other D_0 values available[11, 15, 16]. The data

of low-lying levels were taken from ENSDF, and were corrected and replenished according to the recent data from "Nuclear Data Sheets" (until 1993). Considering the loss of levels, a cut-off energy has been chosen by means of a histogram of low-lying levels for each selected nucleus. Below the cut-off energy, we have counted up the number of levels in group, and drawn the histogram of level numbers for all groups, which will be used to estimate the level density parameters.

An object function is defined as :

$$X^2 = X_N^2 + X_D^2 = \frac{1}{m} \sum_{i=1}^{m} \left(\frac{N_c(i) - N_e(i)}{0.3\ N_e(i)} \right)^2 + \left(\frac{D_c - D_e}{\Delta D_e} \right)^2$$

Where m is the group number, $N_c(i)$ and $N_e(i)$ are calculated and experimental value of level number for the ith group respectively. D_c, D_e and ΔD_e are the calculated, experimental value and experimental error of D_0 respectively. Using GC, BS and GSM formulae to fit the experimental data mentioned above for the 54 nuclides selected, the corresponding two level density parameters for each formula could be obtained when X^2 value achieved the minimum. In general, X_D^2 is very small for each nucleus, if $X_N^2 < 1$, then the $N_c(i)$ values are statistically within their uncertainty $0.3\ N_e(i)$. The X_N^2 distribution of fitting results for each formula are listed in Table 1. The numerals in this table are the numbers of nuclei and percentage.

Table 1 X_N^2 distribution of fitting level numbers with every formula for 54 nuclides

X_N^2	GC	BS	GSM
$X_N^2 < 1$	42 (78%)	21 (39%)	25 (46%)
$1 < X_N^2 < 2$	10 (18%)	11 (20%)	16 (30%)
$2 < X_N^2$	2 (4%)	22 (41%)	13 (24%)

Analyzing calculated results, we can also see :

There are only 18 nuclei, the X_N^2 values of which are all less than 1 for the three formulae. Their results are identical within the statistical error.

The X_N^2 values of 10 nuclei are all larger than 1 for these formulae, and the X_N^2 of GC formula are mostly less than those of BS and GSM formula, the X_N^2 value of other 18 nuclei are also larger than 1 for BS and GSM formula, but less than 1 for GC formula. To sum up, the results of the GC formula to re-

produce the discrete levels seem better than others in low excitation energy region.

1.4 The GDP Sub-library

The GDP-1 sub-library (Version 1)[20] was set up in 1993, but there were giant dipole resonance parameters (GDRP) of only 102 nuclides ranging from ^{51}V to ^{239}Pu compiled by Dietrich and Berman[21] and no data in the region $A<50$. For sake of the systematics approaches and practical application, the collections of experimental data on the photonuclear reactions and estimates of the GDRP for nuclides mass region with $A < 50$ are very important.

In the past year, the experimental cross sections of photoneutron reaction for nuclides ^{12}C, ^{14}N, ^{16}O, ^{27}Al and ^{28}Si[22] were fitted with the Lorentz curve (1) describing the giant dipole resonances of the photonuclear reactions, and the GDRP of these nuclides have been extracted

$$\sigma(E_\gamma)=\sum_{i=1}^{2}\frac{\sigma_{g_i}E_\gamma^2\Gamma_{g_i}^2}{(E_\gamma^2-E_{g_i}^2)^2+D_\gamma^2\Gamma_{g_i}^2} \tag{1}$$

Using these parameters, the integrated cross sections, and their first moments and second moments of the photonuclear reaction giant dipole resonances of these nuclides were calculated. Adjusting the parameters a little, the better coincidences of the excitation curves and integrated cross sections with the experimental data were reached. Finally their GDRP were obtained (Table 2). The comparisons of the calculated results with the experimental data show that the extracted GDRP are reliable.

Table 2 The giant dipole resonance parameters of ^{12}C, ^{14}N, ^{16}O, ^{27}Al and ^{28}Si

Z	A	E_{g_1} / MeV	Γ_{g_1} / MeV	σ_{g_1} / mb	E_{g_2} / MeV	Γ_{g_2} / MeV	σ_{g_2} / mb
6	12	22.60	1.90	6.30	26.50	8.60	2.60
7	14	20.60	4.30	2.90	23.50	4.50	13.90
8	16	24.50	6.20	6.50			
13	27	21.10	6.10	12.50	29.50	8.70	6.70
14	28	20.10	3.90	10.50	26.50	8.70	3.70

The GDRP estimated by us were compiled in the updated edition GDP–1.1 data file. Up to now, it contains the GDRP of 107 nuclides ranging from ^{12}C to ^{239}Pu, extended from $A=51$ to $A=12$. This is useful both for model calculations and systematics approaches of the GDRP.

1.5 The FBP Sub–library

The FBP–1 (Version 1)[23] including three sets of the fission barrier parameters had been finished before the 1st RCM. In the past year the data file has been expanded, a FBP–1 1 data file has been set up, in which the fission barrier heights recommended by Smirenkin[24] are contained.

1.6 The OMP Sub–library

The OMP data file includes the following two parts :

(1). The global and regional optical model potential parameters for six type of projectiles(n, p, d, t, ^3He and alpha) have been collected and compiled respectively.

(2). The nucleus–specific optical model potential parameters

A standard optical potential form of the data file have been determined. About 75 sets of optimum optical model parameters for neutron only, which were used in the calculations of complete neutron data in CENDL–1, 2, have been compiled and submitted to the IAEA

The management retrieval code has been completed. The code can retrieve the parameters (OMPP) for a single and / or several reaction channels from Part A and / or Part B. It can also calculate the cross sections, and compare the results, calculated with different OMPP sets, with experimental data. The code consists of both spherical and deformed potentials. It is suitable for both standard optical potential form and all kinds of global and regional OMPP sets.

2 Activities on CENPL

The following meeting were held in the past year.

The Meeting on "Development of RIPL of the IAEA and Researches of Relevant Nuclear Model Parameters", Oct. 8～9, 1994, Huangshan City, Anhui Province, presented the 1st RCM of the IAEA, arranged the work on the actions determined in the 1st RCM.

The 2nd Workshop on Optical Model Parameters, Dec. 6～ 8, 1994, Tianjin, communicated and reviewed the progress on the CENPL, discussed the

deformed potential parameters, dispersion optical model and problem on the management retrieval code of the OMP sub-library

The Meeting of Sub-Group Head, March 20~21, 1995, Beijing; communicated and reviewed the progress on the CENPL, established the objective to set up the CENPL-2 (Version 2) and worked out a plan on developing the CENPL-2.

The 1st Workshop on Giant Dipole Resonance Parameters, June 19, 1995, Beijing, discussed the problem on extracting the GDRP from the photonuclear reaction data for the nuclides mass region with $A < 50$, and the research on systematics of the GDRP.

3 Conclusions

The remarkable progress on constructing CENPL has been made in the past year :

(1) Six sub-libraries, MCC, DLS, NLD, GDP, FBP and OMP, including their data files and management-retrieval code systems have all been finished basically. All six sub-libraries have been used in nuclear model calculations, nuclear data evaluations and other fields in China. The applied results show that our evaluated nuclear parameter library is satisfactory and convenient, and the project of the RIPL of the IAEA is of great worth.

(2) According to the actions determined in the 1st RCM, the data files with the S-wave average level spacings, level density parameters, discrete level schemes and gamma radiation branching ratios, and optical model parameter sets have been submitted to IAEA.

(3) In the aspect of researches on nuclear model parameters, a new set of GSM level density parameters for 249 nuclides ranging from ^{41}Ca to ^{250}Cf was obtained, the ability describing low lying levels for three level density formulae has been compared, the resolved resonance parameters, taken from BNL-325, ENDF / B-6, JEF-2 and JENDL-3, are being evaluated and recommended, the GDRP of 5 light nuclides were extracted.

Acknowledgement

The authors would like to thank NDS / IAEA and NNDC / BNL for providing us the data on mass excesses, ENSDF and so on.

The project supported in part by the International Atomic Energy Agency and the National Natural Science Foundation of China.

References

[1] G. Audi et al., Nucl. Phys., A565, 1(1993) and 66(1993)

[2] P. Moller et al., (1 August 1994), accepted for publication in At. Nucl. Data Tables

[3] P. Moller et al., At. Nucl. Data Tables, 39, 225(1988) (File as of 1991)

[4] Evaluated Nuclear Structure Data File — a computer file of evaluated nuclear structure data maintained by the NNDC / BNL

[5] N. E. Holden, "Table of the Isotopes", CRC Handbook of Chemistry and Physics 71st edition (1990)

[6] Su Zongdi et al., Commu. Nucl. Data Progress, 11, 103(1994)

[7] Su Zongdi et al., Commu. Nucl. Data Progress, 12, 80(1994)

[8] Huang Zhongfu et al., t be published

[9] S. F. Mughabghab et al., Neutron Cross Sections, Academic Press (NY–London), V. 1, part A, in 1981; part B, in 1984

[10] M. S. Moore et al., Phys. Rev., C18, 1328(1978); G. A. Keyworth et al., Neutron Physics and Nuclear Data, Harwell, 241(1978)

[11] P. Ribon et al., CEA–N–1832, 1617(1975); G. Rohr et al., RIT / FIS–LDN, (1), 80(1979), NEA Data Bank, Newsletter, 27 July 1982

[12] Zhao Zhixiang, Annual Report of CIAE in 1988; Huang Zhongfu et al., Commu. Nucl. Data Progress, No. 5, 59(1991)

[13] A. V. Ignatyuk et al., Sov. Nucl. Phys., 29, 450(1979), O. T. Grudzevich et al., Systematics of Level Densities, Private communication in 1991

[14] A. Gilbert et al., Can. J. Phys., 43, 1446(1965)

[15] J. L. Cook et al., Aust. J. Phys., 20, 477(1967)

[16] Su Zongdi et al., INDC(CPR)–2, 1985

[17] W. Dilg et al., Nucl. Phys., A217, 269(1973)

[18] Huang Zhongfu et al., Chinese J. Nucl. Phys., 13, 147(1991)

[19] Lu Guoxiong et al., to be published

[20] Liu Jianfeng et al., INDC(NDS)–335, p. 75, in 1995, Zuo Yixin et al., INDC(NDS)–335, p. 77, in 1995

[21] S. S. Dietrich et al., Atomic Data and Nuclear Data Tables, 38, 199(1988)

[22] A. I. Blokhin et al., INDC(CCP)–337, 1991

[23] Zhang Limin et al., Commu. Nucl. Data Progress, 10, 88(1993)

[24] G. N. Smirenkin, INDC(CCP)–359, in 1993

CN9700502

Discrete Level Schemes and Their Gamma Radiation Branching Ratios (CENPL-DLS) (II)

Zhang Limin Su Zongdi Sun Zhengjun

(China Nuclear Data Center, CIAE)

1 The DLS Data Files

The DLS data files contains the data and information of nuclear discrete levels and gamma rays. They were transformed from the Evaluated Nuclear Structure Data File (ENSDF)[1], the transformation code was programmed[2], the data were checked and corrected; the levels, for their gamma rays have been determined were deleted; the format was refined. Considering the demands for different kinds of research fields, such as compound nucleus reaction theory, nuclear level density, nuclear structure and so on, most of the evaluated experimental levels and gamma rays in the ENSDF are kept. At present, the file contains 79461 levels and 93177 gamma rays for 1908 nuclides.

For each measured level, order number, energy, spin, parity and half-life, as well as the order numbers to the final levels, branching ratios and multipolarities are contained. The data format as follows.

Z : Charge number, column 1~3.
EL : Element symbol, column 4~6.
A : Mass number, column 7~10

The line marked "L" in 13 column contains the data concerning a level NL, E, dE, J^{π}, IS, $T_{1/2}$ and UC :

NL : Order number of level, column 14~16
E : Level energy in keV, column 17~27.
dE : Standard uncertainty for E, column 28~30
J^{π} : Level spin and parity, column 31~46
IS : Isomer state denoted by "M", column 47.
$T_{1/2}$: Half-life of the level, column 62~72.
d$T_{1/2}$: Standard uncertainty for $T_{1/2}$, column 73~79.

UC : Denoted by character "?" uncertain or questionable level, column 80.

The line marked "G" in 48 column contains the data concerning a gamma ray for the level listed above, *NG*, *Br*, d*Br*, *MP* and *UC* :

NG : Order number to final level for gamma transition,column 49 ~ 51

Br : Branching ratio of gamma ray, column 52~57.

d*Br* : Standard uncertainty of Br, column 58~61.

MP : Multipolarity of gamma transition, column 62~79.

UC : Denotes character "?" uncertain placement of the transition, "s" denotes an expected one, but not yet observed, column 80.

For convenience of retrieval, the DLS data file were divided into 104 data files from " D000.DAT" to " D103.DAT" according the charge number *Z* value

2 DLS Management Retrieval Code DLS

The code can provide two retrieval ways. One is for a single nucleus (SN), and another is for a neutron reaction (NR). The latter contains four kinds of retrieval types corresponding to four types of fast neutron calculation codes (i e. FUP code, code for emitted particles without d,t and ^{3}He, UNF code and MUP code). The data on the discrete levels and gamma rays of the relevant residual nuclei can be retrieved. The code can cut off and select some levels and gamma rays according to user's requirement.

An example is given in Table 1 for ^{56}Fe in (SN).

Table 1 Retrieved DLS for ^{56}Fe (SN)

NL	*E*	d*E*	J^{π}	*IS*	*NG*	*Br*	d*Br*	$T_{1/2}$ or	*MP*	d$T_{1/2}$	*UC*
1	0.0		0^+					STABLE			
2	846.753	5	2^+					6.07	PS	23	
					G 1	100.0		*E2*			
3	2085.054	7	4^+					0.64	PS	12	
					G 2	100.0		*E2*			
4	2657.541	16	2^+					26	FS	7	
					G 1	3.8	38				
					G 2	96.2	29	*M1+E2*			
5	2941.7	3	0^+					0.45	PS	+21 −12	
					G 2	100.0					
•	•	•	•		•	•	•	•		•	
18	3755.54	13	6^+					0.13	PS	2	
					G 3	80.7	32	*E2*			
					G 9	1.6	*LE*				?
					G 11	17.7	8	*M1+E2*			

3 Conclusion Remarks

The DLS sub-library (Version 1) has been set up at the CNDC, and widely used for nuclear model calculations and other field. The data file contains the data from the ENSDF as many as possible, and users can break off and select the levels and gamma rays required so it can satisfy the different demands and very simple and convenient to use.

Acknowledgement

The authors would like to thank NNDC BNL for providing us the ENSDF data

References

[1] Evaluated Nuclear Structure Data File NNDC, BNL (1991)

[2] 1st RCM P. Oblozinsky, INDC(NDS)-335, p. 67 (1995)

VI NUCLEAR DATA NEWS

Activities and Cooperation on Nuclear Data in China During 1995

Zhuang Youxiang

(China Nuclear Data Center, CIAE)

1. The Activities and Meetings in Nuclear Data Field in 1995.

(1) "The Ist plenary session of the second China Committee of Nuclear Data" , June 20~ 21, China Institute of Atomic Energy, Beijing. Summarized the achievements and experiences of nuclear data work during the 8th five-year plan, reviewed and endorsed the 9th five-year plan of nuclear data,

(2) " The celebration activities of the 20th anniversary of the founding of China Nuclear Data Center", June 22, China Institute of Atomic Energy, Beijing. This is a grand gathering of the staff members in nuclear data field in China,

(3) " The Combined Meeting of Nuclear Data Evaluation Working Group and Nuclear Theory Working Group" , Oct. 23~ 27, Taian City, Shandong Province;

(4) "The Meeting of Nuclear Data Measurement Working Group", Dec. 18~ 22, Nanning City, Guangxi Province,

During the mentioned-above meetings, the detailed plans were made to accomplish the third version of the Chinese Evaluated Nuclear Data Library (CENDL-3).

2. The International Meetings and Workshops in Nuclear Data Field Attended by Staff Members of CNDC in 1995.

(1) "The 20th Meeting of International Nuclear Data Committee" , April 3~ 7, Vienna, Austria;

(2) " The IAEA Consultants' Meeting on Technical Aspects of the Cooperation of Nuclear Reaction Data Center", May 2~ 5, Vienna, Austria;

(3) " The 7th Meeting of NEANSC Working Party on International Evaluation Cooperation", May 16～18, Paris, France;

(4) "The Meeting on Technical Aspects of Atomic and Molecular Data Processing and Exchange", July 10～11, Vienna, Austria,

(5) "The CRP Meeting on Improvement of Measurement, Computations and Evaluations on Helium Production Cross Section", Sept 25～29, Japan;

(6) "The CRP Meeting on Development of Reference Input Parameter Library (RIPL) for Nuclear Model Calculations of Nuclear Data", Oct. 30～Nov. 3, Vienna, Austria,

(7) "The 1st CRP Meeting on Development of Reference Charged Particle Cross Section Data Base for Medical Radioisotope Production", Nov 15～17, Vienna, Austria,

(8) "Workshop on Condensed Matter Physics and Physics of the Living State Program", Oct. 25～Nov. 25, ICTP, Italy.

3 The Foreign Scientists in Nuclear Data Field Visited CNDC / CIAE in 1995:

Drs. J. Katakura and A. Ichihara, NDC / JAERI, Japan, March 18～22;
Dr. Robert Russian, RSIC / ORNL, USA, and
Dr. Edward T. Cheng, USA, November.

4 Two staff members of CNDC as visiting scientist worked at NDC / JAERI, Japan and ECN, Netherlands, for one year, respectively.

CINDA INDEX

Nuclide	Quantity	Energy (eV)		Lab	Type	Documentation			
		Min	Max			Ref	Vol	Page	Date
H	total	2.0+7	2.0+9	AEP	Eval	Jour CNDP	15	66	June 96
^{18}O	(p,n)	Thrsh	8.0+7	AEP	Eval	Jour CNDP	15	43	June 96
^{56}Fe	(n,γ)	1.4+7		AEP	Comp	Jour CNDP	15	71	June 96
^{59}Co	(n,x)	Thrsh	1.0+8	AEP	Eval	Jour CNDP	15	50	June 96
	(n,x)	Thrsh	1.0+8	AEP	Theo	Jour CNDP	15	11	June 96
Ni	(n,xα)	1.4+7		HST	Expt	Jour CNDP	15	1	June 96
	(n,p)	Thrsh	2.0+7	SIU	Eval	Jour CNDP	15	60	June 96
^{58}Ni	(n,p)	Thrsh	2.0+7	SIU	Eval	Jour CNDP	15	60	June 96
^{60}Ni	(n,p)	Thrsh	2.0+7	SIU	Eval	Jour CNDP	15	60	June 96
^{61}Ni	(n,p)	Thrsh	2.0+7	SIU	Eval	Jour CNDP	15	60	June 96
^{62}Ni	(n,p)	Thrsh	2.0+7	SIU	Eval	Jour CNDP	15	60	June 96
^{64}Ni	(n,p)	Thrsh	2.0+7	SIU	Eval	Jour CNDP	15	60	June 96
^{77}Se	(p,n)	Thrsh	8.0+7	AEP	Eval	Jour CNDP	15	43	June 96
^{89}Y	(n,γ)	1.4+7		AEP	Comp	Jour CNDP	15	71	June 96
^{93}Nb	(n,γ)	1.4+7		AEP	Comp	Jour CNDP	15	71	June 96
^{90}Zr	(n,x)	Thrsh	1.0+8	AEP	Eval	Jour CNDP	15	68	June 96
	(n,x)	Thrsh	1.0+8	AEP	Theo	Jour CNDP	15	37	June 96
^{186}W	(p,n)	Thrsh	8.0+7	AEP	Eval	Jour CNDP	15	43	June 96
^{238}U	(n,n')	1.4+7	2.0+7	TSI	Theo	Jour CNDP	15	31	June 96

Author, Comments
Liu Tingjin, total CS
Zhuang Youxiang, ^{18}F CS
Fan Sheng+, SPEC
Yu Baosheng+, ^{56,57,58}Co, ^{52,54,56}Mn, ^{59}Fe CS
Shen Qingbiao+, n+^{59}Co
Ye Bangjiao+, CS
Ma Gonggui+, CS
Ma Gonggui+, CS
Ma Gonggui+, CS
Ma Gonggui+, CS
Ma Gonggui+, CS
Ma Gonggui+, CS
Zhuang Youxiang, ^{77}Br CS
Fan Sheng+, SPEC
Fan Sheng+, SPEC
Yu Baosheng+, ^{88,89}Zr, ^{86,87,88}Y CS
Shen Qingbiao+, n+^{90}Zr
Zhuang Youxiang, ^{186}Re CS
Chen Zhenpeng, Direct INEL

(京)新登字 077 号

图书在版编目(CIP)数据

中国核科技报告 CNIC-01075,核数据进展通讯(No 15)/刘挺进等著. —北京:原子能出版社,1996.6
ISBN 7-5022-1502-6

Ⅰ.中… Ⅱ.刘… Ⅲ.①核技术-研究报告-中国②核反应-数据-进展-通讯 Ⅳ.TL-2

中国版本图书馆 CIP 数据核字(96)第 07554 号

原子能出版社出版发行
责任编辑:李曼莉
社址:北京市海淀区阜成路 43 号 邮政编码:100037
中国核科技报告编辑部排版
核科学技术情报研究所印刷
开本 787×1092 1/16·印张 7·字数 110 千字
1996 年 6 月北京第一版 1996 年 6 月北京第一次印刷

ISBN 7-5022-1502-6